Universitetet i Stavanger

Faculty of Science and Technology

MASTER'S THESIS

Study program / Specialization: Industrial Economics / Construction Engineering	Spring semester, 2017 Open access
Author: Henrik Eeg Kjærnsmo	…… (signature of author)
Supervisors: Kjell Tore Fosså Samdar Kakay	
Title of master's thesis: Graphene Oxide – A New Potential Nano Reinforcement	
Credits: 30	
Keywords: *Concrete Technology; Graphene Oxide; Properties of Fresh Cement Mortar; Temperature Development; Mechanical Properties; Microstructure; SEM; EDS.*	Number of pages: 111 + supplemental material/other: 44 Stavanger, 15th of June, 2017

This page intentionally left blank.

Table of Contents

This page intentionally left blank.

Abstract

Graphene oxide (GO) is a new potential nano reinforcement in cementitious composites. In previous research, graphene oxide has shown promising potential for improving mechanical properties, and particularly the tensile strength capacity. The thesis investigates the effect of GO on fresh cement mortar (workability, air content, heat of hydration), microstructure (SEM & EDS) and mechanical strength (Flexural -, compressive -, splitting tensile strength) after 3,7, and 28 days of curing. These properties are studied by introducing various dosages of GO combined with a constant content of polycarboxylate (SP). The selected dosages of GO are 0.03 wt%, 0.05 wt%, and 0.2 wt% of the cement weight. The effects of two different types of GO have been studied: Water dispersed- and fine powder concentrate GO. The results show that the workability decreases correspondingly to the increasing content of water dispersed GO. The heat of hydration is increased for both types of GO which indicate a chemical reaction between GO and cement. The percent air content is almost constant with a GO dosage of 0.03 wt% and 0.05 wt%, but is increased from 3.2 % to 4.9 % with 0.2 wt% water dispersed GO. The increased air content is an indirect outcome of poor compaction and workability. The adverse effects of GO on fresh mortar will consequently influence the mechanical properties. GO has the potential of accelerating the hydration process and enhance the early mechanical strength (3 and 7 days), but has no effect after 28 days of curing. Particularly for the highest content of water dispersed GO, the adverse effect on the workability seems to diminish the mechanical strength after 28 days. No distinct influence of GO on the microstructure has been observed with SEM, except for the presence of GO sheets verified by EDS.

Acknowledgements

I would like to thank my supervisors, Kjell Tore Fosså and Samdar Kakay, for constructive guidance and commitment. It has truly been a privilege to do this research and conducting the experimental program. Further, a great gratitude also goes to John Grønli, who has provided the research with materials, equipment, and facilitated the concrete laboratory.

A great appreciation also goes to Research Fellow Mona Minde, for giving me the opportunity to work in the SEM laboratory and for sharing important knowledge.

Additionally, I would like to offer my special thanks to Associate Professor Mesfin Belayneh Agonafir (UiS, Petroleum Department) and Associate Professor Kidane Fanta Gebremariam (UiS, Museum of Archaeology), for their support and engagement in my work.

Notations

at%	Atomic percentage (Atomic ratio)
Avg.	Average
C-S-H	Calcium Silicate Hydrate
cm	Centimeter
D10	10% percent of the particles have the designated size or smaller.
D50	Mean particle size
$d_{50\%}$	50^{th} percentile
D90	90% percent of the particles have the designated size or smaller.
$d_{95\%}$	95^{th} percentile
dm^3	Cubic decimeter
EC 2	Eurocode 2
EDS	Energy-Dispersive X-ray Spectroscopy
g	Gram
GO	Graphene Oxide
ITZ	Interfacial Transition Zone
Kg	Kilogram
KJ	Kilojoule
L	Liter
m	Meter
m^2	Square Meter
mBar	Millibar
mg	Milligram
mL	Milliliter
mm	Millimeter
MPa	Megapascal
N	Newton
NEC	Nano-Engineered Concrete
nm	Nanometer
ppm	Parts-per-million
SEM	Scanning Electron Microscopy
SP	Superplasticizer
TEM	Transmission Electron Microscopy
wt%	Weight percentage (Mass fraction)
µm	Micrometer
µs	Microsecond
Ø	Diameter
°C	Celsius
2D	Two dimensional
3D	Three dimensional

Definitions

Bridging effect	A toughening mechanism that take place in fracture process zone.
Covalent Bonding	The chemical bond is formed by the sharing of electron pairs between two atoms.
Hydrophilic	Water Dispersive
Hydrophobic	Not (or almost not) water dispersive (dissolvable).
Interfacial Transition Zone (ITZ)	The zone between the aggregate or the sand particle and the bulk cement paste. Generally considered as the weakest link of the chain and the strength-limiting phase (Metha & Monteiro, 2006).
SP^2 Hybridization	Each carbon atom in the hexagonal network is bonded to three other carbon atoms by SP^2 - hybridization. The SP^2- hybridization determines the flat structure and also the chemical- and physical properties. There are three s-bonds per carbon atom which creates the 2D structure, and one free p-electron located in a p-orbital. The free p-electron makes graphene to an excellent heat - and electrical conductor. (Ghavanini & Theander, 2015)
Stiff Plastic	A fresh mortar consistency designation with the following external feature according to Magne et al. (2016): *At tilting the concrete forms a flat heap that flows quite easily under vibration. The concrete sticks to the hand and can be shape into a ball in the hand.*
Toughening Mechanism	Fracture Mechanics: *Energy absorbing mechanism.*

1 Introduction

This chapter will present background, motivation, objectives, scope, and thesis structure.

1.1 Background and Research Motivation

In recent years, it has been a rapid development of new nanomaterials which can be used as additives to improve the properties of cementitious materials. Graphene is a relatively "new" material with a size of only a few angstroms (1×10^{-10} meter), and it is about 200 times stronger than steel (Vjayaraghavan, 2017). Moreover, graphene is known for its superb material properties and has shown a great potential in other industries, such as electronics and polymer composites. Graphene Oxide (GO) is a derivate from graphene, and previous research has shown that GO can be used as an additive in cement mortar with the potential of providing a nano reinforcement (Wang et al., 2015). With only a small dosage, GO has the potential of improving the mechanical properties, and particularly the tensile capacity. Furthermore, it is important to empathize that this field of research is still at an early stage. In the context of this, the thesis will look more into GO as a potential nano reinforcement in cement mortar and other side-effects, with the purpose of increasing the understanding of this potential new wonder material.

1.2 Objectives and Scope

The prime objective is to investigate the effect graphene oxide (GO) on cement mortar. The thesis scope is limited to focusing on the following properties of cement mortar:

1. **The effect of GO on fresh cement mortar**
   - Workability
   - Air content
   - Density
   - Heat of hydration

2. **The effect of GO on mechanical properties**
   - Flexural strength,
   - Compressive strength
   - Splitting Tensile Strength
   - Ultrasonic Velocity

3. **The effect of GO on the microstructure**
   - The interfacial transition zone & the bulk cement paste

1.3 Thesis Structure

The potential effects of GO will be elaborated and discussed both through a literature review of previous research (Chapter 2) and by conducting an experimental program (Chapter 3 to 5) in the Concrete -, Petroleum - and Nano Laboratory at University of Stavanger, Spring 2017. An overview of the thesis is presented in Figure 1.

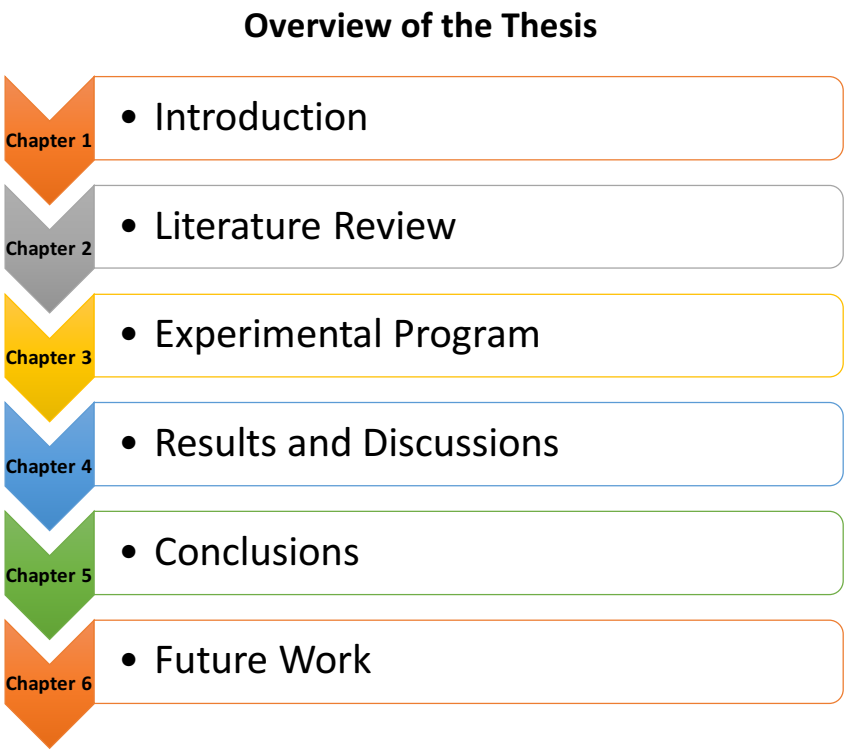

Figure 1. Overview of the thesis (Kjaernsmo, 2017)

2 Literature Review

The purpose of this chapter is to provide the reader with relevant theory within the field of graphene and graphene oxide. This will be followed by a review of previous research on graphene oxide as an additive in cementitious mortar and cement.

2.1 Graphene – The New Wonder Material

In 2010, the Nobel Prize in Physics was awarded to Geim and Novoselov for their groundbreaking research regarding the two-dimensional (2D) material graphene, and graphene became well known to the world as the possible new wonder material. (NobelMedia, 2014)

Graphene has a thickness of only one atom, and its 200 times stronger than steel (Vjayaraghavan, 2017). According to atomic force microscopy, the intrinsic strength is 130 GPa and the Young´s modulus is 1TPa for a single layer graphene sheet (Tang, Liu, Wang, & Ye, 2014). Graphene consist of a characteristic hexagonal network of carbon atoms, illustrated in Figure 2.

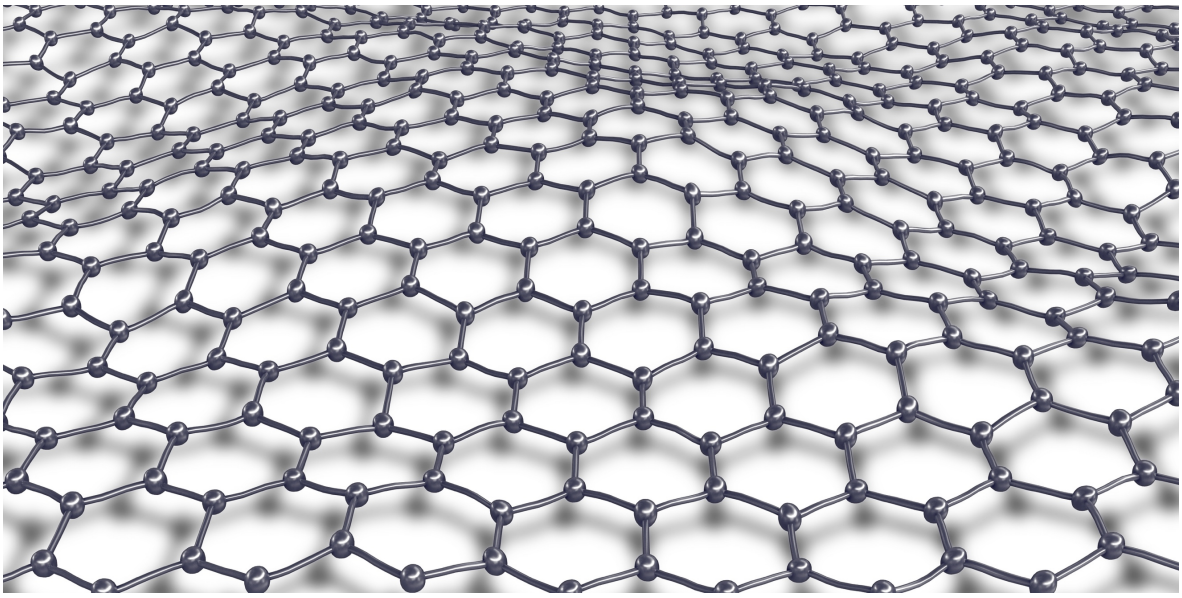

Figure 2. Graphene consist of a hexagonal (honeycombed) network of carbon atom. (TheManufactor, 2016)

Graphene is a form of carbon in a 2D single layer sheet made of a hexagonal (honeycombed) network of carbon atoms (Chuah, Pan, Sanjayan, Wang, & Duan, 2014). Each carbon atom is covalently bonded to three carbon atoms with a SP^2 - hybridization. The strong covalent bonds (carbon-carbon bonds) provide the distinct flat plane and the superb mechanical strength (Ghavanini & Theander, 2015). The SP^2 - hybridization determines the chemical- and physical properties of graphene. Diamond also has a similar type of carbon-carbon bonding, but the carbon atoms are bonded by a tetrahedral SP^3 - hybridization which creates a 3D structure. The hybridization of the carbon atom is illustrated in Figure 3 and is a result of the electron configuration.

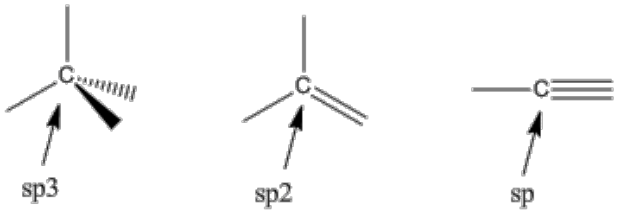

Figure 3. The hybridization of the carbon atom. (Quoracdn, 2017)

Furthermore, graphite and graphene are also related, since graphite consist of a large number of 2D single-layer graphene sheets bonded by Van der Waals forces. The carbon-carbon bonding can be categorized into intramolecular attractions, and the Van der Waals forces are defined as intermolecular attractions. The strong intramolecular attractions hold the atom together within a molecule, while intermolecular attractions are weak and exist between the molecules. The hydrogen bonding is another example of intermolecular attractions which can be broken by heat, pressure or oxidation. This will be further elaborated in Section 2.3. The structural molecular differences between diamond, graphite and graphene is illustrated in Figure 4. The dashed green lines (graphite) represent the intermolecular attractions.

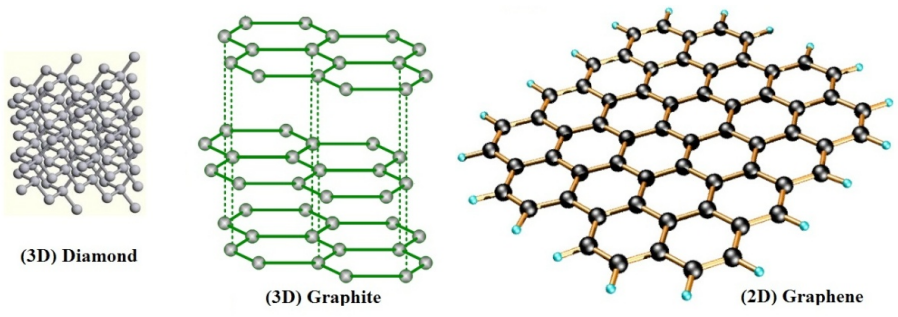

Figure 4. The molecular structure – Diamond (left), Graphite (center), and Graphene(right). (InTechopen, 2017)

2.2 Material properties of Graphene & Possible Areas of Interest

According to Ghavanini and Theander (2015), graphene has the following unique combination of material properties:

- *Thinnest imaginable material*
- *Largest surface area (~2.700 m^2 per gram)*
- *Strongest material 'ever measured' (theoretical limit)*
- *Stiffest known material (stiffer than diamond)*
- *Most stretchable crystal (up to 20 % elastically)*
- *Record thermal conductivity (outperforming diamond)*
- *Highest current density at room temperature (106 times of copper)*
- *Completely impermeable (even He atoms cannot squeeze through)*
- *Highest intrinsic mobility (100 times more than in Si)*
- *Conducts electricity in the limit of no electrons*
- *Lightest charge carriers (zero rest mass)*
- *Longest mean free path at room temperature (micron range)*

There are several possible areas where graphene can be utilized within the field of civil engineering and transportation infrastructure. From a graphene feasibility study conducted by the Norwegian Public Roads Administration and Chalmers Industriteknik, the following possible areas of interest were identified (Ghavanini & Theander, 2015):

- *Construction material (Concrete, steel, polymers).*
- *Sensor of measuring surrounding environment.*
- *Energy harvesting*
- *Heat transfer in roads*
- *Coating and barrier materials*
- *Communication, vehicle to vehicle, vehicle to road*

2.2.1 Functional Groups – From Graphene to Graphene Oxide (GO)

Graphene is hydrophobic in nature which is characterized by flocculation and settles down when it is mixed with water. By introducing oxygen-containing functional groups (oxidation), graphene transforms into a hydrophilic material and becomes graphene oxide (Chuah et al., 2014). The hydrophilic property of GO makes it possible to disperse in water. Graphene oxide (GO) consists of a characteristic hexagonal network of carbon atoms with several functional groups such as hydroxyl, epoxide, carboxyl, and carbonyl(Chuah et al., 2014). The characteristic hexagonal carbon network with functional groups is illustrated in Figure 5.

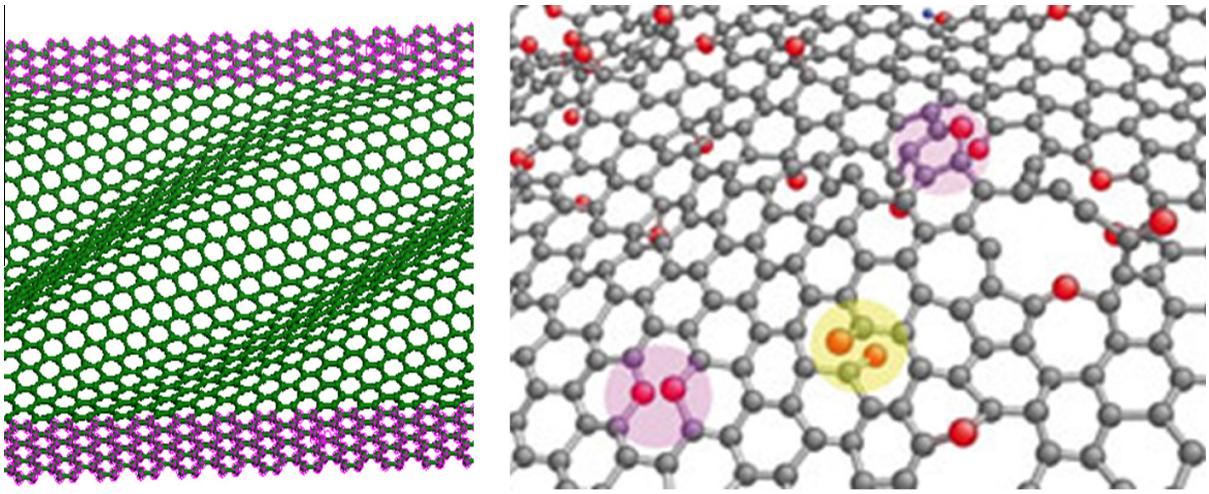

Figure 5. Graphene Oxide - A Hexagonal Network of Carbon (Chuah et al., 2014)

Graphene oxide (GO) must be modified, or functionalized, by increasing the number of functional groups on the GO surface in order to be combined with cementitious materials. According to Tang et al. (2014), the objectives with the functionalization are:

1) Oxygen-containing functional groups are required in order to achieve a stable dispersion in the solvent.

2) The functional groups provide a better interfacial interaction with the cement hydrates.

A schematic illustration of the chemical reaction between GO and cement hydration products is presented in Figure 6. As illustrated, the oxygen-containing functional groups attached on GO surface reacts with the cement hydration products.

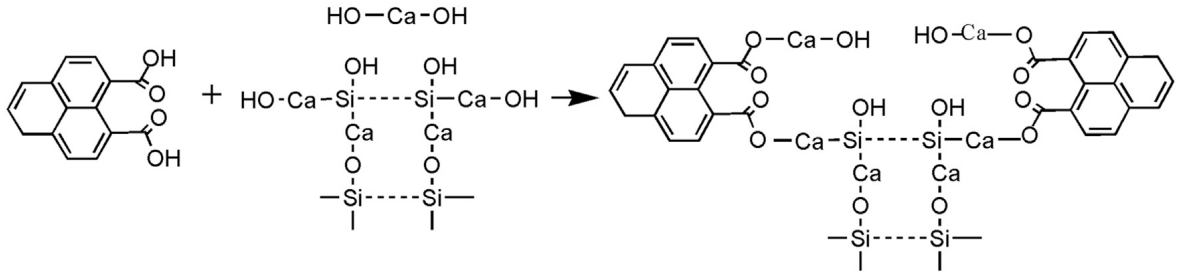

Figure 6. Chemical reaction between GO and cement hydration products (CH & C-S-H). (Zhao et al., 2017)

2.3 Graphene oxide (GO) - A New Nano Reinforcement

Graphite is a 3D material which contains millions of 2D single-layer sheets of graphene held together by electrostatic forces (Van der Waals bonding). By chemically separating these layers into monolayers or just a few layers, you get graphene oxide (GO). Ultrasonic treatment can further increase the number of monolayers. The modified Hummer´s method is a common technique in graphene oxide manufacturing and involves chemical oxidation of graphite powder (Gong et al., 2015). A simplified illustration of the production technique is illustrated in Figure 7. There are also several other methods used in graphene and graphene oxide manufacturing (e.g. UV-light), but they are not further elaborated in this thesis.

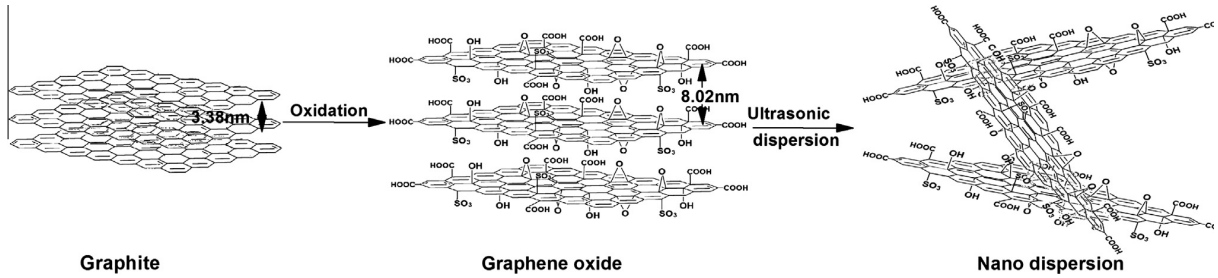

Figure 7. Preparation of Graphene Oxide. (Lv et al., 2013)

2.4 Nano-Engineered Concrete (NEC)

Graphene Oxide is categorized into Nano-Engineered Concrete (NEC). Figure 8 compares graphene oxide with other cementitious materials and aggregates. NEC is still at the early research stage, but in the future, nano-additives have the potential of solving many issues we are struggling with today. For instance, within concrete 3D printing, a major challenge is the placing of reinforcement which interrupts the production process. One of the objectives of developing NEC is to construct a reinforcement at the nanoscale. A nano-reinforcement which controls nano-cracks by either preventing or delaying the initial nano-cracks to propagate into micro cracks.

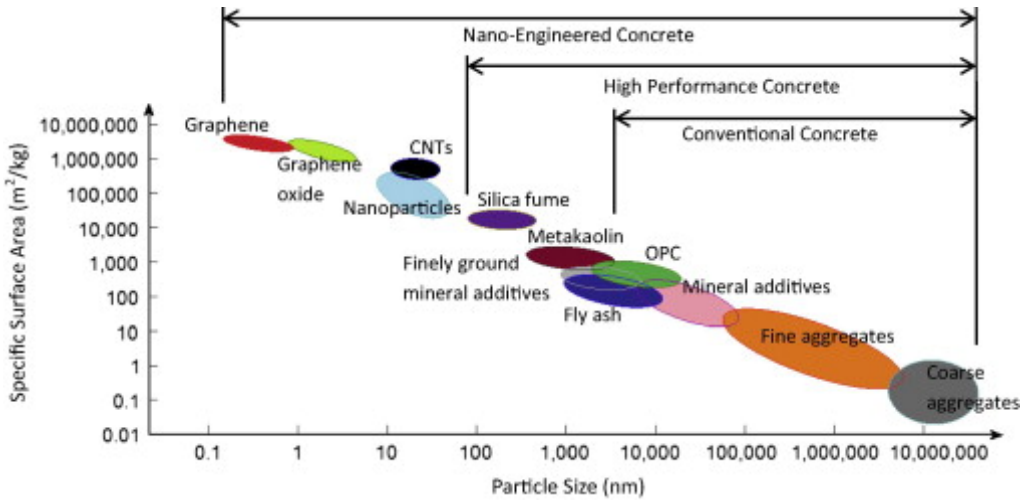

Figure 8. Graphene Oxide compared to other materials. (Chuah et al., 2014)

2.4.1 The mechanisms behind the improved mechanical properties

Since this field of research is at an early stage, there are several interpretations of why graphene oxide has the potential of improving the mechanical properties of cementitious mortar and cement.

According to Kang, Seo, Lee, and Chung (2017), GO nanosheets improve the mechanical strength by acting as a bridge in the cement mortar. Equivalent to fiber reinforced concrete and aggregate bridging in the fracture process zone, which considered as toughening mechanisms. The bridging effect of GO acts at the nano-scale and prevent or delay the nano-cracks to form into micro cracks. In other words, GO sheets create a nano reinforcement. The microstructure of the cement based composite and GO sheets are illustrated in Figure 9.

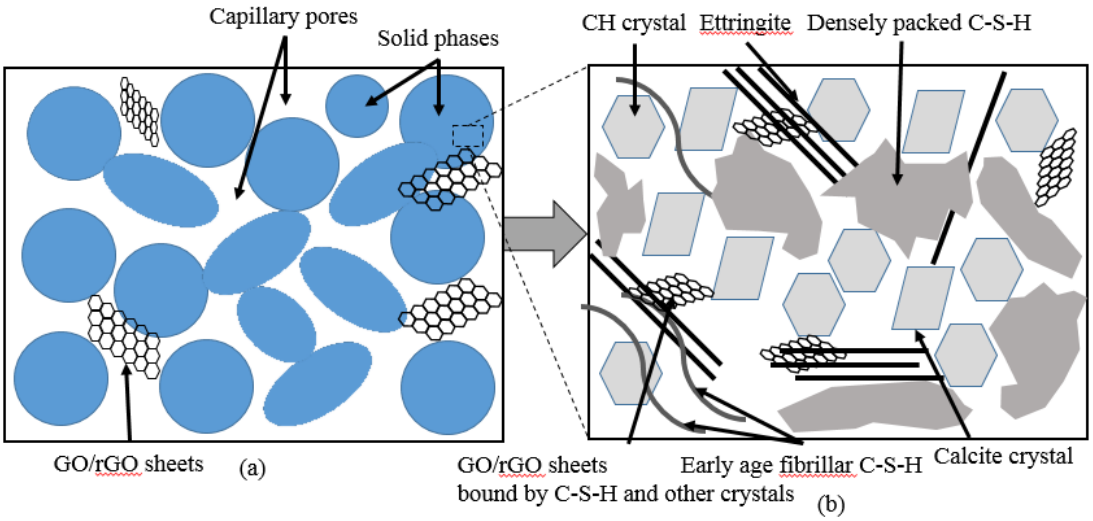

Figure 9. The microstructure of the cement paste with GO sheets.(Muhit, 2015)

The bridging effect can only be achieved through strong covalent bonding with the C-S-H. In a chemical perceptive, strong covalent bonds between graphene oxide and the cement hydration components formed on the interface of the graphene oxide are essential, in order to incorporate the mechanical properties of GO to the cement mortar (Chuah et al., 2014). Without these strong covalent bonds, the intrinsic mechanical properties of GO will not be utilized. Because of crack initiation can propagate in a potential weak transition between the GO sheets and the bulk cement paste.

On the other hand, according to Zhao et al. (2017), the improved mechanical properties are caused by crack deflection between the cement matrix and the GO sheets. The crack deflection absorbs energy and is also defined as a toughening mechanism. The crack deflection is illustrated in Figure 10.

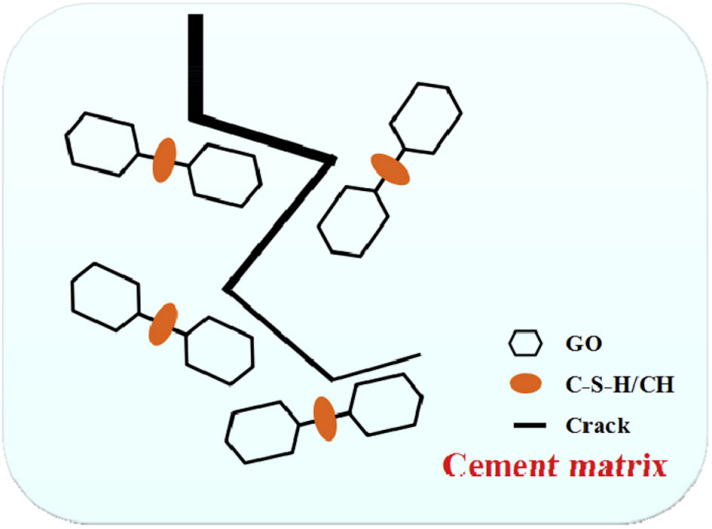

Figure 10. Deflection of cracks in the cement matrix. (Zhao et al., 2017)

Furthermore, according to Gong et al. (2015), the enhanced mechanical strength can also be a result of a refinement of the pore structure because GO increases the degree of hydration.

2.5 Previous research

The following sections will present previous research on graphene oxide mixed with cement or cementitious mortar. The designated previous research is selected in terms of the experimental program. The following results and observations are based on a literature study performed by this thesis author, Spring 2017.

2.6 Mechanical Properties

2.6.1 Flexural Strength

One of the main objectives of adding GO is to improve the flexural strength by reinforcing the cementitious mortar at the nanoscale. The majority of the previous research presents results which indicate an enhanced flexural strength because of GO, but the opposite has also been reported, where there are non-improvements or even a decreased flexural strength. The flexural strength is a combination of the compressive and tensile strength and is usually determined by a three- or a four-point bending test.

Wang et al. (2015) reported that the flexural strength of the cementitious mortar increased by 69.4 %, 106.4 %, and 70.5 % after three, seven, and 28 days, respectively. The content of GO was 0.05%. To the author's knowledge (of this thesis), these results are the largest improved flexural strength obtained by adding GO. Others can report an improved flexural strength in the range of 30,37 % - 60,7 % (Zhao et al., 2017), (Pan et al., 2015) & (Lv et al., 2013).

2.6.2 Compressive Strength

The compressive strength, determined by a conventional test, is a combination of both the compressive- and tensile capacity of cement mortar. For instance, if the flexural strength increases there is a high probability of an improved compressive strength. Wang et al. (2015) observed that the compressive strength also increased by 43.2 %, 33 %, and 24.4 % at three, seven, and 28 days of curing. Figure 11 presents the corresponding flexural and compressive strength results presented by Wang et al. (2015). Similar observations are also reported by Zhao et al. (2017), Pan et al. (2015) and Lv et al. (2013), where the compressive strength increased in the range of 15 - 38.9 %.

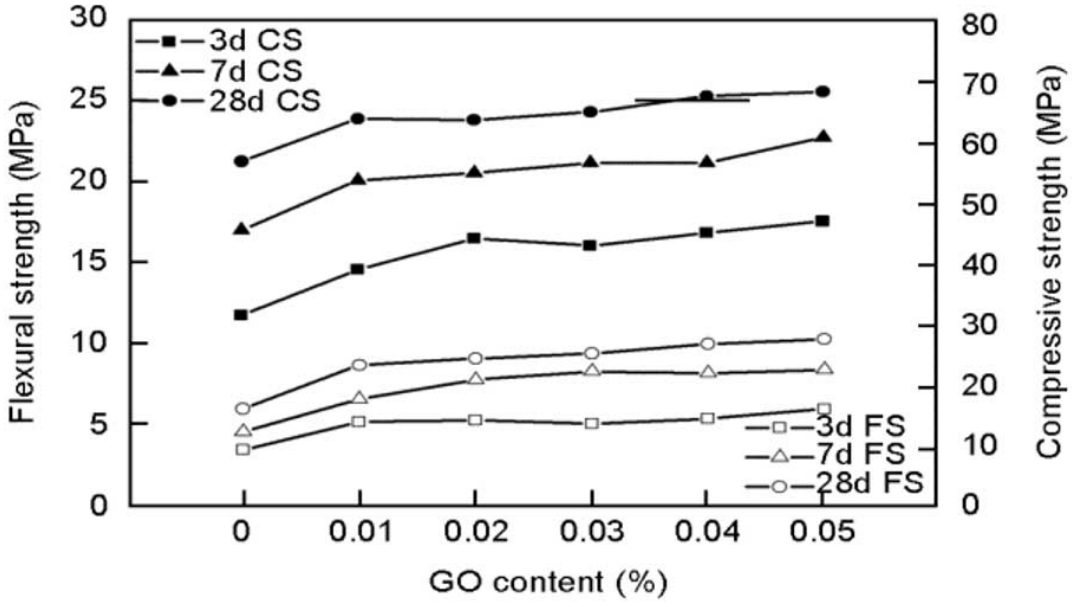

Figure 11. The flexural and compressive strength of cementitious mortar. (Wang et al., 2015)

2.6.3 Splitting Tensile Strength

X. Li et al. (2016) reported an increased splitting tensile strength for cement mortar containing 0,02 % and 0.04 % GO nano sheets. For the cement mortar containing 0.02 % GO, the tensile splitting strength increased by 21 %, and 18 % after seven and 28 days, respectively. But after three days of curing, there was no substantial change in the splitting tensile strength. Also, Gong et al. (2015) observed an enhancement of approximately 50 % with a GO content of 0.03 % GO after 28 days of curing. More results regarding the splitting tensile strength have not been found during the literature review.

Additionally, Lv et al. (2013) observed that the direct tensile strength of cement increased by 78,6 % with a GO content of 0.03 %. The result was obtained by testing dumbbell (dog-bone shape) specimens under direct tension. However, it is important to emphasize that direct tensile strength is not directly comparable. Since the splitting tensile strength generally overestimates the tensile strength by 10 % to 15 % (Metha & Monteiro, 2006). The splitting tensile strength will be further elaborated in Section 3.4.9.

2.7 Fresh Properties

2.7.1 Workability

A reduced workability is one of the challenges with graphene oxide. Consequently, can a reduced workability cause poor compaction and therefore influence the mechanical properties. The impaired workability can be explained by a reduced amount of free-water since GO has a significant high specific surface area which can result in a high water absorbency. In some of the previous research, the reduced workability has been solved by adding superplasticizer (SP) made of polycarboxylate, but potential side-effects because of the chemical reaction between SP and GO, are unknown to the author.

According to Gong et al. (2015), the mini-flow diameter is reduced by 34.6 % with a GO content of only 0.03 wt%. Their observations are illustrated in Figure 12. Equivalent results are also reported by Pan et al. (2015), Shang, Zhang, Yang, Liu, and Liu (2015) and Tang et al. (2014).

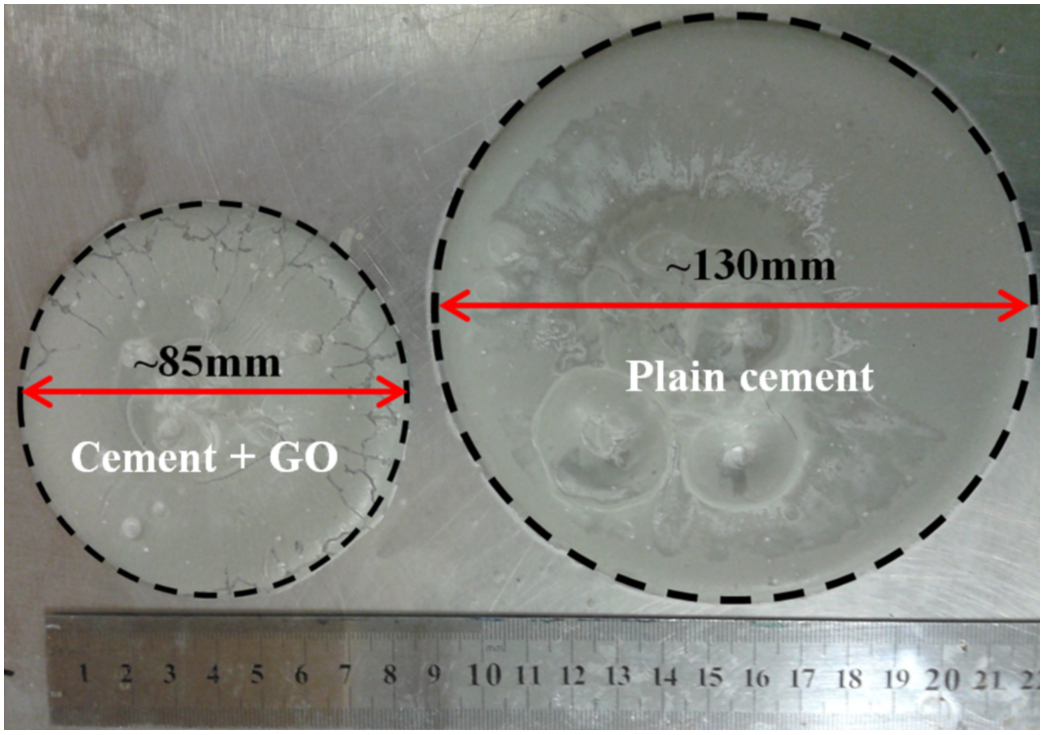

Figure 12. The mini-slump diameter after 10 minutes. (Gong et al., 2015)

Shang et al. (2015), also observed that the mini-flow diameter decreases with an increasing content of GO. This illustrated in Figure 13. The mini-flow diameter is reduced by 36.2 % with a GO content of 0.08 wt%. According to Chuah et al. (2014), similar results are also observed with other nanomaterials, such as nano silica and carbon nano tubes (CNT).

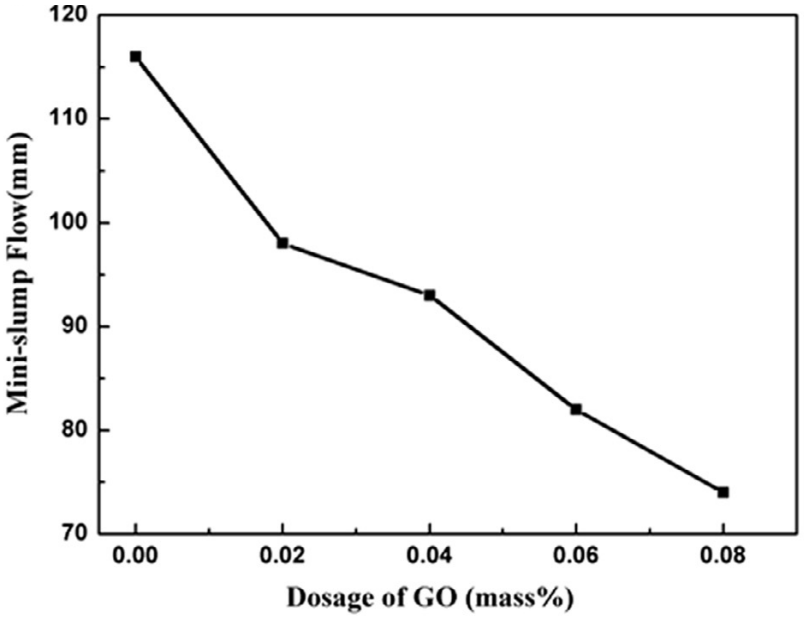

Figure 13. Mini-flow diameter for various dosages of GO. (Shang et al., 2015)

2.8 Heat of hydration

According to the author's knowledge, the influence of GO on the heat of hydration is not clarified well in previous research. During the literature study, only two research articles with results regarding the heat of hydration were found. Moreover, the research articles are also presenting opposite results. Zhao et al. (2017) reported that GO increases the maximum cement hydration exothermal rate, illustrated in Figure 14, while Wang et al. (2015) observed the opposite, illustrated in Figure 15. Alternatively, the distinct contradicting results can also be a consequence of adding polycarboxylate. Also, in this case, potential secondary effects of mixing graphene oxide and polycarboxylate are unknown to the author.

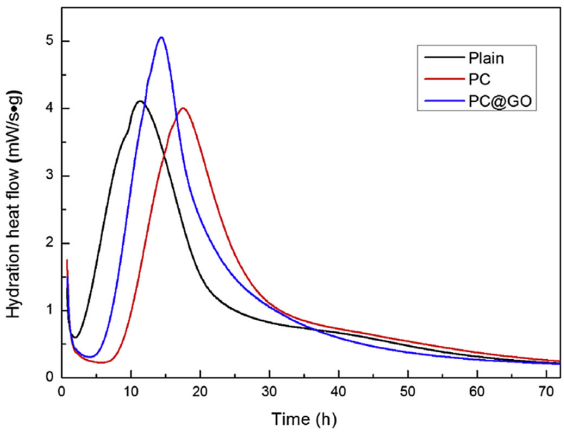

Figure 14. Cement hydration exothermic rate (PC = Polycarboxylate superplasticizer). (Zhao et al., 2017)

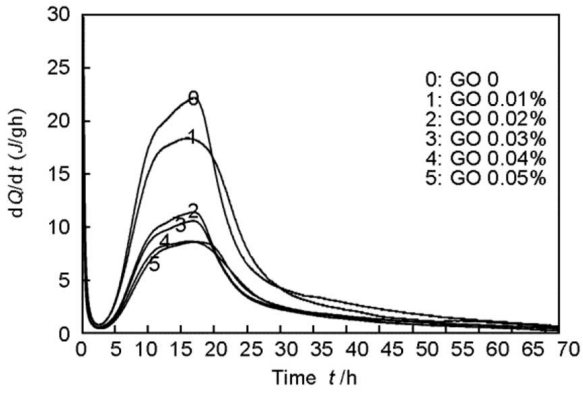

Figure 15. Cement hydration exothermic rate. (Wang et al., 2015)

Figure 16 illustrates the corresponding effect of GO on cement hydration heat (J/g) reported by Wang et al. (2015).

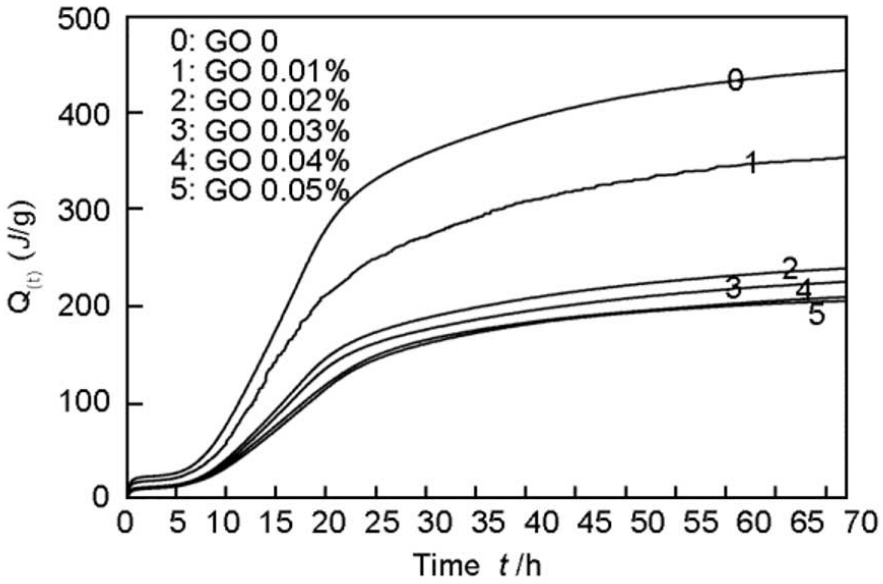

Figure 16. The effect of GO on the Cement Hydration Heat reported by Wang et al. (2015)

2.9 The Microstructure

Xiangyu Li et al. (2016) observed GO aggregation located in the cement paste, as illustrated in Figure 17. The corresponding energy dispersive X-ray spectrum (EDS) is presented in Figure 18, and verifies the aggregation of GO by quantifying a high content of carbon.

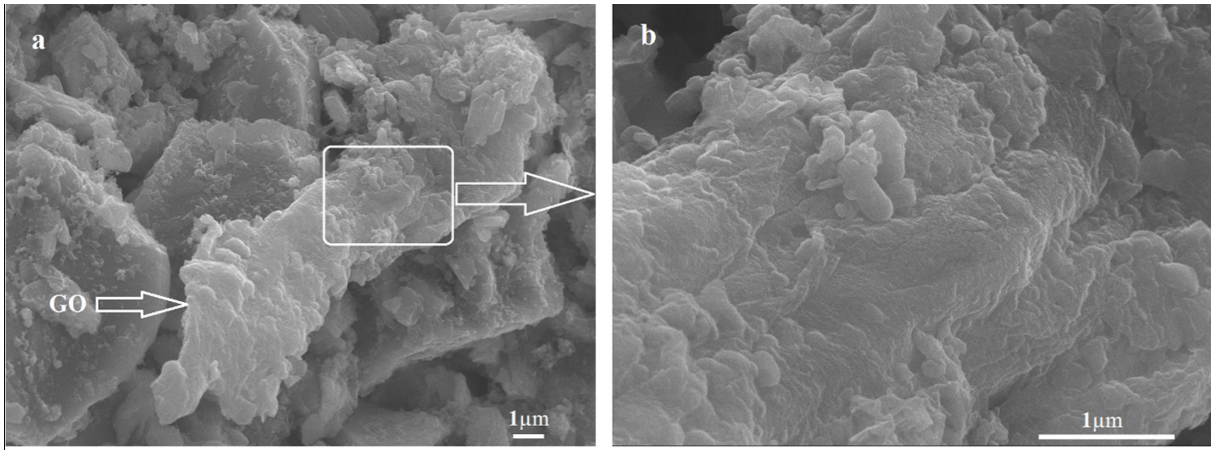

Figure 17. GO aggregates in cement paste observed with SEM.(Xiangyu Li et al., 2016)

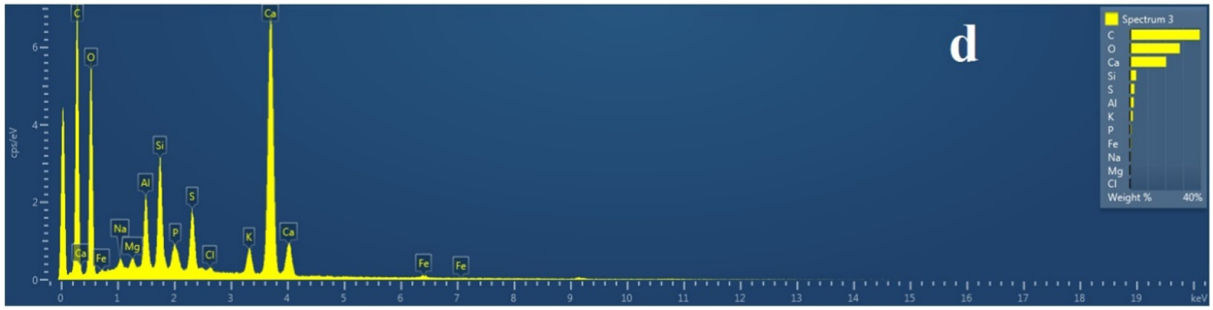

Figure 18. EDS analysis. (Xiangyu Li et al., 2016)

This page intentionally left blank.

3 Experimental Program

This chapter is organized into sections that follow the logical order of performing the experimental program: The experimental work plan is presented in Section 3.1. Section 3.2 presents the materials. Preparation of the cement mortar specimens is described in Section 3.3. The different types of experiments followed by the test setup are presented and illustrated in Section 3.4.

The objective of the experimental program is to investigate the effect of graphene oxide on cement mortar. Several different experiments are performed with the purpose of increasing the understanding of how graphene oxide influences both fresh mortar, mechanical properties, and the microstructure. An overview of chapter three is presented in Figure 19.

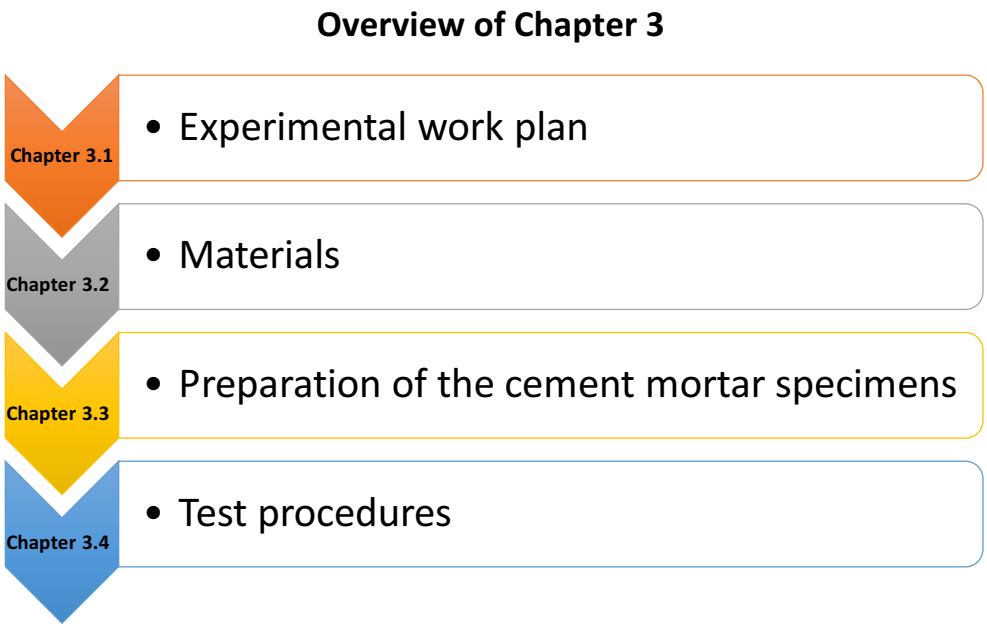

Figure 19. Overview of Chapter 3 (Kjaernsmo, 2017)

3.1 Experimental work plan

The experimental work plan is illustrated by Figure 20. The program is performed with cement mortar containing the following dosages of GO: 0 wt% (reference), 0.03 wt%, 0.05 wt%, 0.2 wt% of cement weight (Table 1). The mechanical properties are tested with three specimens for each cement mortar composition (Table 2).

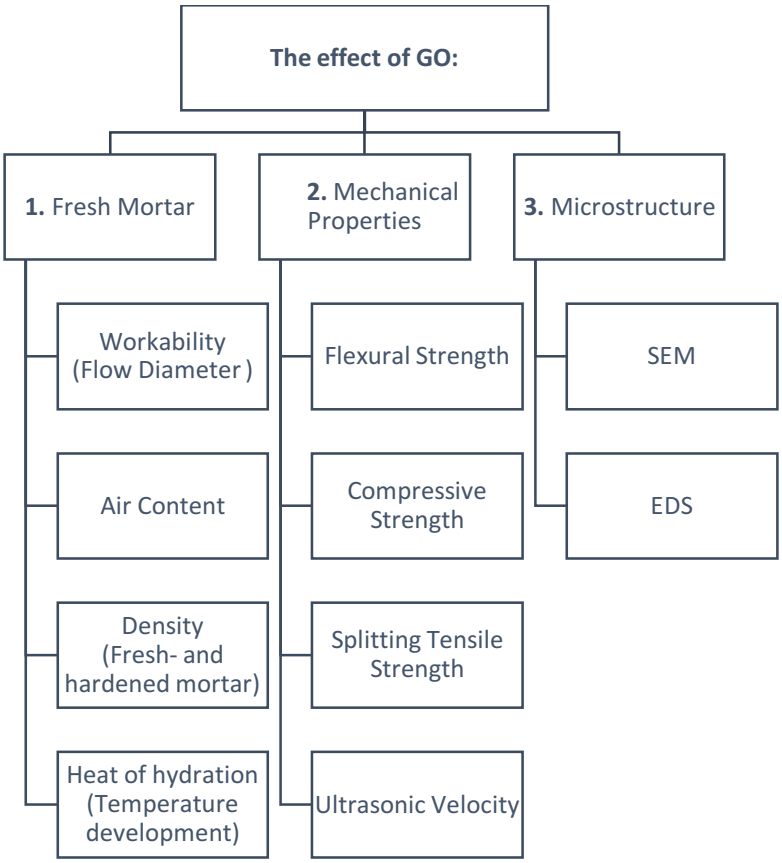

Figure 20. Experimental work plan (Kjaernsmo, 2017)

3.1.1 Overview of the various contents of GO

Table 1 highlights an overview of the various contents of GO introduced to the mortar composition.

Table 1. Overview of the various amounts of GO introduced to the mortar composition.

Type	**Content of GO [wt% of the cement weight]**
Reference	0
Graphenea (Water dispersed)	0.03
	0.05
	0.2
Graphitene (Fine powder)	0.03
	0.05
	0.2

3.1.2 Overview of the number of specimens

An overview of the number of specimens prepared for each mechanical test and per mortar composition is presented in Table 2.

Table 2. Overview of the number of specimens prepared for each mechanical test per mortar composition.

Type of Mechanical Test	**Number of Specimens**
Flexural Strength	3 prisms
Compressive Strength	(6 prism ends)
Splitting Tensile Strength	3 cylinders
Ultrasonic Velocity	3 cylinders

3.1.3 NS-EN 196-1:2016 – Methods of Testing Cement

The primary framework behind the experimental program is *NS-EN 196-1:2016 – Methods of testing cement "Part 1: Determination of Strength".* The standard is only used as a framework in order to reduce the number of variables, and therefore, some modifications are found to be more appropriate. These modifications are clarified when the selected method, procedure or test setup deviate from the standard.

3.2 Materials used for the Experiments

3.2.1 Standard Cement

Standard cement is provided by Norcem, Brevik, and satisfies the requirements for Portland Cement EN 197-1-CEM I 42.5R. Chemical and physical data are listed in Table 3.

Figure 21. Standard Cement, Norcem- Brevik (Kjaernsmo, 2017)

Table 3. Norcem Standard Cement- Chemical and Physical Data. (Norcem, 2017)

Norcem Standard Cement	
Chemical Data	
Fineness (Blaine)	370 m^2/kg
Tricalciumaluminate C_3A	7 %
Alkali (Equiv. Na_2O, NB21)	1.3 %
Mineral additives	4 %
Loss on ignition	2.5 %
Insoluble residue	1 %
Sulfate content (as SO_3)	3-4%
Chloride content	< 0.085 %
Water-soluble Cr^{6+}	< 2 ppm
Specific weight	3.15 kg/dm^3
Physical Data	
Compressive strength – 1 day	21 MPa
Compressive Strength – 2 days	32 MPA
Compressive Strength – 7 days	42 MPa
Compressive Strength – 28 days	52 MPa
Initial setting time	130 min
Soundness (expansion)	1 mm

3.2.2 CEN Reference Sand

CEN Reference Sand is selected according to NS-EN 196-1:2016, Methods of Testing Cement. The CEN Reference Sand is provided by Norcem, and initially produced by Normensand in Beckum, Germany.

Figure 22. CEN Reference Sand- Pre-weighted, 1350g (Kjaernsmo, 2017)

<u>According to NS-EN 196-1:2016:</u>

CEN Reference Sand is a natural, siliceous sand with rounded particle shape and with a silica content of at least 98 %. The moisture content shall be less than 0.2 %.

The speedy moisture test showed a moisture content of 0 % which satisfies the requirement. A detailed overview of the speedy moisture test procedure is shown in Appendix B.

Table 4. CEN Reference Sand, Particle Size Distribution. (NS-EN 196-1:2016)

Particle size distribution of CEN Reference Sand according to *NS-EN 196-1:2016*

Square mesh size [mm]	2.00	1.60	1.00	0.50	0.16	0.08
Cumulative sieve residue [%]	0	7 ± 5	33 ± 5	67 ± 5	87 ± 5	99 ± 1

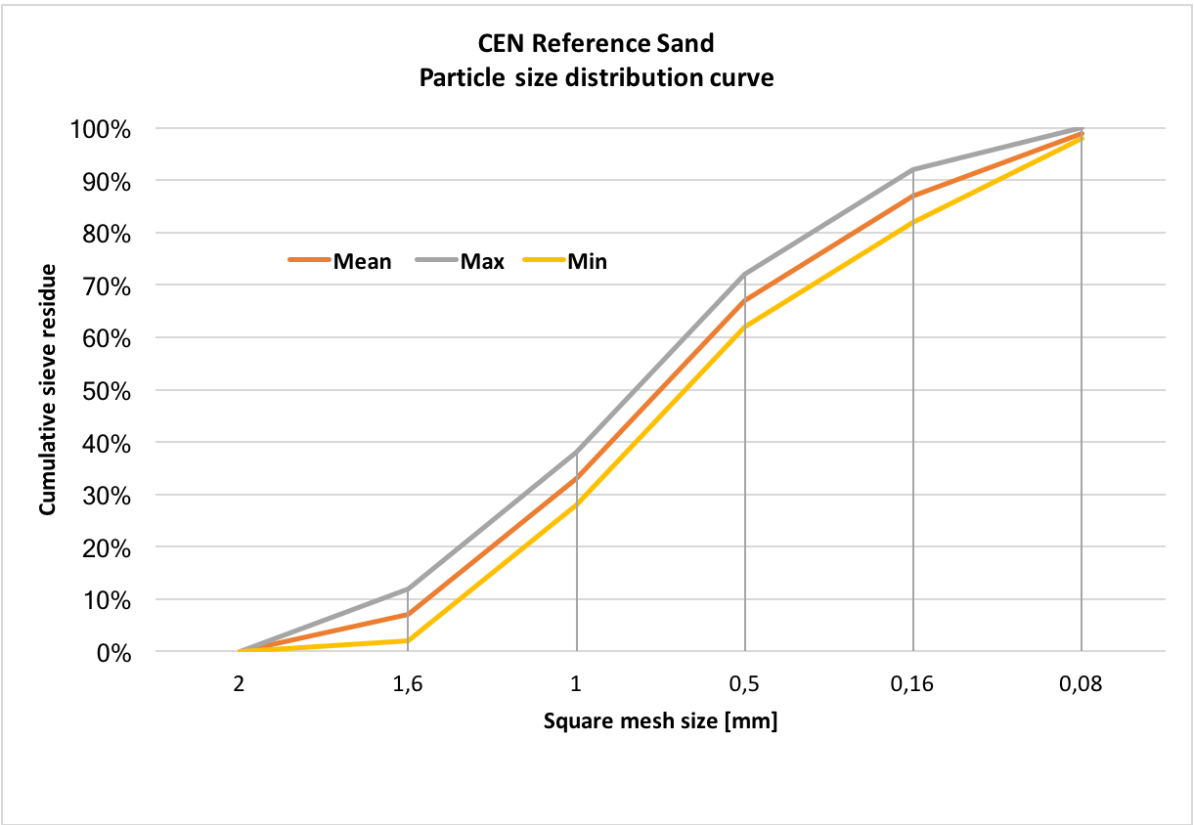

Figure 23. CEN Reference Sand, Particle Size Distribution Curve (Redrawn with data from NS-EN 196-1:2016

3.2.3 Graphene Oxide (GO)

3.2.3.1 Graphitene – Fine powder Concentrate GO

Fine powder concentrate graphene oxide is provided by Graphitene Ltd., UK. The concentration of graphene oxide is 20 % of the fine powder. The components and the percent concentrations are listed in Table 5. Characteristic properties of Eco Graphene Oxide produced by Graphitene Ltd. are presented in Table 6.

Table 5. Graphitene Fine Powder Components. (GraphiteneLdt, 2017a)

Graphitene Graphene Admixture for Cement – Fine Powder

Component	Concentration
Eco Graphene Oxide	20 %
Carbon Black	1 %
Sand	79 %

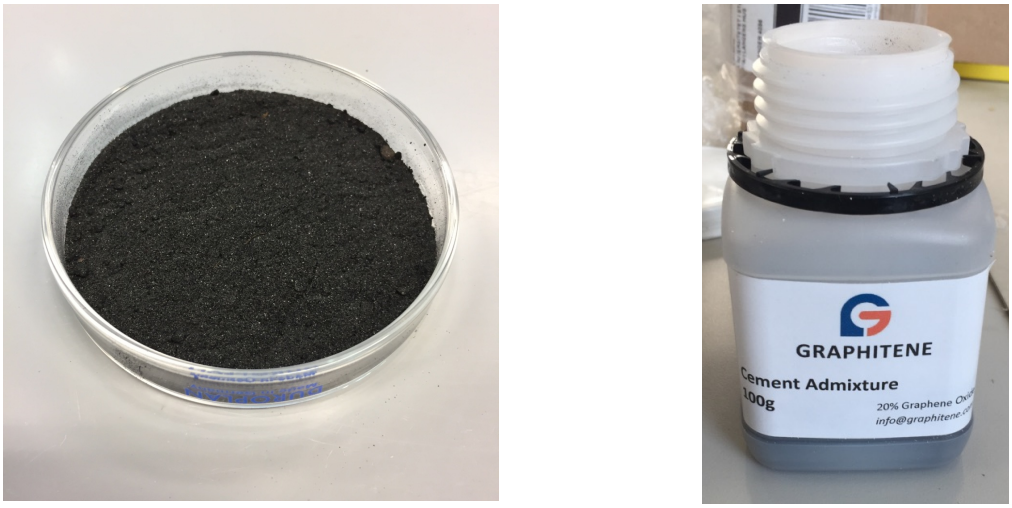

Figure 24. Graphitene fine powder concentrate, 100 g, 20% Graphene Oxide. (Kjaernsmo, 2017)

Table 6. Eco Graphene Oxide Properties.(GraphiteneLdt, 2017b)

Eco Graphene Oxide Properties

Characteristics	Value	Unit
Color	Yellow – Brown	
Form	Powder / Suspension	
Solubility	Dispersible in polar solvents	
Carbon content	75-85	at%
Oxygen content	15-25	at%
Sulfur content	< 1	at%
Nitrogen content	< 0.1	at%
Flake thickness	1-5	layer
Flake size	0.5-5	µm

3.2.3.2 Graphenea – Water Dispersed GO

Water dispersed graphene oxide is provided by Graphenea, Spain. The concentration of graphene oxide is 0.4 mg/mL. The characteristic properties are listed in Table 7, and an element analysis of the graphene oxide in dry condition is presented in Table 8.

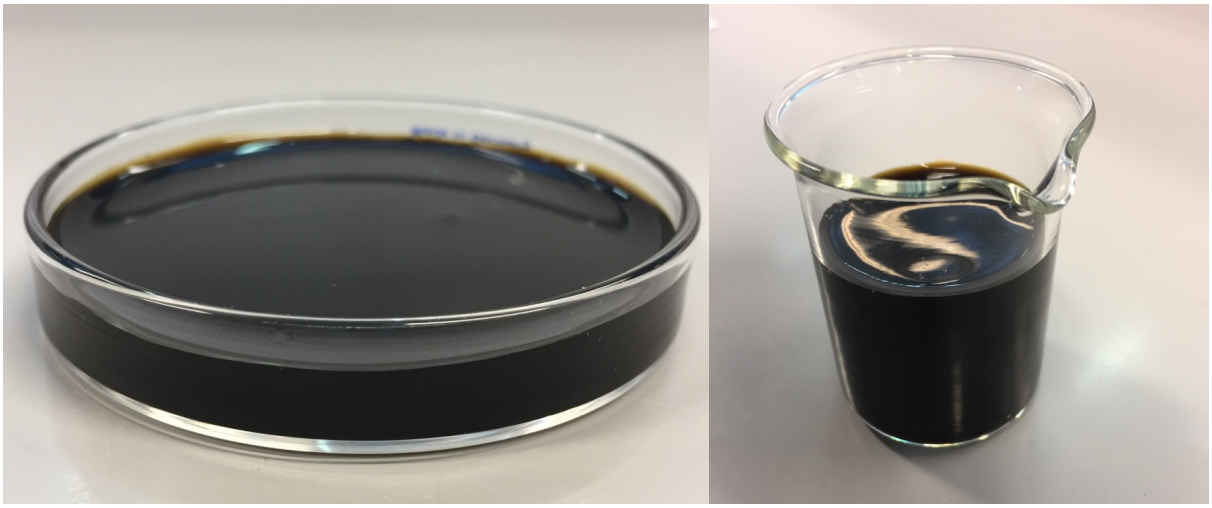

Figure 25. Water dispersed graphene oxide provided by Graphenea (Kjaernsmo, 2017)

Figure 26. Graphena, 5000 ml, Graphene Oxide 4 mg/mL (Kjaernsmo, 2017)

Table 7. Product Datasheet – Graphenea Graphene Oxide (GO) Properties. (Graphenea, 2017)

Graphenea - Properties

Form	Dispersion of graphene oxide sheets
Particle Size	D90 29.05 – 32.9 µm
	D50 14.30 – 16.6 µm
	D10 5.9 – 6.63 µm
Color	Yellow-Brown
Odor	Odorless
Dispersibility	Polar Solvents
Solvents	Water
Concentration	4 mg/mL
pH	2.2 – 2.5
Monolayer Content (measured in 0,5 mg/mL)	>95 %*

(*) 4mg/ml concentration tends to agglomerate the GO flakes and dilution followed by slight sonication is required in order to obtain a higher percentage of monolayer flakes

Table 8. Product Datasheet – Graphenea Graphene Oxide (GO) Element Analysis. (Graphenea, 2017)

Element Analysis*

Carbon	49-56%
Hydrogen	0-1%
Nitrogen	0-1%
Sulfur	2-4%
Oxygen	41-50%

* Sample preparation: 2g of 4 wt% GO in water were dried under vacuum at 60°C overnight.

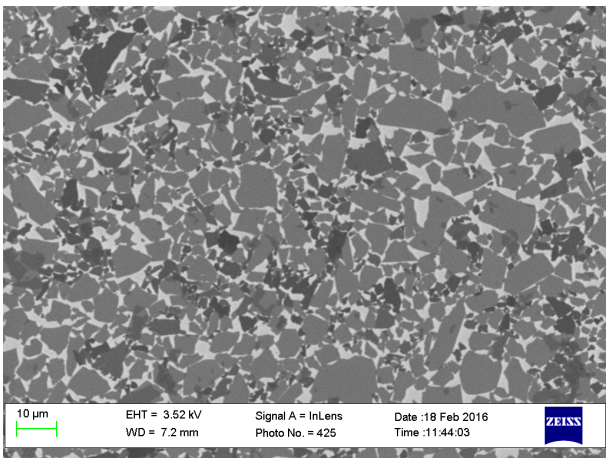

Figure 27. SEM image of Graphenea (Graphenea, 2017)

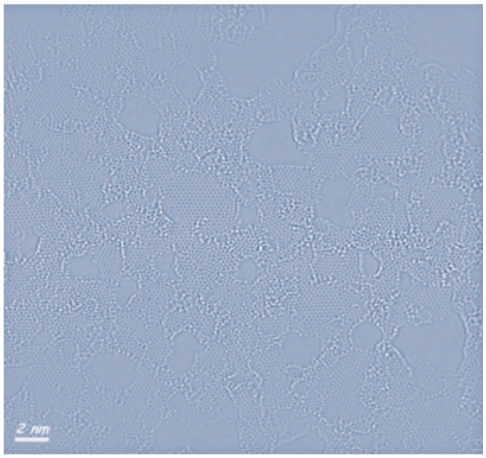

Figure 28. TEM image of Graphenea(Graphenea, 2017)

3.2.4 Quartz Sand

One cement mortar batch is prepared with fine powder quartz sand - W12 instead of graphene oxide (GO). The content of quartz sand is 2.0 wt% of the cement weight which is equivalent to the highest selected content of GO. The objective of replacing GO with quartz sand is to investigate how a “no- or less-reactive” material influences the workability and the flexural- and compressive strength after 28 days of curing. Quartz sand - W12 (white powder) is illustrated in Figure 29.

The quartz sand - W12 has an average grain size of 16 µm ($d_{50\%}$), and an upper grain size of 50 µm ($d_{95\%}$). The average grain size is approximately within the same dimensional range as the particle size for the graphene oxide produced by Graphenea, but the upper grain size is substantially larger. The results must therefore only be interpreted as indications. The quartz sand - W12 is produced by Quarzwerke GmbH. A detailed product data sheet is presented in Appendix E.

Figure 29. Fine Powder Quartz Sand (Kjaernsmo, 2017)

3.2.5 Superplasticizer (Polycarboxylate)

MasterGlenium ACE 434 is a superplasticizer (SP) admixture based on polymers of polycarboxylate with long chains. The polymers have a dispersing effect because of both electrostatic repulsion and steric hindrance effect. The recommended dosage is 0.2 – 1.4 % of cement content. (MasterBuildersSolution, 2013).

Table 9. Technical Data MasterGlenium ACE 434. (MasterBuildersSolution, 2013)

Technical Data	
Consistency	Viscous liquid
Color	Yellowish
Solids	26.8 ± 1.5 %
Density	1.07 ± 0.02 kg/L
pH – value	5,0 ± 1,5
Equivalent Na_2O	< 1.0%
Chloride Content	< 0.01 %

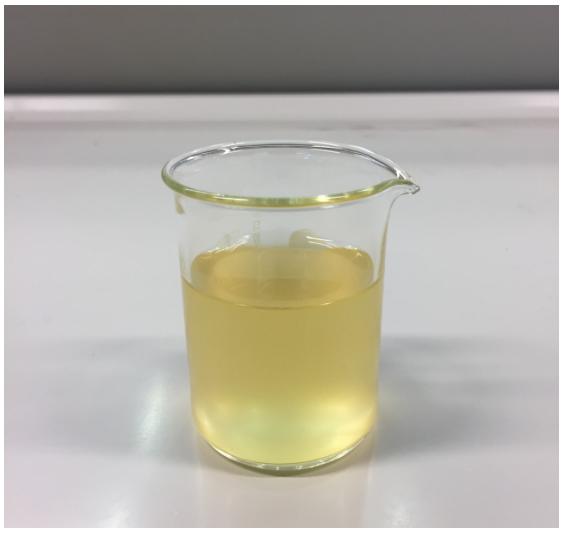

Figure 30. MasterGlenium ACE 434, Superplasticizer (Kjaernsmo, 2017)

3.2.6 Mixing Water

The quality of regular tap water is considered as acceptable. The mixing water is tapped 24 hours prior to mixing, and the water container is stored in a water bath at a constant temperature of 20 °C.

3.3 Preparation of cement mortar specimens

3.3.1 Mix Design

The mix design is adapted to the procedure described in *NS-EN 196-1:2016 – Methods of testing cement* and modified by adding superplasticizer (polycarboxylate) and various content of graphene oxide (GO). The mix design is listed in Table 10.

The previous research (Wang et al., 2015) reported enhanced mechanical properties with the dosages of 0.03 wt% and 0.05 wt% GO of the cement weight. This is presented in Section 2.6. The selection of 2.00 wt% GO is based on the research methodology of study the extreme with the purpose of observing a large variation in the mortar properties.

Table 10. The Mix Design with various dosages of GO (Kjaernsmo, 2017)

Materials	Quantity [g]
Standard Cement	450 ± 2
CEN Reference Sand	1350 ± 5
Water	225 ± 1
Superplasticizer (SP) MasterGlenium ACE 434	0.8 wt.% of the cement weight
Graphene Oxide (GO) Graphenea & Graphitene	[0.00, 0.03, 0.05%, 0,2%] wt.% of the cement weight

- Water/cement ratio = 0.5
- The cement, sand, and water have a temperature of 20±2 °C.
- All the materials are stored in a controlled laboratory environment (temperature of 20±2 °C). The cement is kept in an airtight container, and the CEN Reference Sand is preserved in pre-weighted plastic bags (1350±5 g).
- The weight of the fine powder graphene oxide and the superplasticizer are measured with 0.001 g precision.

3.3.2 Molds

3.3.2.1 Prisms (mini-beams) – Flexural- and compressive strength test

The molds are coated with form oil prior to casting (Figure 31).

Dimensions: Length: 160 mm Height: 40 mm Width: 40 mm

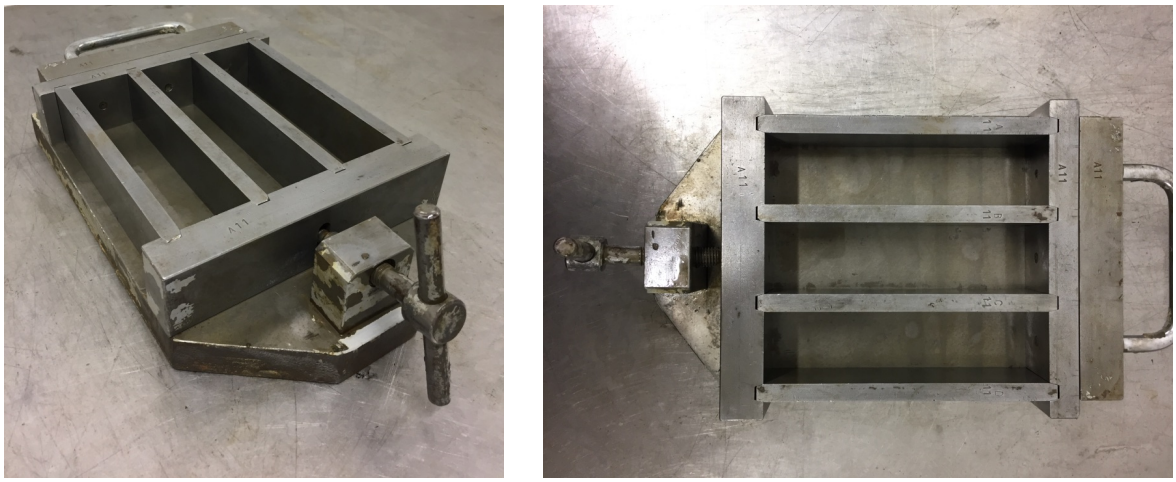

Figure 31. Prismatic specimen mold, 160 mm x 40 mm x 40 mm. (Kjaernsmo, 2017)

3.3.2.2 Cylinders - Splitting tensile strength- and Ultrasonic test

The plastic molds (Figure 32) were not coated with form oil prior to casting because of the glossy plastic surface and the demolding technique which is described in Section 3.3.5.2.

Dimensions: Height: 65 mm Diameter: 33 mm

The length of the cylindrical plastic mold is two times the diameter which satisfies the dimensional requirement for the splitting tensile test according to NS-EN 12390-1.

Figure 32. Cylinder mold H: 65 mm & D: 33 mm (Kjaernsmo, 2017)

3.3.3 Mixing of Mortar

3.3.3.1 Hobart Mixer

The mixing procedure is adapted to a mixing regime developed by X. Li et al. (2016) because of their positive results with the same type of graphene oxide produced by Graphenea. The regular mixing procedure which can be found in *NS-EN 196-1:2016* is modified by first mixing water with GO and sand, rather than water with GO and cement. The intentions with this modification is both to mechanically separate the GO nanosheeds by utilizing the sand particles, and to improve the interfacial transition zone (ITZ) by covering the sand particles with GO (X. Li et al., 2016). ITZ is the space between the sand particle and the bulk cement paste, and is generally the weakest link in the cement mortar (Metha & Monteiro, 2006). An overview of the modified mixing procedure is presented in Table 11.

Type of mixer: Hobart N-50

Table 11. The Modified Mixing Procedure developed by X. Li et al. (2016)

Overview of the Modified Mixing Procedure

Step	Total Time	Procedure
1	0 sec	Place water and water dispersed graphene oxide (GO)* into the bowl
2	60 Seconds	Mix water and GO for 60 seconds at medium (2) speed
3	1 min 30 sec	Add sand for 30 seconds Continuously mixing at low speed (1)
3	2 min	Add cement over for 30 seconds Continuously mixing at low speed (1)
4	2 min 30 sec	Stop mixer, add Superplasticizer (SP) Continue mixing at medium speed (2) for 30 seconds
5	4 min	Stop mixing for 90 seconds, scrape the side of the bowl during the first 30 seconds
6	5 min	Mix for 60 seconds at medium speed
*Graphitene GO powder was first dispersed in water in a shear mixer. See section 9.5.2.		

Table 12. Speeds of Mixer Blade according to NS-EN 196-1:2016

Speeds of Mixer Blade

	Rotation [min^{-1}]	Planetary movement [min^{-1}]
Low Speed **= Hobart N-50 Low (1) 136 RPM**	140 ± 5	62 ± 5
High Speed **= Hobart N-50 Intermediate (2) 281 RPM**	285 ± 10	125 ± 10

Figure 33. Hobart N-50 Mixer (Kjaernsmo, 2017)

Figure 34. Flat Beater (Kjaernsmo, 2017)

3.3.3.2 High-Speed Shear Mixer - Hamilton Beach

The fine powder graphene oxide powder from Graphitene Ltd. is first dispersed in water with a high-speed shear mixer for two minutes (Figure 35). Immediately afterwards, the water dispersed graphene oxide (Graphitene) is placed in the Hobart mixer bowl, and the mixing process continues with the modified mixing procedure described in Table 11. The intention with the high-shear mixing is to prevent potential flocculation of graphene oxide powder in the cement mortar.

Type of mixer: High-speed shear mixer - Hamilton Beach

Selected Speed: 17 000 RPM, High (3)

Figure 35. High-Speed Shear Mixer - Hamilton Beach (Kjaernsmo, 2017)

3.3.4 Molding and Compaction procedure using vibrating table

A jolting compaction equipment should be used according to *NS-EN 196:2016*, but this type of equipment is not available in the laboratory. The compaction can also be performed with a vibrating table according to *NS-EN196-1:2016, Annex A - Alternative vibration compaction equipment and procedure validated as equivalent to the reference jolting compaction equipment and procedure.* The procedure has a compaction duration of 120 seconds, and the molds compartments are filled within the first 45 seconds. Since the cement mortar in this experimental program contains superplasticizer, the total compaction duration is reduced to 60 seconds with the purpose of decrease the probability of segregation. The modified compaction procedure is presented in section 3.3.4.1.

3.3.4.1 The modified compaction procedure based on NS-EN196-1:2016

The vibration table with empty molds is first controlled to be in horizontal level. Then, two equal layers are vibrated for 30 seconds each. The vibrating table is switched off when the cement mortar is placed into the molds. The cement mortar is evenly placed from one end into the mold compartments over a period of 30 seconds.

Type of compaction equipment	Vibrating table

Figure 36. The vibrating table (Kjaernsmo, 2017)

3.3.5 Curing conditions

3.3.5.1 Curing conditions before demolding – Climatic chamber

Impermeable plastic wrap is placed over the mold compartments after casting. The molds are stored in a climatic chamber for 24 hours at a temperature of 20 °C and 90 percent relative humidity (%RH) according to NS-EN 196-1:2016.

Type of Climatic Chamber:	Clima Temperatur Systeme (CTS) C-40/600
Temperature Range:	-40 °C to 180 °C
Humidity Range:	10 %RH to 98 %RH

Figure 37. Climatic Chamber (Kjaernsmo, 2017)

3.3.5.2 Demolding

The specimens are demolded after 24 hours of curing in the climatic chamber.
The prism specimens are demolded as usual. While, the cylinders are demolded by first making a small cut the plastic mold with a utility knife, and then twisted out of the plastic compartments.

3.3.5.3 Curing conditions after demolding – Curing in water

The prisms are cured in a water bath at the constant temperature of 20 °C for three, seven and 28 days. The water bath system with integrated cooling and heating elements is illustrated in Figure 38 and Figure 39.

Water bath system: Lauda E100 Temperature Control Unit/Circulator & RE-120 Chiller

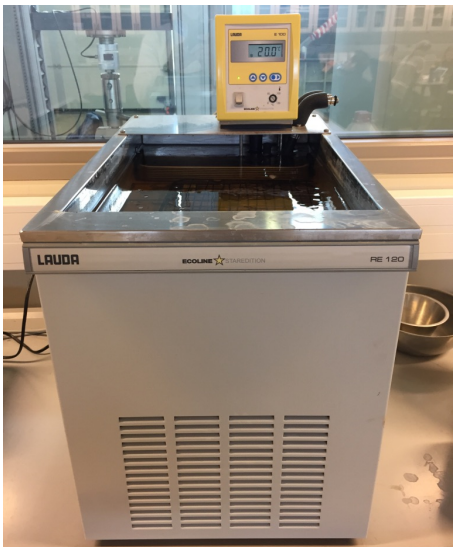

Figure 38. Lauda water bath system (Kjaernsmo, 2017)

Figure 39. Lauda Temperature Control Unit & Circulator (Kjaernsmo, 2017)

The cylinders are cured in a water bath system with only heating elements. This is illustrated in Figure 40. The temperature is set to 20 °C, and room temperature varies in the range of 20±2 °C. Also, the cylinders are cured in water for three, seven and 28 days.

Water bath system: VWR Unstirred Water Bath 12L

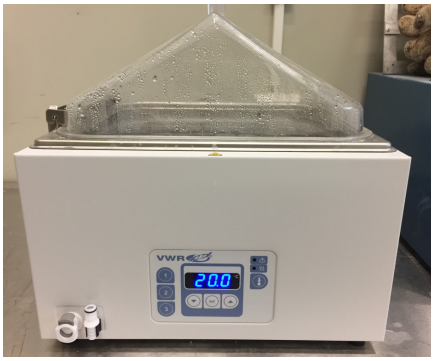

Figure 40. VWR Unstirred Water Bath 12 L (Kjaernsmo, 2017)

3.3.6 Additional preparations of the cylinders

The non-destructive ultrasonic velocity test requires a straight cylinder edge which is perpendicular to the length. Unevenness or roughness on the cylinder edge surface can influence the sonic measurement because of poor contact between the transmitter- or the receiver probe. As illustrated in Figure 42, the edge of the cylinder is cut by only 3 mm because of the dimensional requirement of the splitting tensile test (Length = 2 x Diameter).

Figure 41. Concrete Saw (Kjaernsmo, 2017)

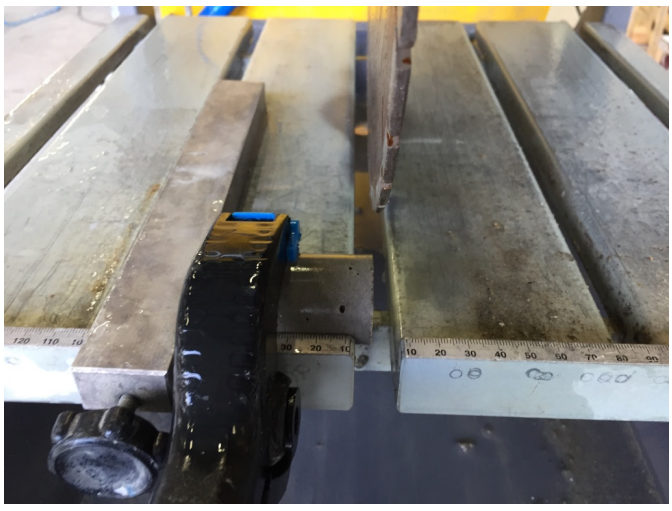

Figure 42. The cylinder was attached to the concrete saw by a clamp (Kjaernsmo, 2017)

3.4 Test Procedures

3.4.1 Density of Fresh Mortar

The density of fresh mortar is determined according to *NS-EN 1015-7: Determination of air content of fresh mortar*, and calculated by the following equation:

$$\text{Density} = \frac{m_2 - m_1}{V} = [kg/m^3]$$

where

V – Volume of the test pot [m^3]

m_1 – Mass of the empty test pot [kg]

m_2 – Mass of the test pot with the fresh mortar [kg]

3.4.2 Determination of air content of fresh mortar

The air content of the fresh mortar is determined with a mortar air entrainment meter according to *NS-EN 1015-7: Determination of air content of fresh mortar*. The mortar air entrainment meter and the manometer are illustrated in Figure 43 and Figure 44, respectively.

Type of Air Entrainment Meter: Form+Test Mortar Air Entrainment Meter 1 Liter

Figure 43. Mortar Air Entrainment Meter 1 Liter (Kjaernsmo, 2017)

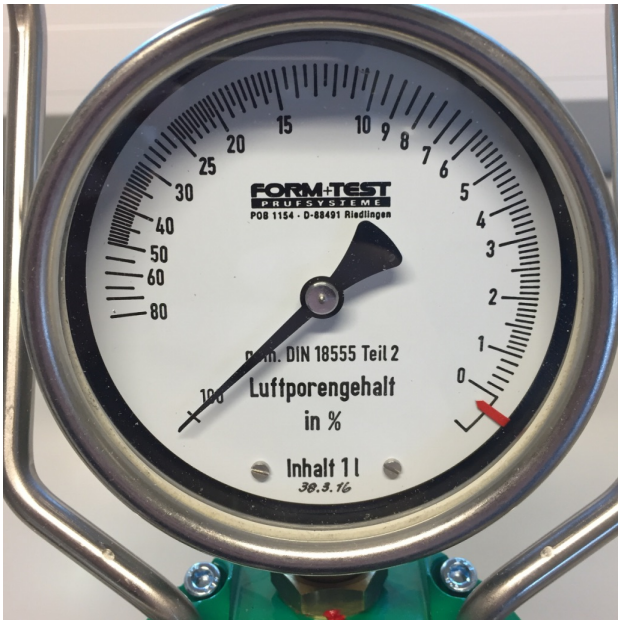

Figure 44. Air Entrainment Manometer (Kjaernsmo, 2017)

3.4.3 Temperature - and Heat Development

The fresh mortar is placed in insulated polystyrene boxes with the dimension of 100 mm x 10 mm x 100 mm. The thickness of the polystyrene walls and the lid is 20 mm. Two thermocouples are then arranged in the center of each box in case of one of them fails. The temperature is measured by the data acquisition system illustrated in Figure 45, and the measurements last until the cement mortar reaches the room temperature. The cumulative isothermal heat development is estimated with a curing box spreadsheet developed by Sverre Smedplass, Skanska. A detailed overview of the input parameters is presented in Appendix C.

Data Acquisition System: Hewlett Packard 34970A

Logging interval: 10 minutes

Type of thermocouples: J

Figure 45. HP349670 A data acquisition unit (Kjaernsmo, 2017)

Figure 46. Test setup (Kjaernsmo, 2017)

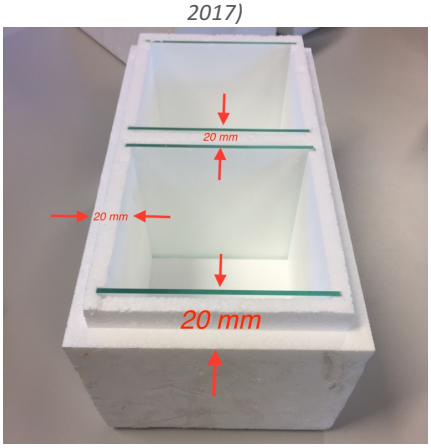

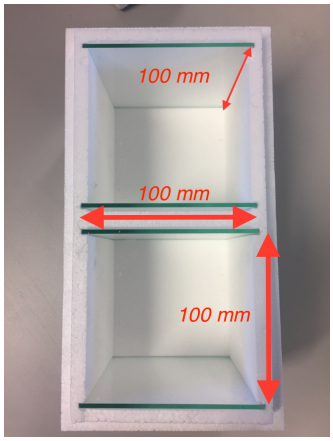

Figure 47. Insulated Polystyrene box, 100 mm x 100 mm x 100 mm (Kjaernsmo, 2017)

3.4.4 Mini-Flow Test

The mini-flow test procedure is described in detail since the selected method is not according to the conventional procedure.

The Heidelberg measurement board is first controlled to be in horizontal level. Figure 49 and Figure 50 illustrate the mini-flow test equipment. Immediately after the mixing process, the fresh mortar is evenly poured into the cone, and then the cone is lifted slowly over a five seconds period. After two minutes, when the mortar has come to rest, the average flow diameter is determined by taking two measurements (D_1 & D_2) perpendicular to each other.

$$\text{Flow Diameter [cm]} = \frac{D_1 + D_2}{2}$$

The flow diameter results, presented in Section 4.1.1, is the average of two individual batches for a mortar composition.

Dimensions of the Mini-flow cone

Top diameter (T.D.):	70 mm
Bottom diameter (B.D.):	100 mm
Height (H):	60 mm
Volume:	0,344 Liter

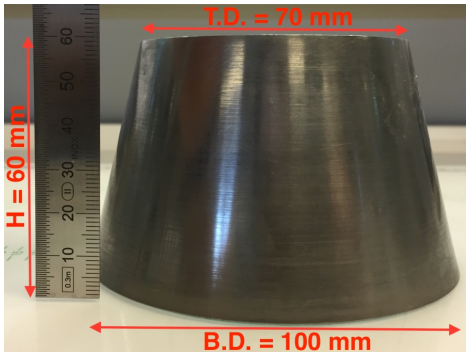

Figure 48. Mini-flow cone(Kjaernsmo, 2017)

3.4.4.1 Additional procedure of determining the workability

Slump measurements are more appropriate if the cement mortar has a stiff consistency. The slump can be determined by the following procedure:

Three layers of mortar are evenly placed into the cone and compacted 15 times each with a stamper. The cone is then lifted slowly over a five seconds period, and the slump is measured immediately afterwards.

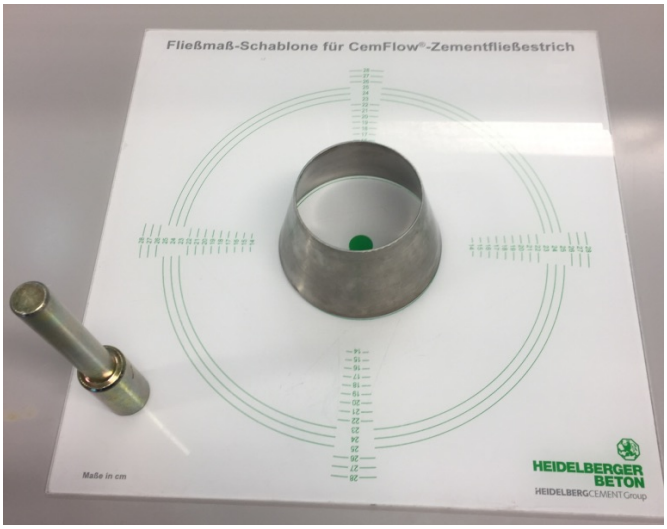

Figure 49. Heidelberg Mini-Flow Equipment (Kjaernsmo, 2017)

Figure 50. Heidelberg Mini-Flow Measuring Board & Cone (Kjaernsmo, 2017)

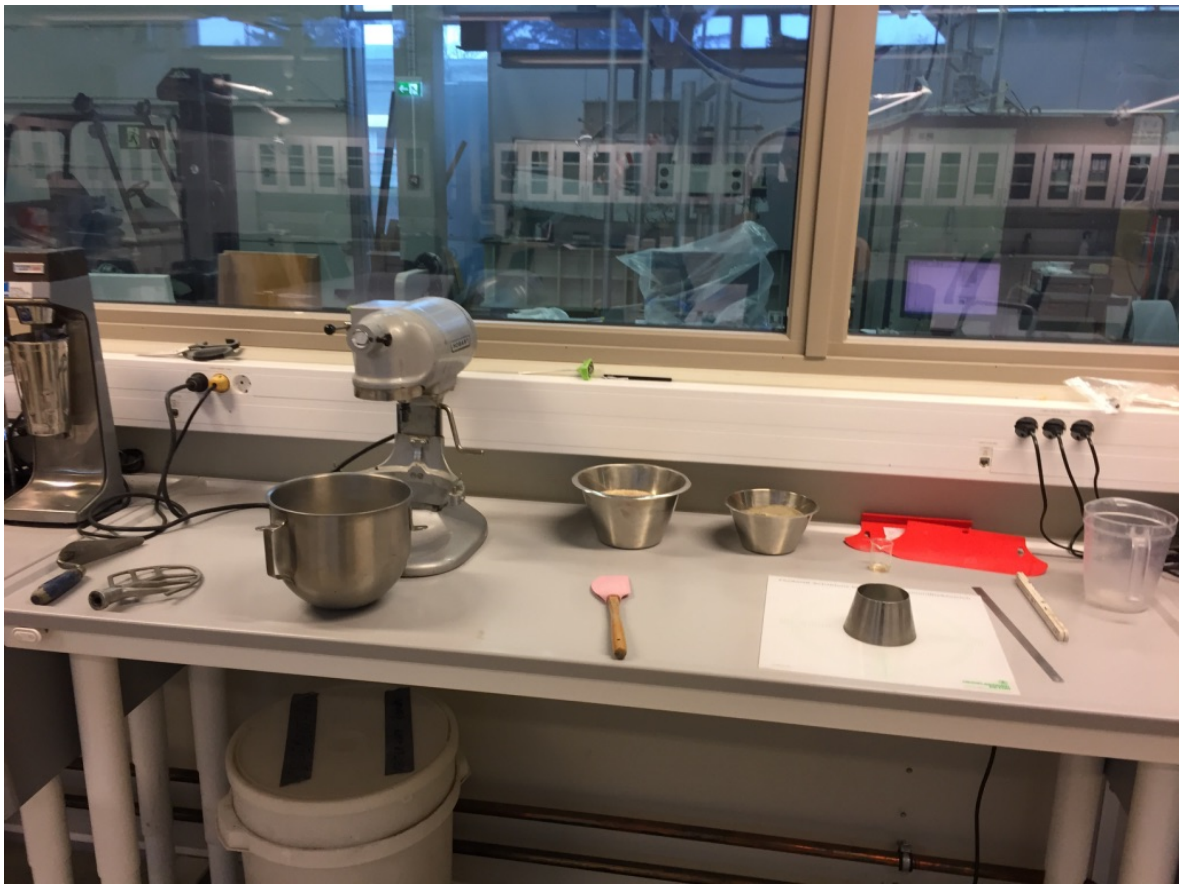

Figure 51. Mini-Flow Test - Overview of the test setup (Kjaernsmo, 2017)

3.4.5 Density of hardened mortar

The density of the hardened mortar is determined by the Archimedes´ principle according to *NS-EN 12390-7 – Part 7: Density of hardened concrete.* The specimens are tested in water saturated condition, and with an alternative setup. Because of the size of the prism specimen, a customized hook is used to hang the specimen in the water bucket. The conventional hook is not appropriate because it fits traditional cubes with the dimensions of 10 cm x 10 cm x 10 cm. The weight is determined with 0.1 g precision.
The alternative test setup is illustrated in Figure 52.

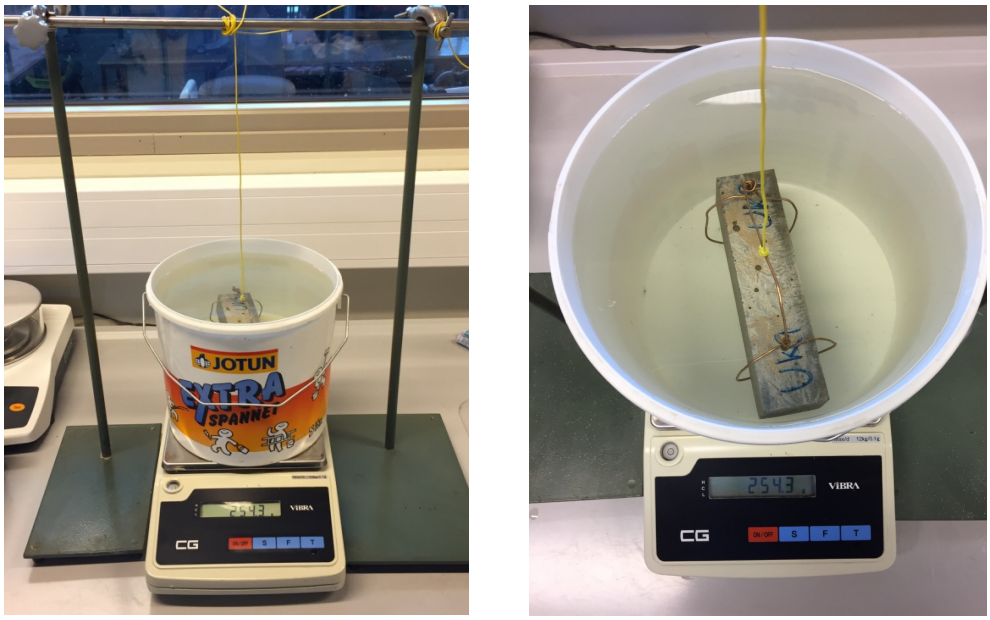

Figure 52. Test setup - Density of hardened mortar(Kjaearnsmo, 2017)

3.4.6 Ultrasonic Velocity Test

The ultrasonic velocity test is a non-destructive method, which determines a special type of modulus of elasticity, and should not be confused with the more conventional E-modulus or Young´s Modulus (the ratio of stress to strain). The modulus of elasticity (M) determined by the ultrasonic velocity test is a combination of the bulk modulus (K) and 4/3 shear modulus (G), as expressed in equation (1) (Sheriff & Geldart, 1995). The sonic velocity meter, illustrated in Figure 53, measures the travel time for the sonic signal through the material. The sonic travel time (t) is measured by using a transmitter - and receiver probe which are in contact with the cylinder. It is also necessary to determine density (ρ) of the cylinder in order to calculate the modulus of elasticity.

$$M=\left(K+\frac{4}{3}G\right)=V_p^2\cdot(\rho) \qquad (1)$$

$$\rho=\text{density}=\frac{\text{mass}}{\text{volume}} \qquad (3)$$

$$V_p=\text{Sonic Velocity}=\frac{L}{\Delta t}=\frac{10^{-6}\cdot\frac{L}{1000}}{\Delta t} \qquad (4)$$

Where K is the bulk modulus and G the is shear modulus. M is the modulus of elasticity in a combination of the bulk modulus, K, and 4/3 shear modulus, G.

3.4.6.1 Procedure – Ultrasonic Velocity Test

The sonic velocity meter is first calibrated by using the calibration cylinder with a sonic travel time of 25.2 µs. The calibration cylinder is illustrated in Figure 54. After the calibrating the system, place the mortar cylinder and the plastic centering ring inside the plastic pipe as shown in Figure 53. By switching on the air pressure, the receiver probe will be pushed against the mortar cylinder and creates contact between the two probes and the cylinder. Start the sonic velocity meter, and read off the sonic travel time in µs (10^{-6} x seconds).

Sonic Velocity meter: CNS Farnell Pundit 7

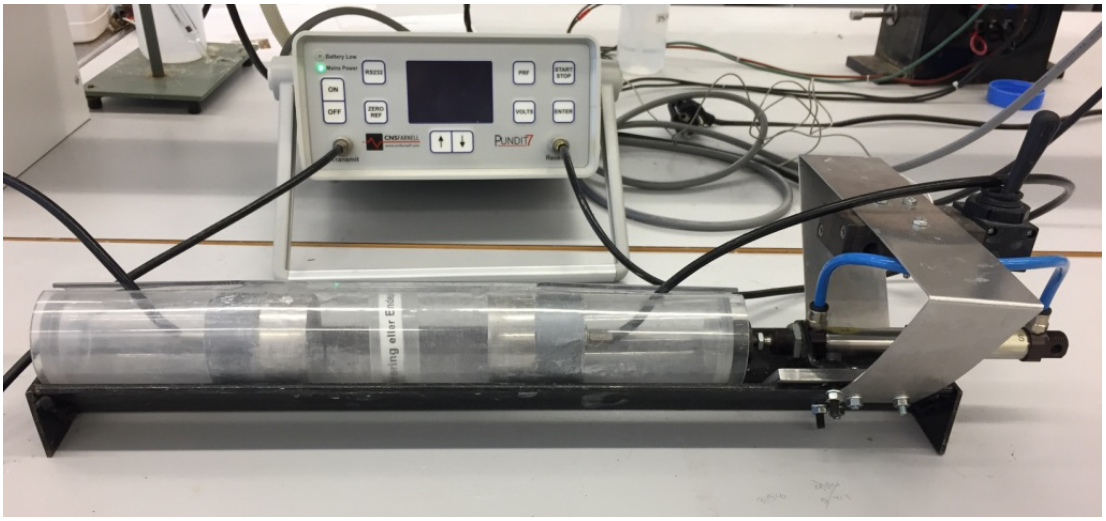

Figure 53. Ultrasonic Pulse Velocity System (Kjaernsmo, 2017)

Figure 54. Calibration Cylinder (Kjaernsmo, 2017)

3.4.6.2 Calculation of Modulus of Elasticity

The modulus of elasticity is calculated by the following equations (Sheriff & Geldart, 1995):

$$M = \left(K + \frac{4}{3}G\right) = V_p^2 \cdot (\rho) \qquad (1)$$

$$\text{Volume} = \pi \cdot r^2 \cdot L \qquad (2)$$

$$\rho = \text{density} = \frac{\text{mass}}{\text{volume}} \qquad (3)$$

$$V_p = \text{Sonic Velocity} = \frac{L}{\Delta t} = \frac{10^{-6} \cdot \frac{L}{1000}}{\Delta t} \qquad (4)$$

where

M – Modulus of elasticity [GPa]

K – Bulk modulus [GPa]

G – Shear modulus [GPa]

V_p – Sonic Velocity [m/s]

3.4.7 Three-Point Bending Test Setup

The prism specimen (mini-beam) is arranged in the testing jig according to *NS-EN 196-1:2016*. Both the flexural strength testing machine and the load arrangement fulfill the requirements in *NS-EN 196-1:2016*.

According to the *NS-EN 196-1:2016* the loading rate should be 50 N/s, during the initial testing, the loading rate of 50 N/s caused a sudden failure, and therefore the test procedure was modified by selecting a low position controlled displacement rate of 0.1 mm/min.

Position controlled:	0,1 mm/min
Type of flexural strength testing machine:	Zwick Z020
Type of flexural strength testing jig:	ELE International
Load capacity:	20 kN

Figure 55. Flexural strength testing jig with tilting roller supports (Kjaernsmo, 2017)

The flexural testing jig, illustrated in Figure 55, has two supporting rollers that are capable of tilting slightly in order to prevent torsional stresses during the loading sequence.

3.4.7.1 Calculation of Flexural Strength

The flexural strength is calculated according to *NS-EN 196-1:2016*:

$$R_f = \frac{1{,}5 \cdot F_f \cdot L}{b^3}$$

where

R_f – is the flexural strength [MPa]

b – is the side of the square section of the prism [mm]

F_f – is the load applied of the prism at fracture [N]

L – is the distance between the supports [mm]

According to *NS-EN 196-1:2016*, the arithmetic mean of three individual result should be expressed to the nearest 0,1 MPa.

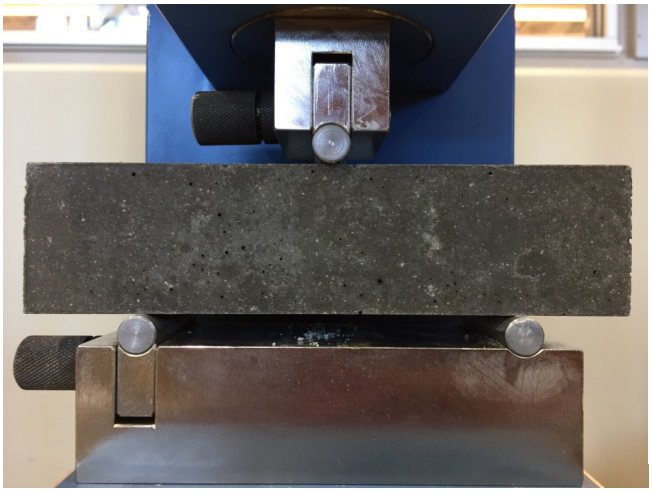

Figure 56. Three-point bending test (Kjaernsmo, 2017)

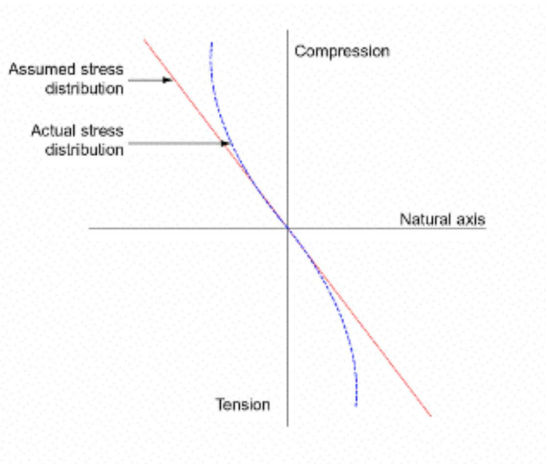

Figure 57. Flexural test - Assumed Vs. Actual stress distribution. (Metha & Monteiro, 2006)

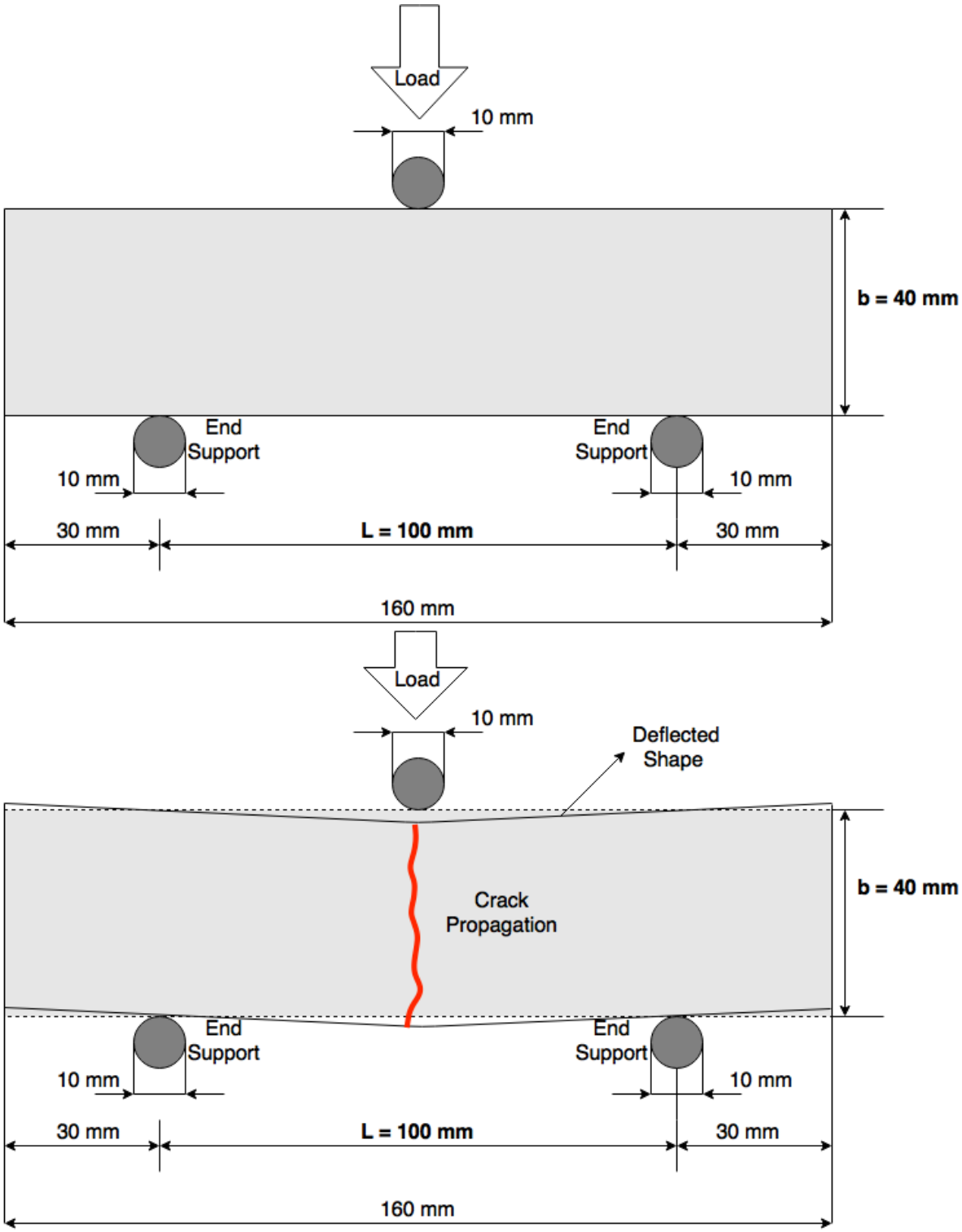

Figure 58. Test setup for Three-point bending test. Redrawn from (Muhit, 2015) and adapted to NS-EN 196-1:2016

3.4.8 Compressive Strength Test Setup

The prism half from the flexural strength test is arranged in the compressive testing jig according to *NS-EN 196-1:2016*. The upper and lower plates, illustrated in Figure 59, have a dimension of 40 mm x 40 mm which is equal to the width of the beam. The end face of the prism overhangs the plates by 10 mm.

Type of compressive testing machine:	Toni Technik / Toni Trol
Type of compressive testing jig:	ELE International
Loading rate (according to NS-EN 196-1:2016):	2 400 N/s
Load capacity (compressive testing jig):	250 kN

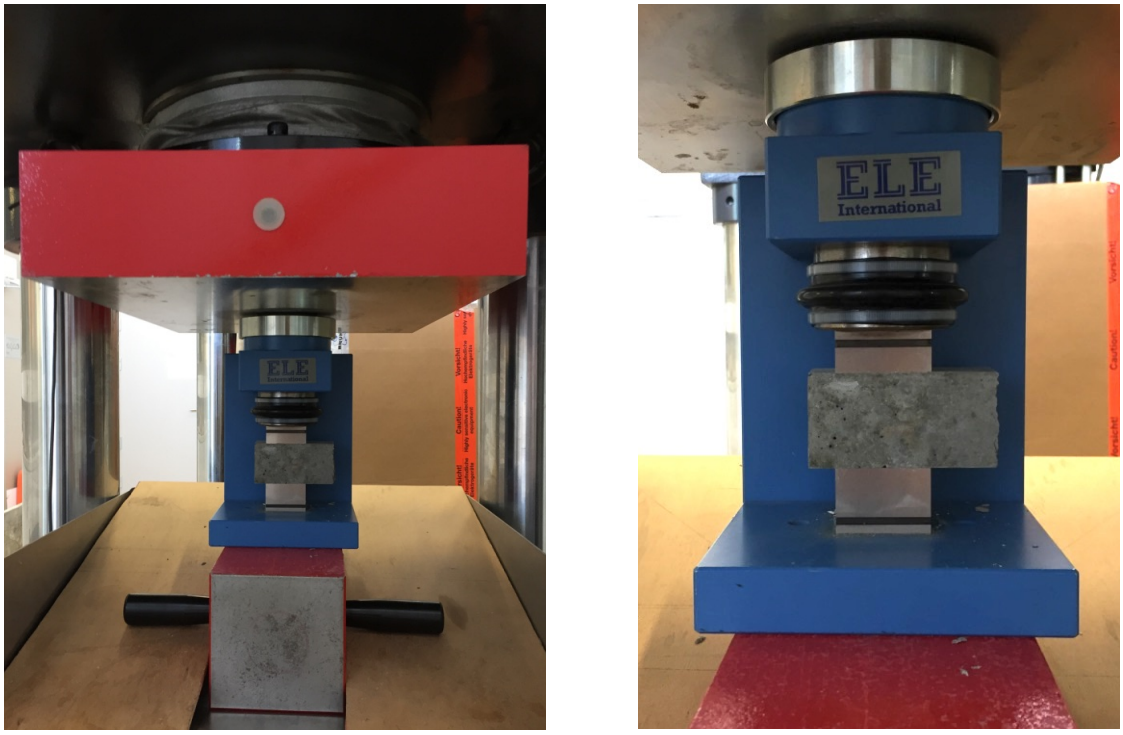

Figure 59. Test setup - Compressive Strength Test (Kjaernsmo, 2017)

3.4.8.1 Calculation of Compressive Strength

The compressive strength is calculated according to *NS-EN 196-1:2016*:

$$R_C = \frac{F_c}{1600}$$

where

R_C – is the compressive strength [MPa]

Fc – is the maximum load at fracture [N]

1600 – is the area of the platens or auxiliary plates (40mm x 40mm), in square millimeters [mm^2]

According to *NS-EN 196-1:2016*, if one results within six individual results varies by more than ± 10 % from the mean, discard this result and calculate the arithmetic mean of the five remaining results. If one result within the five remaining results varies by more than ± 10 % from their mean, discard the set of results and repeat the determination. The arithmetic mean of three individual results should be expressed to the nearest 0.1 MPa.

The validation procedure described in *NS-EN 196-1:2016* is made with the intention of cement certification and factory quality control, which is not the objective of this type of experimental program. The aim is to investigate the effect of graphene oxide (GO) on the mechanical strength, where a possible effect can be an increased uncertainty within a set of results. By eliminating a set of results, according to *NS-EN 196-1:2016*, these types of effects would not be reported precisely. Therefore, the compressive strength results are presented as they were observed and the uncertainty within a set of results is expressed by an error bar. The error bar represents the maximum and minimum compressive strength within a set of results. In addition, the results should only be interpreted as indications since a set of results contains three specimens. A detailed overview of the results is presented in Appendix C.

3.4.9 Splitting Tensile Test Setup

The cylinder is marked with a centerline on the cylinder faces, as illustrated in Figure 61. The centerlines make it easier to control that the cylinder is correctly placed in the testing jig. If the cylinder is not arranged precisely, the fracture will not occur along the center of the cylinder length, thus rendering results invalid. Two small pieces of plywood are then arranged as illustrated in Figure 61. The final test setup is illustrated in Figure 60.

Type of testing machine:	Zwick Z020
Loading capacity	20 kN
Loading rate:	20 N/s

Figure 60. Test Setup - Splitting Tension Strength Test

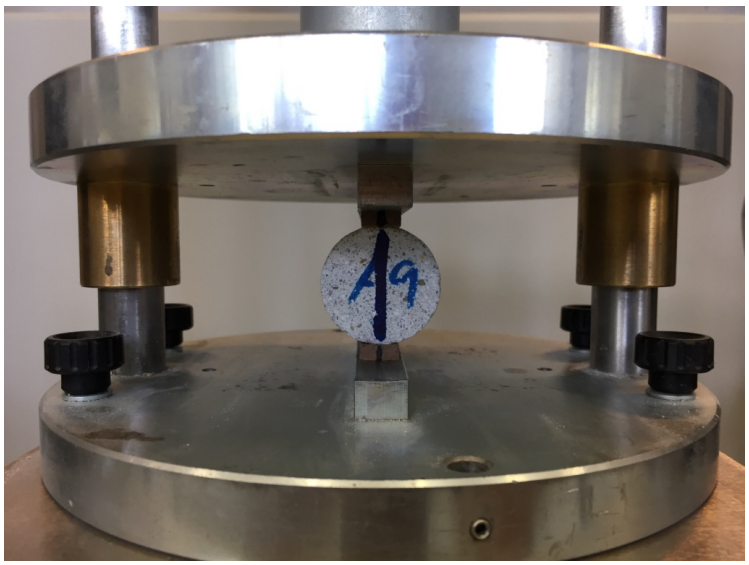

Figure 61. The marked cylinder arranged in the testing jig and supported by two pieces of plywood (Kjaernsmo, 2017)

3.4.9.1 Calculation of Splitting Tensile Strength

The splitting tensile strength is calculated by the following equation according to *NS-EN 12390-6: Tensile Splitting Strength of test specimens*:

$$T = \frac{2 \cdot F}{\pi \cdot L \cdot D}$$

where

T – Splitting tensile strength [MPa]

F – Failure load [N]

L – Length of specimen [mm]

D – Diameter [mm]

3.4.9.2 Splitting tensile test vs theoretical cylinder stress distribution

The theoretical cylinder stress distribution for the splitting tensile test is illustrated in Figure 62. The top and bottom part of the cylinder face is subjected to compression, while the middle is exposed to tension. The stress distribution changes from compression to tension at approximately D/12 from the cylinder edge. In this case, with a diameter of 33 mm, the change should occur approximately 2.75 mm from the cylinder edge.

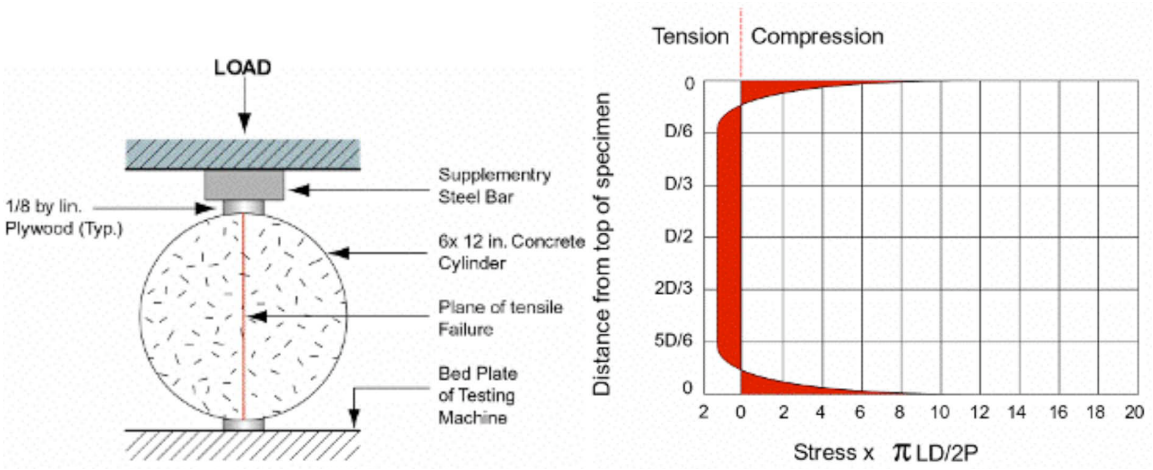

Figure 62. Splitting tensile test - Stress distribution according to the theory. (Metha & Monteiro, 2006)

3.4.10 Strain distribution with Digital Image Correlation (DIC)

The objective of using a high-speed strain camera is to analyze the strain distribution during the three-point bending test. The strain distribution is interesting because the prism ends are used to determine the compressive strength after the three-point bending test. In other words, the prism ends are assumed not to be subjected to substantial forces during the three-point bending test. The strain camera can investigate this assumption and validate the method. The test setup for the three-point bending test with the strain camera is illustrated in Figure 63.

The strain camera measures strain distribution by analyzing the movement of several pre-defined points on the specimen surface during the load sequence. The strain camera analyses how the points are moving with respect to each other both in the X-, Y-, and Z-axis. Moreover, the specimen is also spray painted with the purpose of increase the number of points on the surface. This will improve the quality of the strain analysis and reduce the level of noise in the strain distribution image. The camera system is calibrated by using the calibration plate illustrated in Figure 64.

Strain Camera System: LaVision StrainMaster Portable

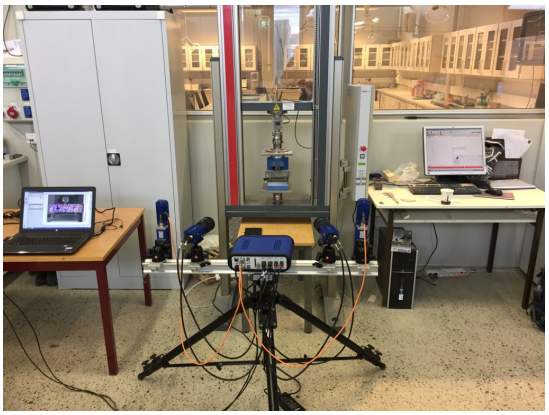

Figure 63. Test Setup - Strain Camera (Kjaernsmo, 2017)

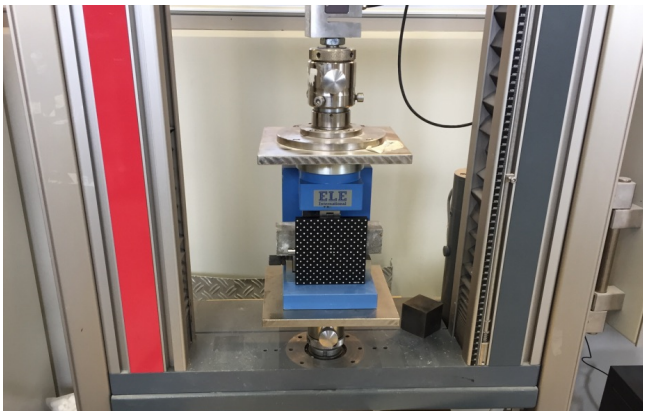

Figure 64. Calibration plate (Kjaernsmo, 2017)

The strain camera is also used to analyze the strain distribution during the compressive strength test. The objective is to validate the method since the compressive strength is not determined by traditional cubes or cylinders. Figure 65 illustrates the compressive test with the strain camera.

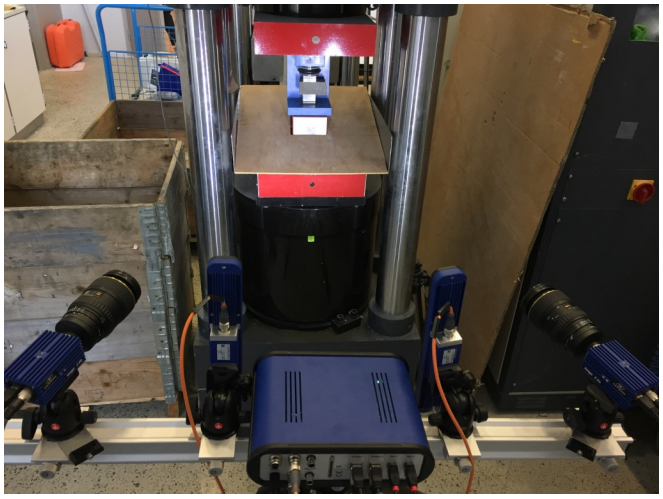

Figure 65. Test Setup - Compressive test with the strain camera (Kjaernsmo, 2017)

The objectives of analyzing the strain distribution during the splitting tensile test are both to validate the selected test setup and compare the strain distribution with the theory. According to the theory, presented in Section 3.4.9.1, the top and bottom part of the cylinder face is subjected to compressive stress, and the middle part is subjected to tensile stress. The test setup for the splitting tensile test and strain camera is illustrated in Figure 66.

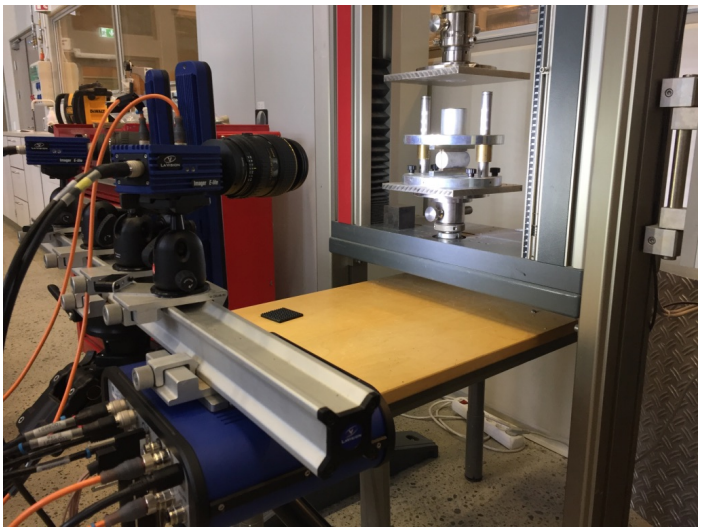

Figure 66. Test Setup - Splitting Tensile Test with strain camera (Kjaernsmo, 2017)

3.4.11 Microstructure - Scanning Electron Microscopy (SEM)

Scanning Electron Microscopy (SEM) utilizes electrons to create an image of the microstructure. The electron gun shoots a focused beam of electrons, these electrons interact with atoms in the sample, and several different detectors examine the emitted signals from this interaction process. SEM can analyze both the topography and the sample composition. The element composition for a specific point is analyzed by Energy Dispersive X-ray Detector Spectroscopy (EDS) and provides an element spectrum for the specific point. The working principles of EDS will be further elaborated in chapter 3.4.11.3.

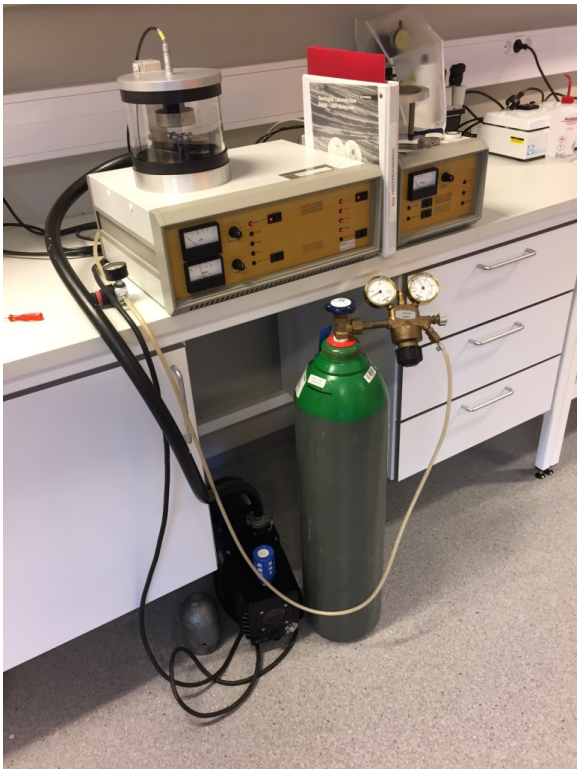

Figure 67. The samples were covered with Palladium (Kjaernsmo, 2017)

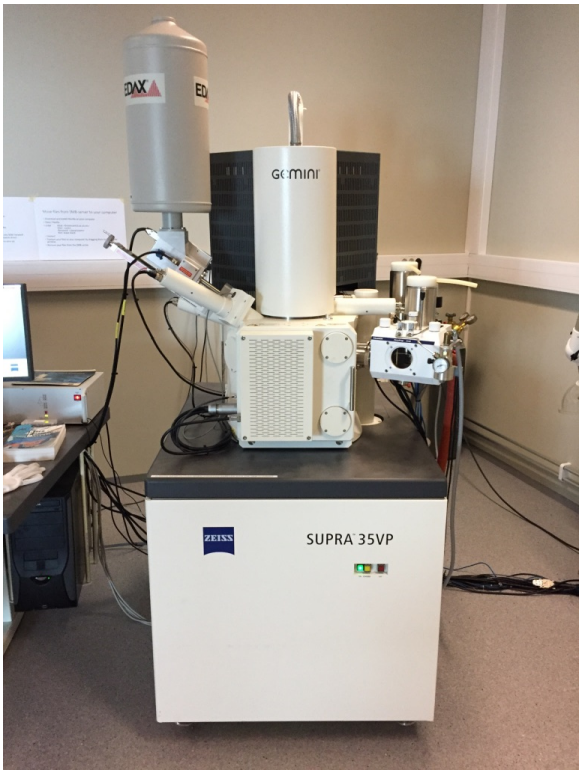

Figure 68. Zeiss Supra 35VP Scanning Electron Microscope (Kjaernsmo, 2017)

3.4.11.1 SEM Preparations

Small samples, approximately 10 mm x 10 mm, were taken from central parts, i.e. the fracture zone of each specimen, and taped to a small sample disc (Ø 10 mm) with conductive carbon tape. The purpose of conductive carbon tape was to conduct the electric current away from the sample. The electric current can also accumulate on the surface of the sample. Therefore, each sample was covered with palladium (Pd) for the purpose of conduct the electric current away. Figure 70 and Figure 71 illustrates the process of covering the samples with palladium. The samples were first placed into a vacuum chamber with 0.07 mBar, and then covered with palladium for 2.5 minutes. Alternatively, the samples could have been covered with carbon particles. Since graphene oxide is made of carbon, palladium was selected as the optimum cover material. The purpose of these preparations was to achieve high-quality SEM image without any electric charge accumulation which creates noise (white spots in the SEM image).

Figure 69. Small samples were taken from central parts from the fractured surface (Kjaernsmo, 2017)

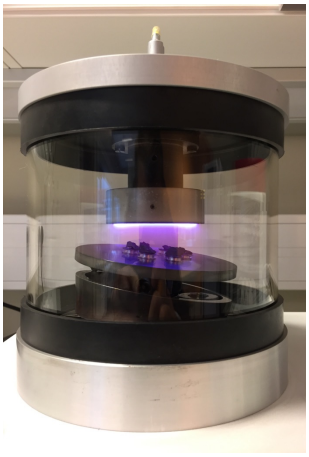

Figure 70. The samples were covered with palladium in a vacuum chamber (Kjaernsmo, 2017)

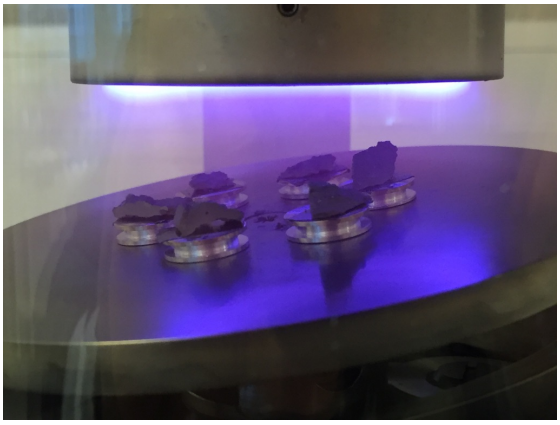

Figure 71. The samples were covered with palladium (Kjaernsmo, 2017)

Figure 72. The samples with palladium cover (Kjaernsmo, 2017)

3.4.11.2 Framework for the SEM Analysis

The objective of this framework is to produce SEM images which make it possible to compare the different samples. All the samples were taken from the specimens after 28 days of curing. For each sample, both the interfacial transition zone(ITZ) and the bulk cement paste were analyzed, as illustrated in Figure 73. All the images were taken with scan speed six with the purpose of achieving high-quality images. Table 13 presents an overview of the framework.

Table 13. SEM Framework

Framework for SEM analysis				
#	Microstructure	Scan speed	Magnification	EDS
1	Interfacial Transition Zone	6	2 000	Counts: 1000-5000
			2 000	
			6 000	
			10 000	
2	Interfacial Transition Zone	6	2 000	Counts: 1000-5000
			6 000	
			10 000	
3	Bulk Cement Paste	6	2 000	Counts: 1000-5000
			6 000	
			10 000	

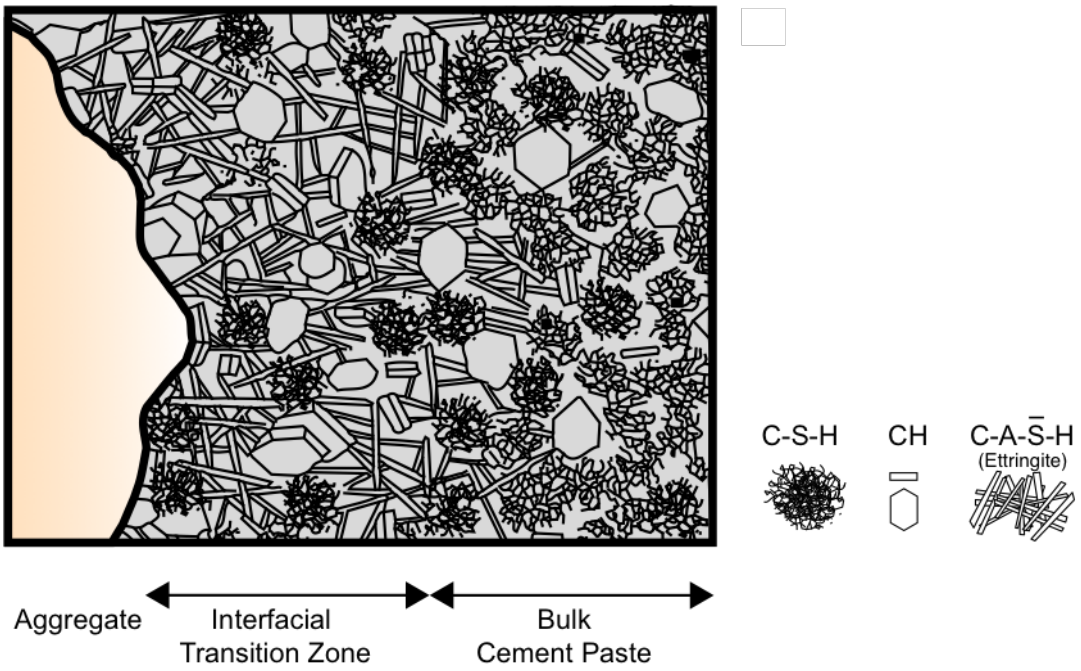

Figure 73. Microstructure – Interfacial Transition Zone and Bulk Cement Paste (Metha & Monteiro, 2006)

3.4.11.3 Energy Dispersive X-ray Spectroscopy (EDS)

Energy dispersive X-ray spectroscopy identifies the element composition by detecting the characteristic X-ray from a selected spot on the SEM sample. The characteristic X-ray is emitted because of electrons are knocked out of their original position (orbital/shell) in the atom by using an high-energy beam of particles (Leng, 2013). The high-energy particles are either x-ray photons, electrons or neutrons (Leng, 2013). The knocked-out electron leaves a vacant position, and an electron from a higher-energy orbital is dropped down to fill this vacancy. In the transition from a high-energy orbital to a lower-energy orbital, the electron releases energy as a characteristic X-ray. According to the law of energy of conservation, the total energy of an isolated system remains constant and can only be transformed. Before the electron drops down to a lower-energy orbital, the electron has electrostatic energy (potential energy). In the transition, the electron gives off electromagnetic energy (kinetic energy), and the total energy remains constant since the energy is transformed from electrostatic to electromagnetic (characteristic X-ray). The working principles of energy dispersive x-ray are illustrated in Figures 74, Figure 75, Figure 76, and Figure 77.

The energy dispersive X-ray detector generates an element spectrum by analyzing the emitted energy (X-ray photons). In the spectrum, the x-axis expresses the emitted energy in electron volts (eV), and the y-axis represents the number of detected X-ray photons (counts). The spectrum is also proportional to the relative element concentrations in the selected spot area. The EDS software estimates the percent chemical element composition by analyzing the energy dispersive X-ray spectrum.

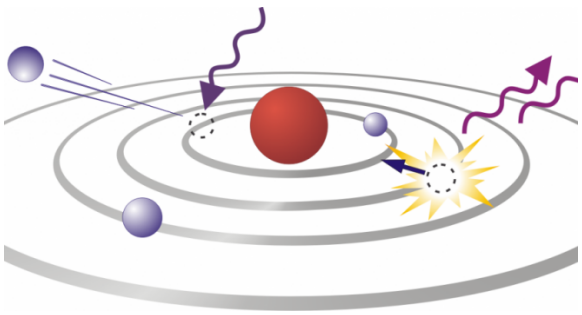

Figure74. The working principles of EDS. (LearnXRF, 2017)

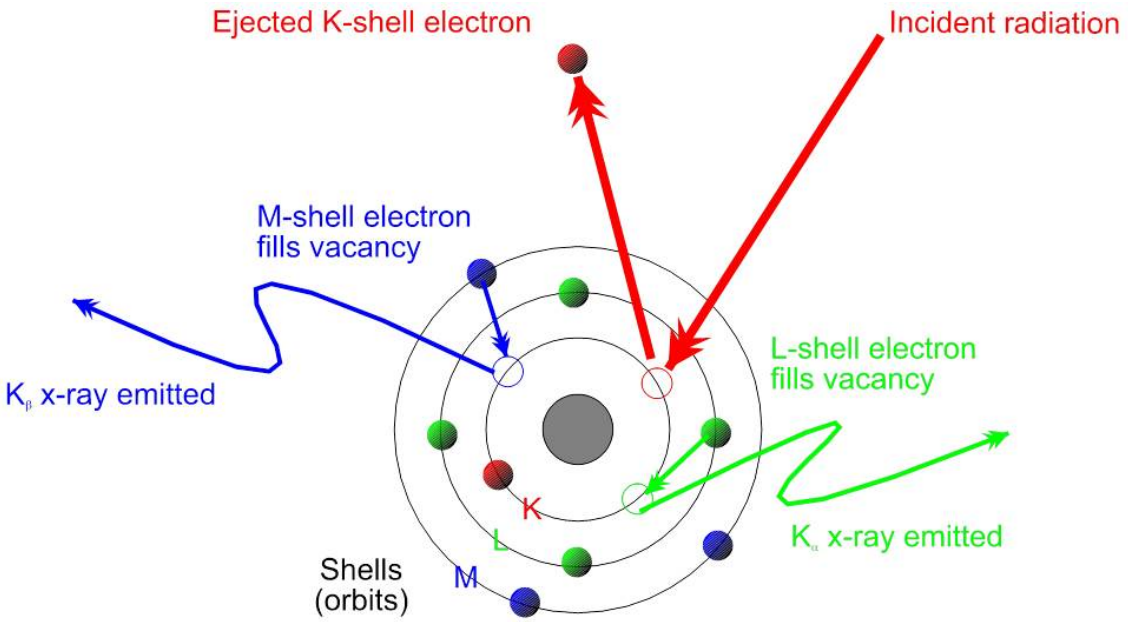

Figure 75. Characteristic X-ray. (Bruker, 2017)

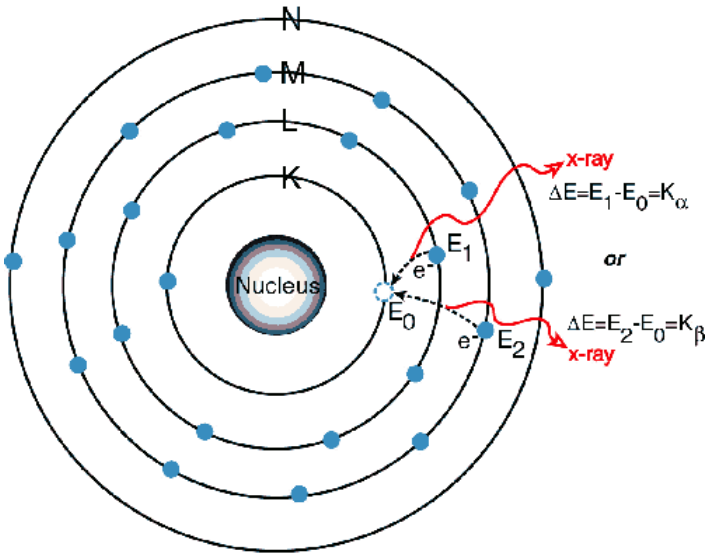

Figure 76. X-ray emission & the law of energy of conservation. (Bedwani, 2017)

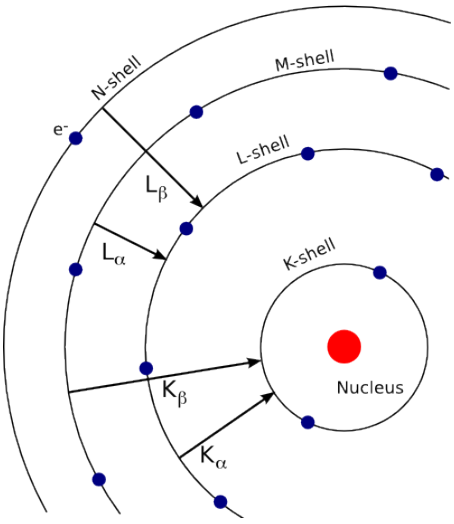

Figure 77. Electrons in a higher-energy orbital drops down to fill the vacant positions. (UCL, 2007)

EDS signals are emitted from a pear-shaped volume on the sample, as illustrated in Figure 78. The pear-shaped volume is also called the volume of interaction or emission volume and creates uncertainty in the element spectrum. Elements or objects located under the selected point or object can emit EDS signals and influence the energy dispersive X-ray spectrum. This uncertainty can be reduced by analyzing multiple points on the selected object and by identifying other objects that are located nearby. Potential interference due to a low take-off angle, illustrated in Figure 79, can also influence the element spectrum. Take-off angle is the angle between the plane of sample surface and the detector. For instance, if the selected point of interest is located in a valley on the sample surface and the x-ray detector identifies elements located above this valley. This potential issue is illustrated by Figure 79. Uncertainty in potential interference can be reduced by increasing the take-off angle (rotating the sample) or by selecting a sample with a flat surface (or less roughness). (Leng, 2013)

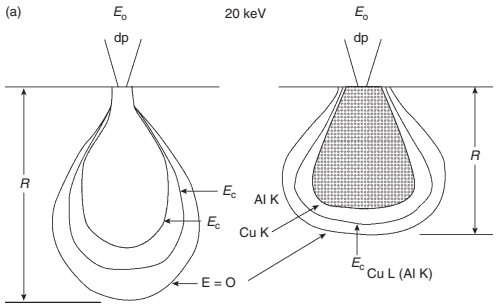

Figure 78. EDS signals are emitted from a pear-shape volume of interaction. (Leng, 2013)

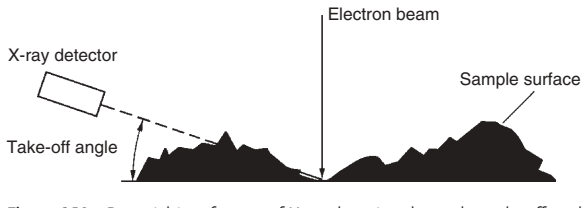

Figure 79. A low take-off angle can create potential interference. (Leng, 2013)

4 Results and Discussions

In this chapter, the results and findings based on the experimental program are presented as well as discussed. The results and discussions will be presented according to the experimental work plan. This is illustrated in Figure 80.

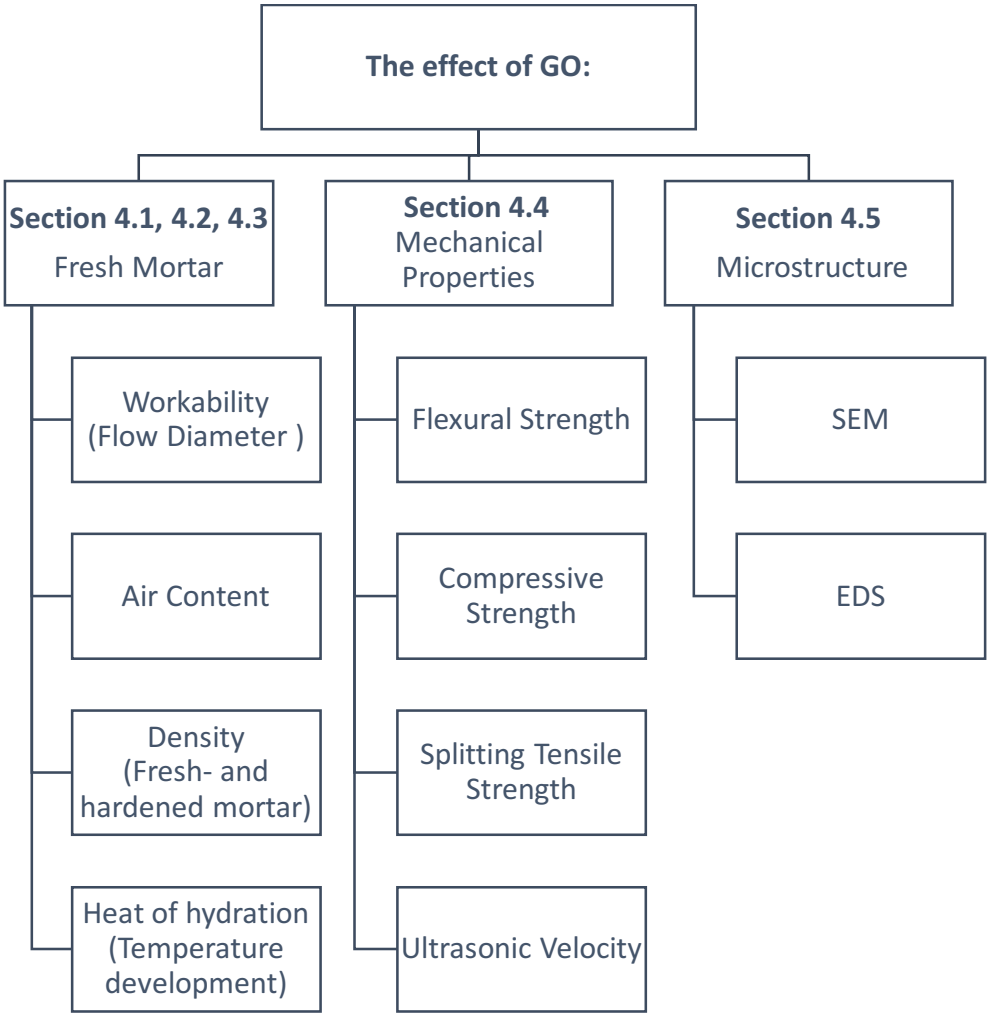

Figure 80. Experimental Work Plan - Overview of Results and Discussions (Kjaernsmo, 2017)

4.1 The Effect of GO on Fresh Mortar

4.1.1 Flow Diameter (Workability)

The results from the mini-flow test are presented in Figure 81. The flow diameter (cm) is presented on the left vertical axis and the percent changes with respect to the reference mortar on the right vertical axis. The flow diameter is the average of two individual batches of a mortar composition.

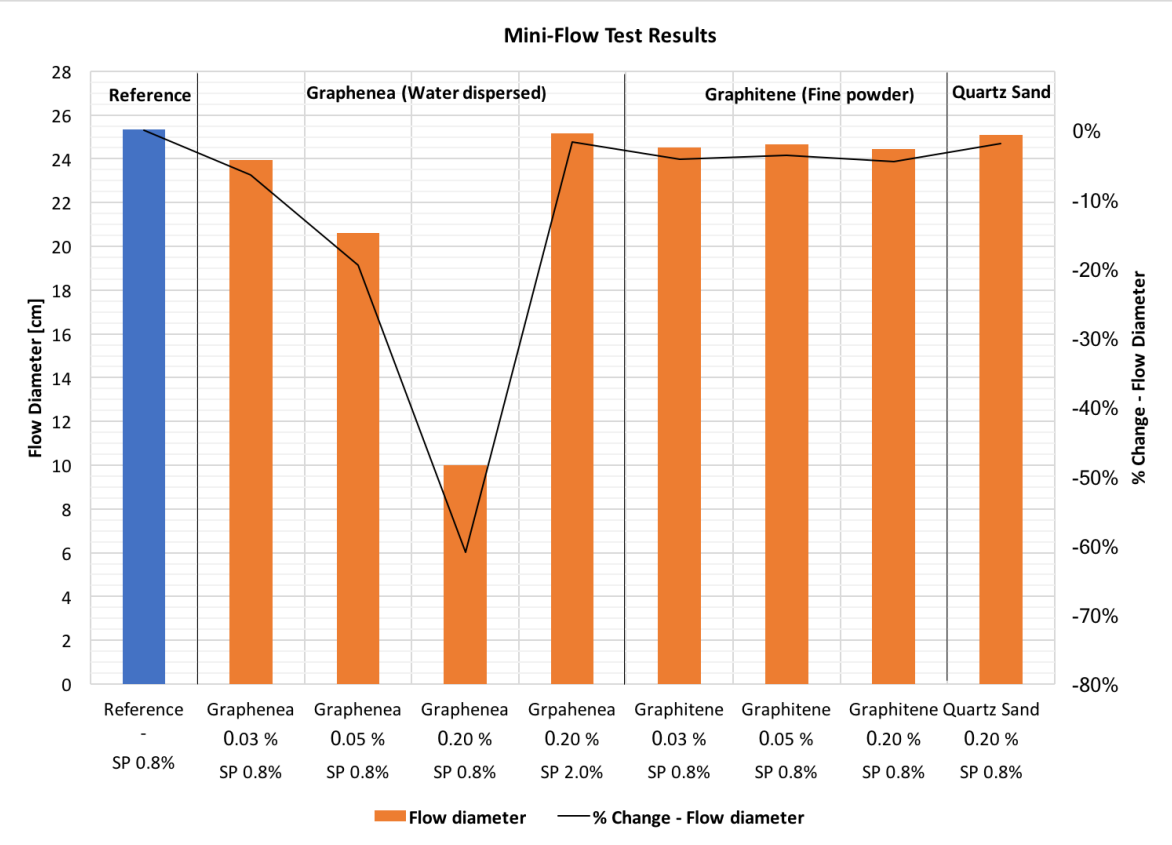

Figure 81. Mini-Flow Test Results (Kjaernsmo, 2017)

There is a correlation between the increased content of Graphenea (water dispersed) and the reduced flow diameter. For Graphitene (fine powder), there is only a small change in the flow diameter with increasing content of GO, but no correlation between the percent GO and the flow diameter.

The cement mortar with Graphenea 0.20% & SP 0.8% had a stiff plastic consistency after mixing. The flow diameter was measured to only 10 cm, which equal to zero flow since the bottom diameter (B.D.) of the cone is 10 cm.

4.1.1.1 Graphenea 0.2 % & SP 2.0 %

A reduced flow property indicates poor workability and self-compact ability which can cause large embedded air voids that decrease the mechanical strength. Therefore, a new mix design was developed for the cement mortar containing Graphenea 0.20% and tested after 28 days of curing. The goal was to reach a flow diameter equal to the reference mortar by adding SP in the increments of 0.2%.

Procedure of increasing the flow diameter equivalent to the reference mortar

After increasing the SP content by 0.2 %, the cement mortar was remixed at medium speed for one minute, and the flow diameter was measured. This process was repeated until the required flow diameter was reached at the SP content of 2.0 %. The mixing and mini-flow test were repeated six times, and mixing sequence lasted for 14 minutes. The SP content increased from 0.8 % to 2.0 %. This improved the flowability, and from observations, the mortar became also highly viscous compared to the other mortar compositions. On the second mini-flow test, the same mortar composition was very stiff after completing the mixing procedure described in Section 3.3.3.1, Table 11. The slump was only 12.5 mm, and the flow diameter was 11 cm, where 10 cm is equal zero flow on the flow board. Because of a possible delay in the chemical reaction between the mortar and the SP, the mortar rested for 5 minutes and then remixed for 1 minute at medium speed. The flow diameter increased from 11 cm to 24.25 cm which is almost equal to the reference mortar (Figure 82). This observation indicates that a mortar with such a high content of SP and GO needs time for the chemical reactions to occur, but can also be a result of increasing the SP content more than recommended by the supplier.

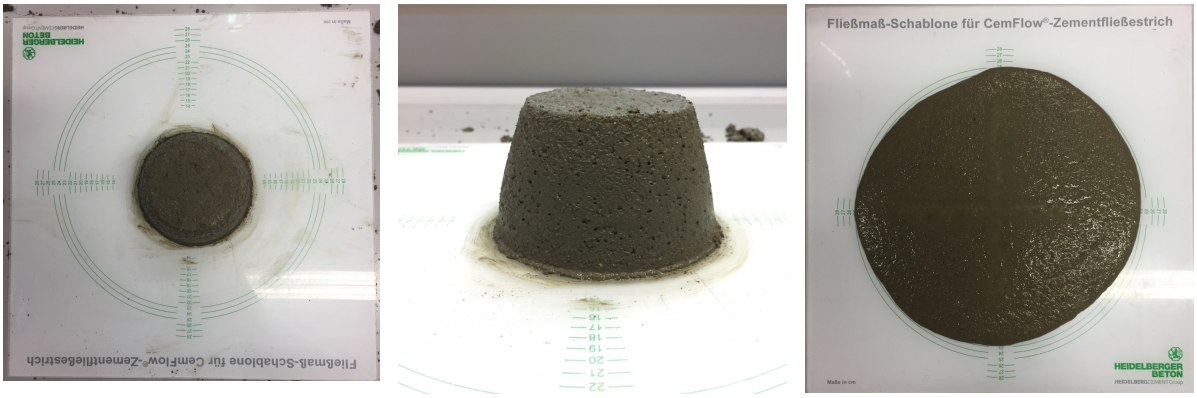

Figure 82. Mini-Flow Test - 0.2% Graphenea & 2.0% SP (Kjaernsmo, 2017)

The reduced flow property is most likely a consequence of the high specific surface area of GO which absorbs the free-water in the cement mortar. Equivalent results have also been reported in the previous research presented in section 2.7.1.

4.1.2 Percent Air of Fresh Mortar

The percent air content varies between 2.5 % to 3.4 %, except for the mortar composition containing Graphenea 0.2%. The air content of 4.9 % for Graphenea 0.2% can be explained by the stiff plastic consistency that was observed during the mini-flow test, presented in Section 4.1.1. A reduced workability can influence the compaction which consequently increases the air content. Also, the mortar containing Graphenea 0.2% & SP 2.0% has almost the same air content and approximately equal flow diameter as the reference mortar.

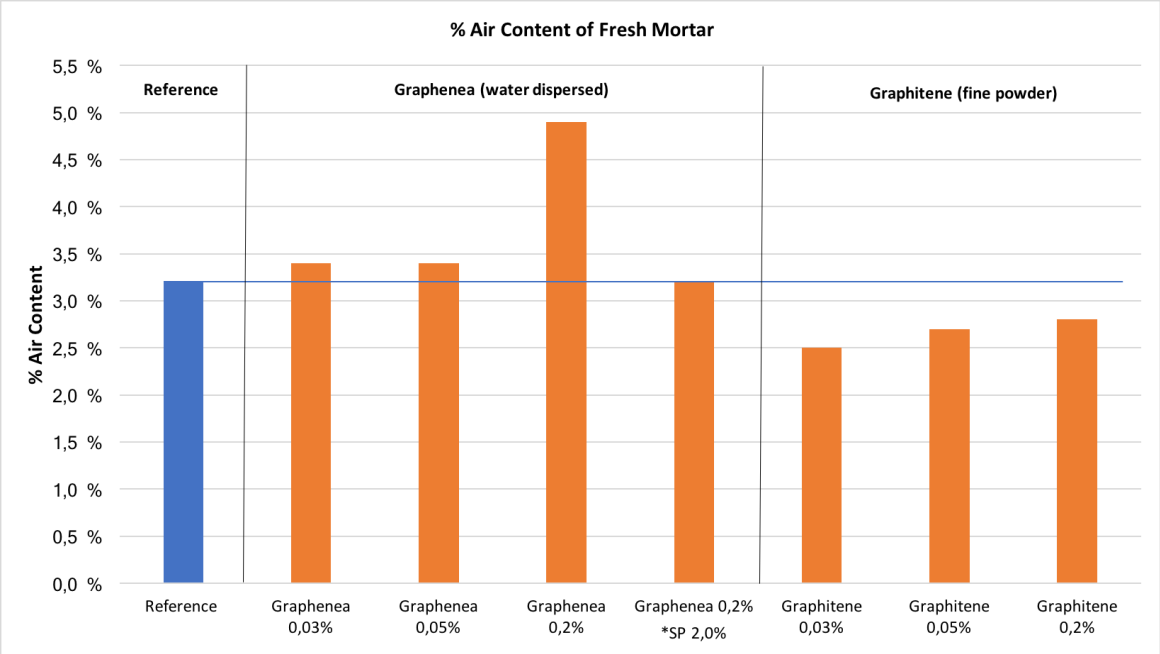

Figure 83. Percent Air Content (Kjaernsmo, 2017)

4.1.3 Density of Fresh Mortar

The fresh mortar densities are within the range of 2.22 to 2.3 kg/m^3. The results are presented in Figure 84. The small reduction in density for Graphenea 0.2% seems to be a result of the reduced workability which was observed during the mini-flow test. The result also corresponds with the increased air content of the fresh mortar reported in Section 4.1.2. Although, the percent change in density between Grapehenea 0,2% and the reference mortar is only 3.31 %.

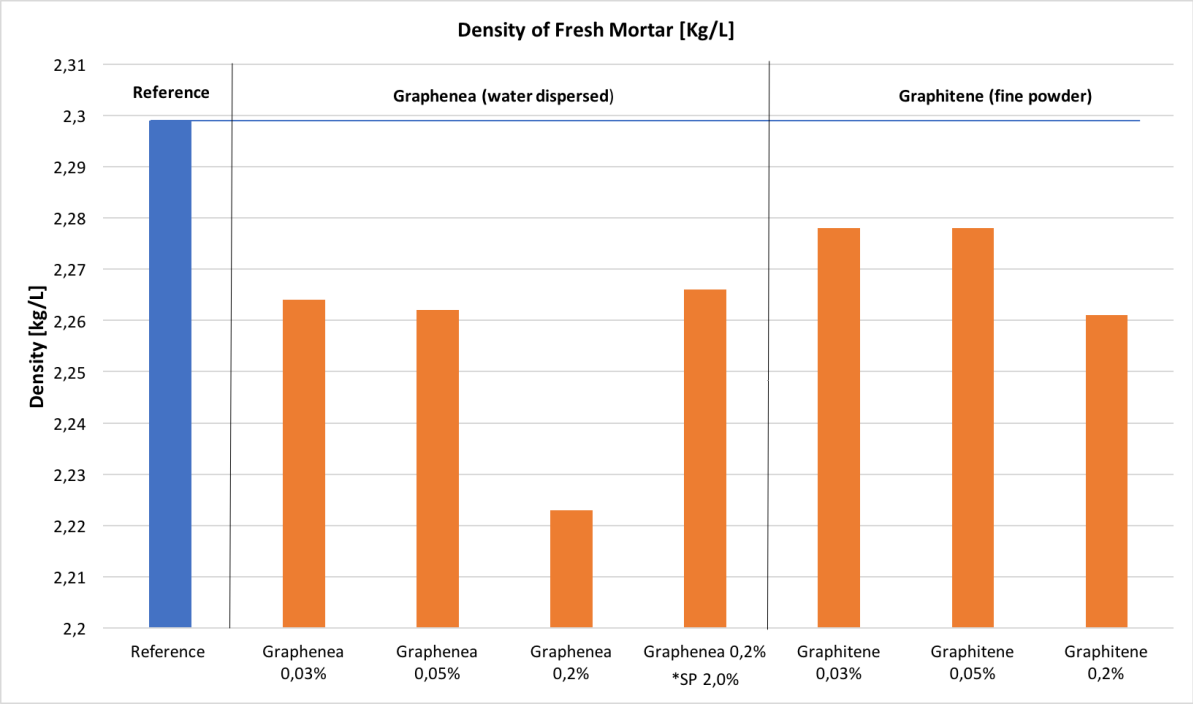

Figure 84. Density of Fresh Mortar (Kjaernsmo, 2017)

4.2 The effect of GO on Temperature- & Heat Developments

4.2.1 Temperature Developments

The temperature development of cement mortar has been recorded until reaching to room temperature, which took three days. The temperature developments for the different mortar compositions are presented in Figure 85. The results show an earlier temperature development and a higher maximum temperature for the cement mortar containing graphene oxide (GO). These results indicate that graphene oxide reacts chemically with the cement mortar components, and therefore increasing the exothermal heat development. The maximum (peak) temperatures and the percent changes with respect to the reference mortar are presented in Figure 86 and Figure 87, respectively. Moreover, the results also indicate that water dispersed GO (Graphenea) has a greater effect on the temperature development compared to GO in powder form (Graphitene). There is also a correlation between the content of the water dispersed GO (Graphenea) and maximum (peak) temperature.

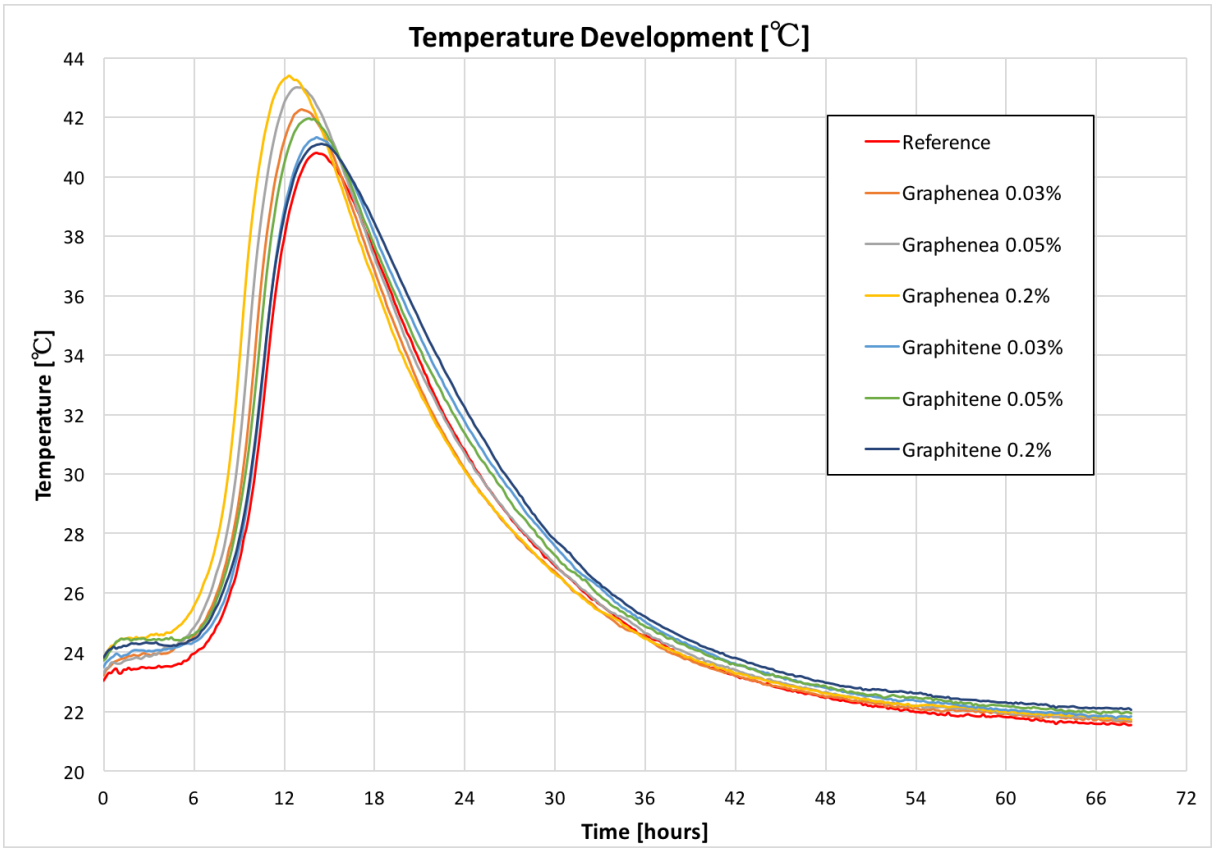

Figure 85. Temperature development after 3 days (Kjaernsmo, 2017)

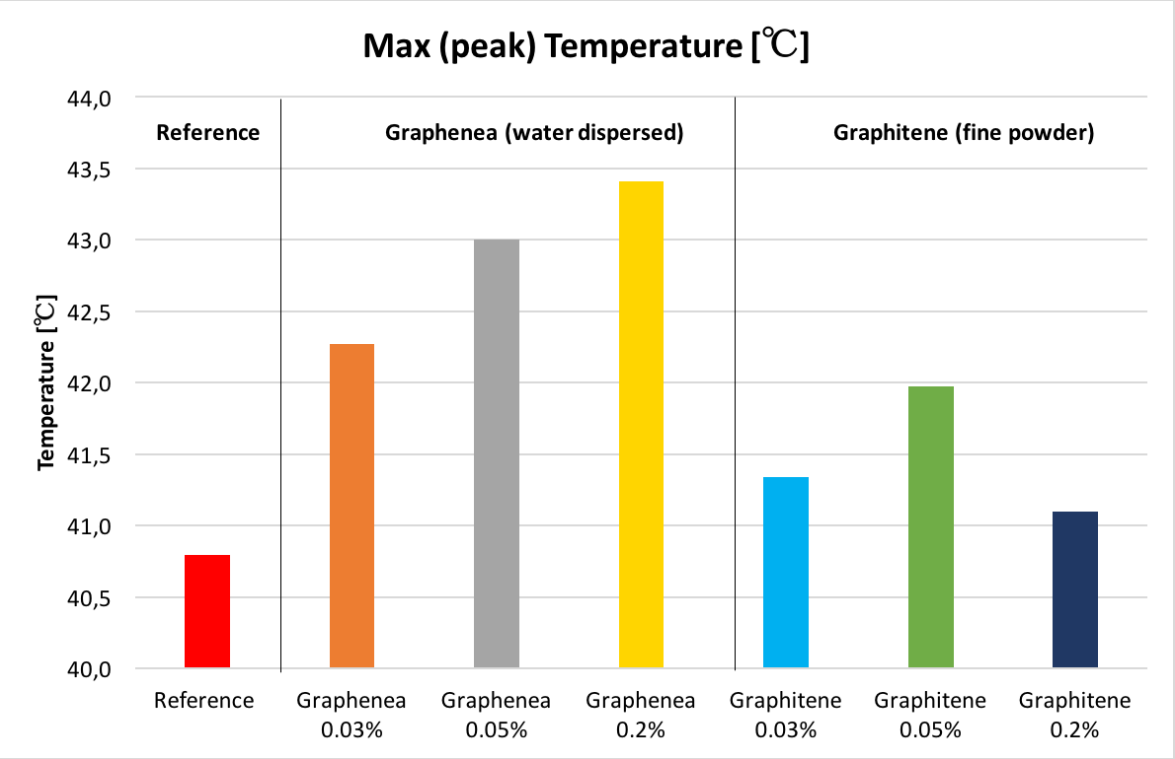

Figure 86. Max Temperature (Kjaernsmo, 2017)

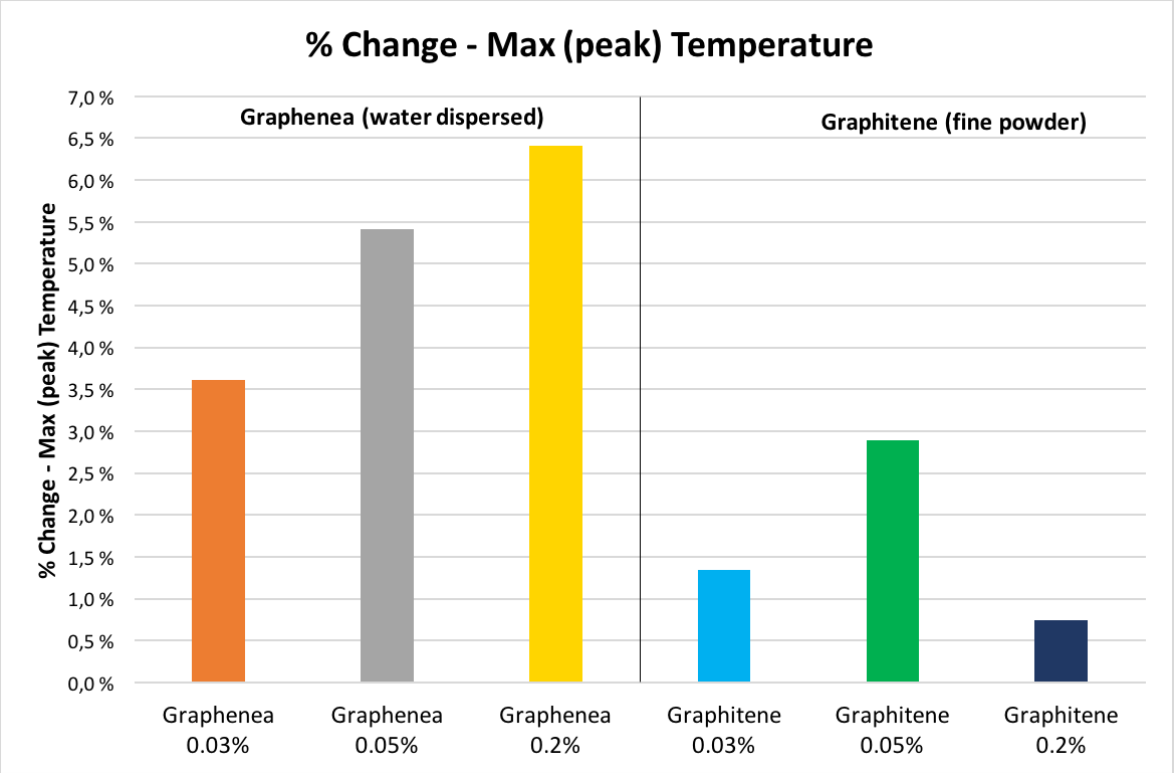

Figure 87. Percent change in the max temperature with respect to the reference cement mortar (Kjaernsmo, 2017)

4.2.2 Cumulative Isothermal Heat Developments

The cumulative isothermal heat developments are estimated with a curing box spreadsheet developed by Sverre Smedplass, Skanska. The estimates are based on the temperature measurements presented in Section 4.2.1. The results are presented in Figure 88. A detailed overview of the spreadsheets is presented in Appendix Appendix C.

The observed effect of GO on the cement hydration heat is opposite compared to Wang et al. (2015) findings. Their results are presented in Section 2.8, Figure 16. Furthermore, the results are more equivalent to the observation reported by Zhao et al. (2017). Presented in Section 2.8, Figure 14. However, secondary effects of mixing graphene oxide and polycarboxylate are unknown and require more research in order to clarify the effect of GO on the heat of hydration.

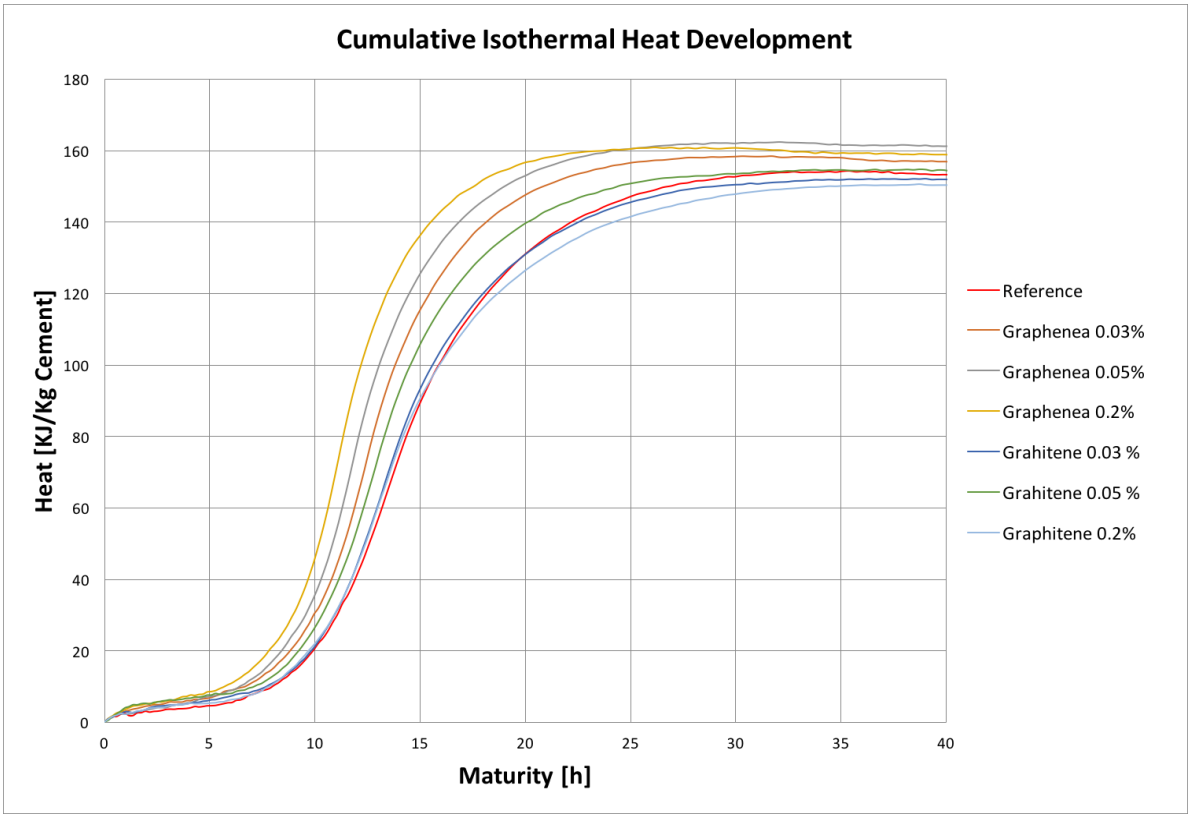

Figure 88. Cumulative Isothermal Heat Development (Kjaernsmo, 2017)

4.3 The effect of GO on the Density of Hardened Mortar

The hardened mortar densities for the various contents and type of graphene oxide are presented in Figure 89. The percent changes with respect to the reference mortar are presented in Figure 90. The results show a reduced density for the mortar compositions containing Graphenea. There is also a correlation between the content of Graphena (0.03%, 0.05%, & 0.2%) and the reduced density. Moreover, the density results correlate also with the flow diameter presented in Section 4.1.1. This correlation indicates that the reduced density is a consequence of poor workability which can increase the content of embedded air bubbles and voids. Except for Graphenea 0.2%, there are no distinct correlations between the densities of the hardened mortar and the percent air of fresh concrete (Section 4.1.2). This can be a consequence of the less reliable air entrainment test or caused by other factors.

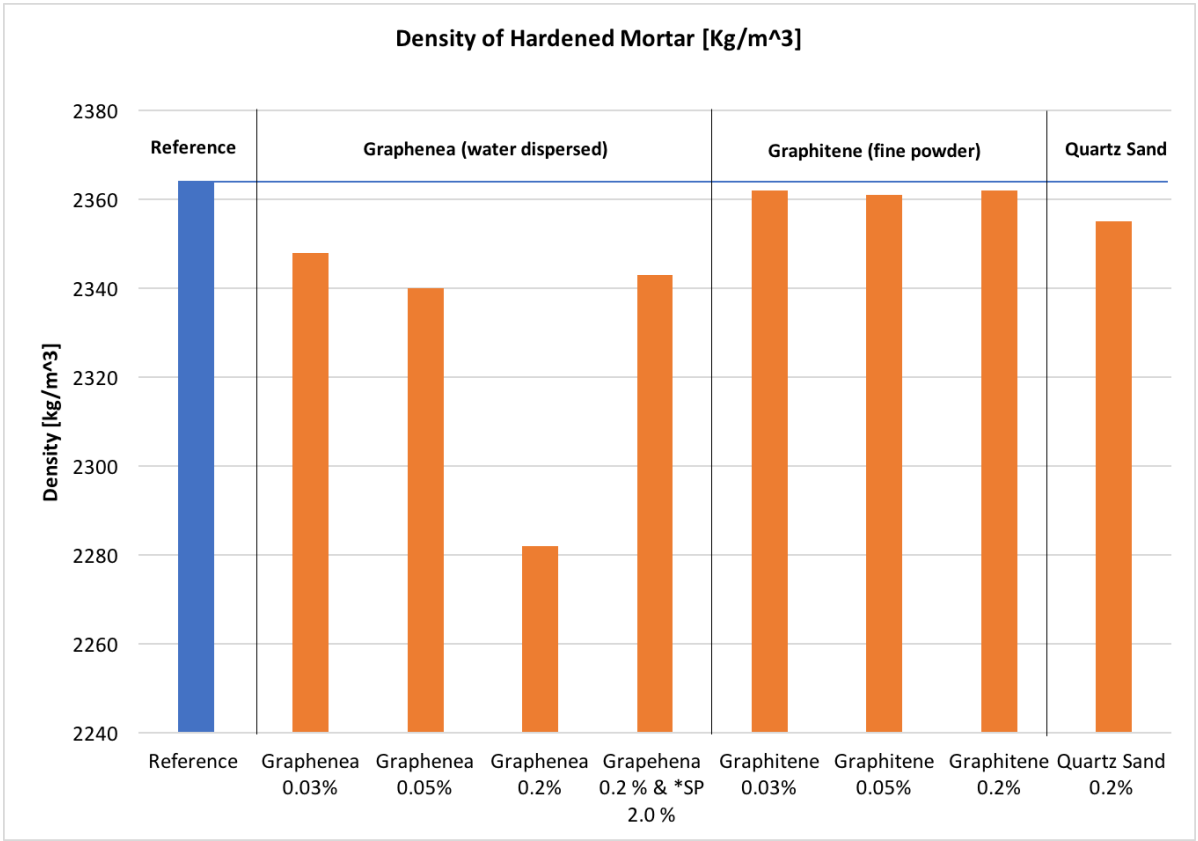

Figure 89. Density of Hardened Mortar (Kjaernsmo, 2017)

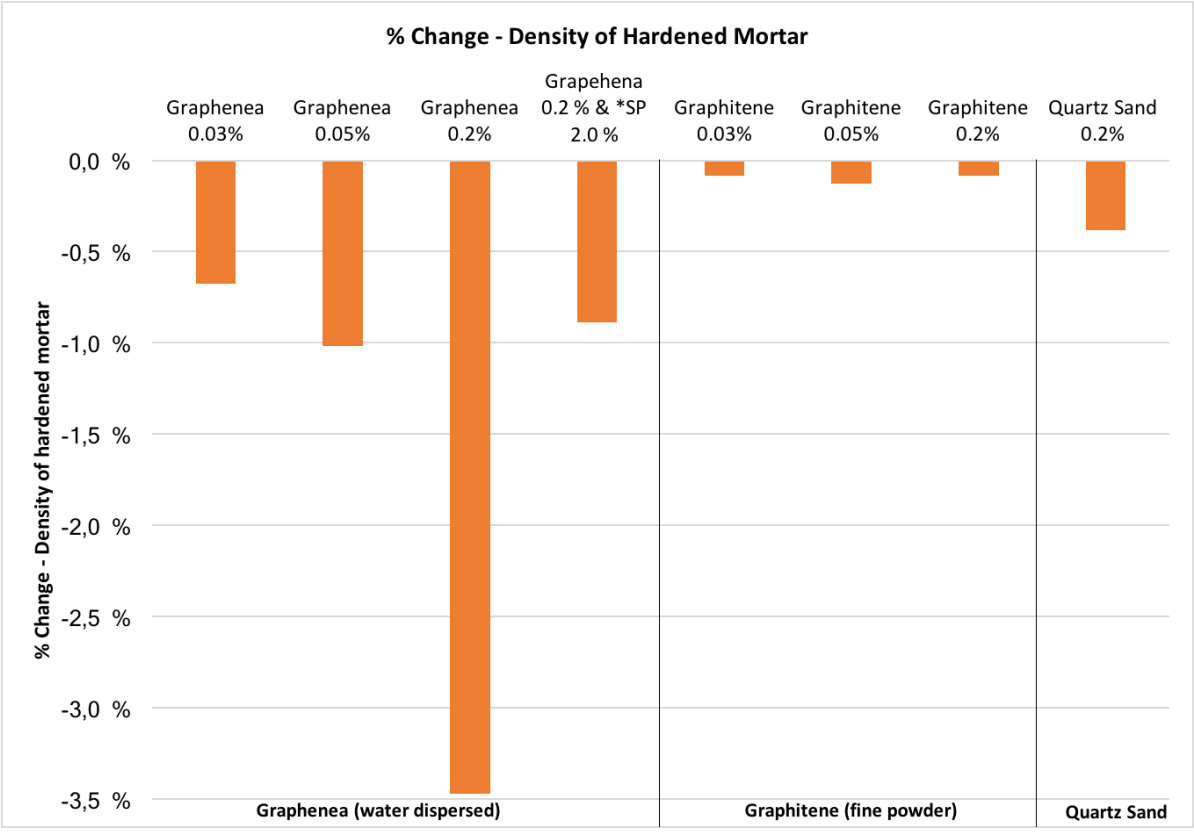

Figure 90. Percent Change - Density of Hardened Mortar (Kjaernsmo, 2017)

4.4 The effect of GO on Mechanical Properties

4.4.1 Flexural Strength

4.4.1.1 Strain Camera – Verification of the Three-Point Bending Test

The typical strain distribution during the three-point bending test is presented in Figure 91 and Figure 92. The red area indicates that the strain arises and propagates in a very concentrated part of the specimen. The prism ends are not subjected to substantial strain during the three-point bending test, and therefore, validates the method of using the prism ends to determine the compressive strength.

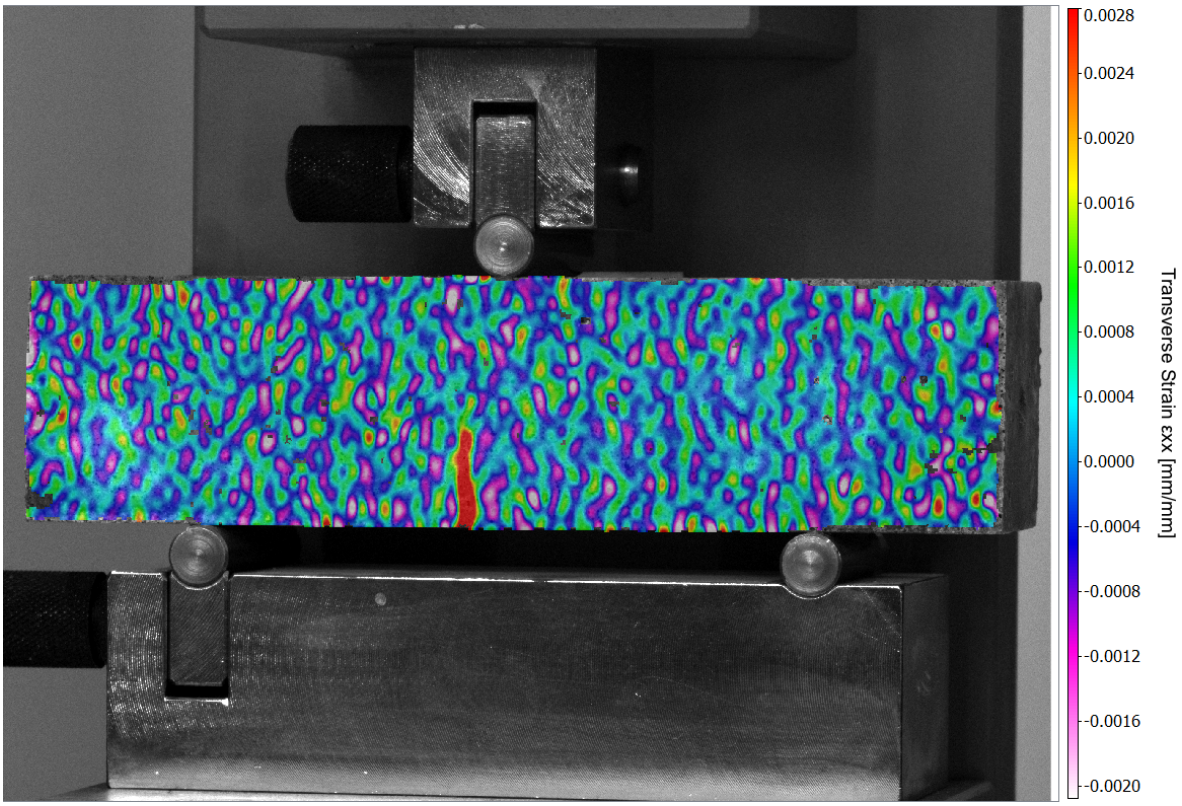

Figure 91. Transverse Strain distribution in x-direction (Horizontally). (Kjaernsmo, 2017)

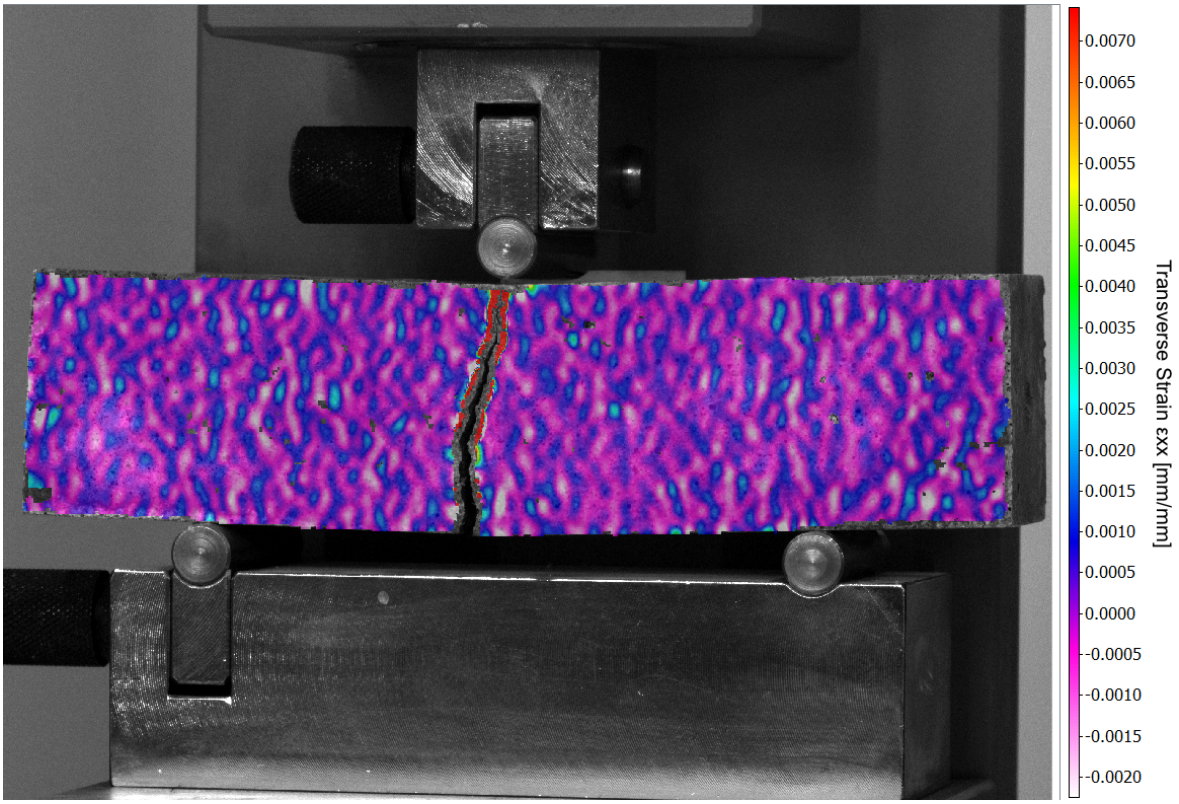

Figure 92. Typical fracture pattern after the three-point bending test (Kjaernsmo, 2017)

4.4.1.2 Flexural Strength Results

The flexural strength after three, seven and 28 days of curing is presented in Figure 93. The percent changes and the flexural strength developments are presented in Figure 94 and Figure 95, respectively.

Graphene oxide seems to improve the early flexural strength after three and seven days, but has no effect after 28 days. No distinct variation between the content or type of graphene oxide and the flexural strength is observed. The percent flexural strength development from three to 28 days is also lower compared to the reference mortar. The improved flexural strength after three and seven days can be a consequence of the increased heat of hydration reported in Section 4.2. This indicates that graphene oxide has a potential of accelerating the hydration process which increases initial flexural strength development.

Furthermore, the influence of GO on the flexural strength is not equivalent to the results reported in the previous research presented in Section 2.6.1.

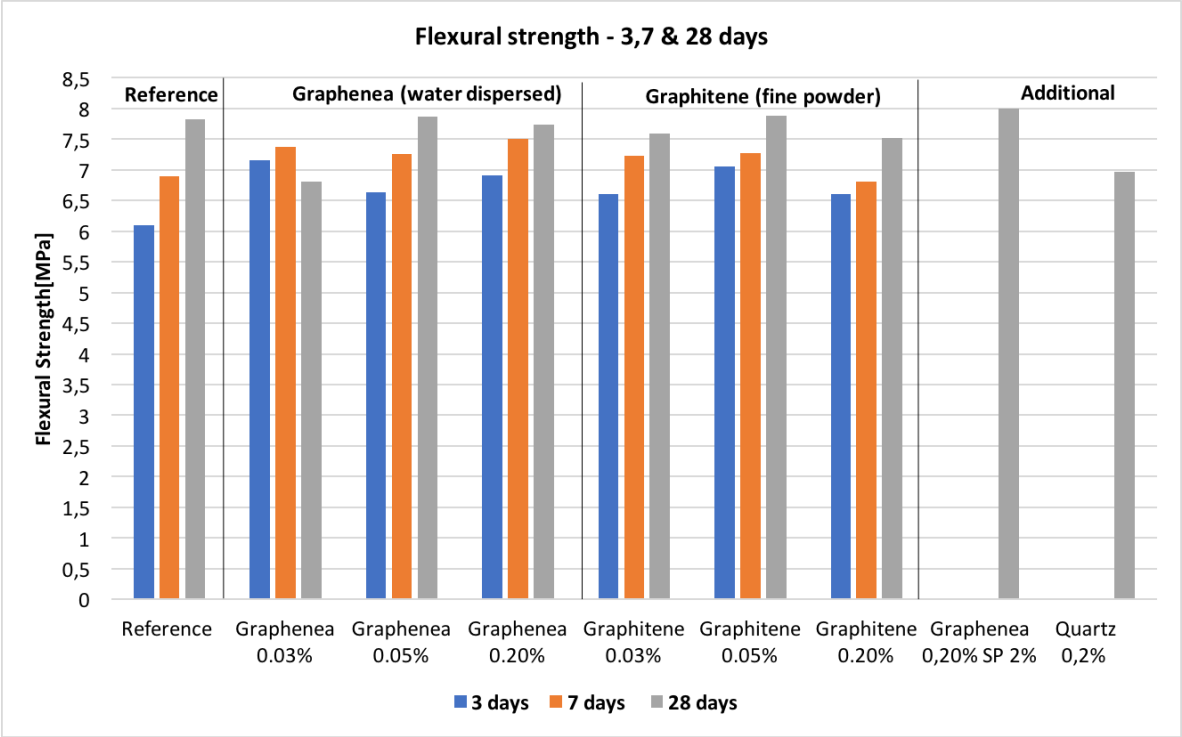

Figure 93. Flexural Strength after 3,7 & 28 days of curing (Kjaernsmo, 2017)

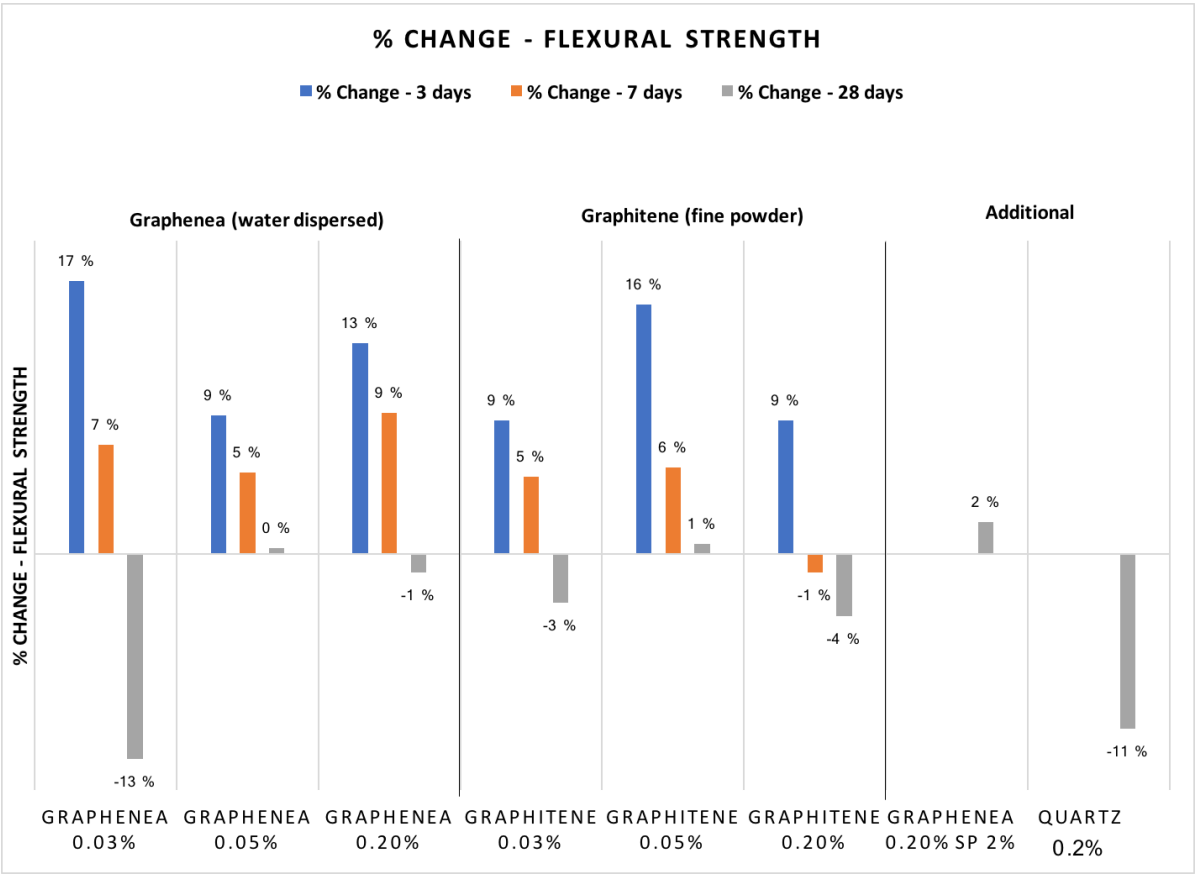

Figure 94. Percent change in the flexural strength with respect to the reference mortar (Kjaernsmo, 2017)

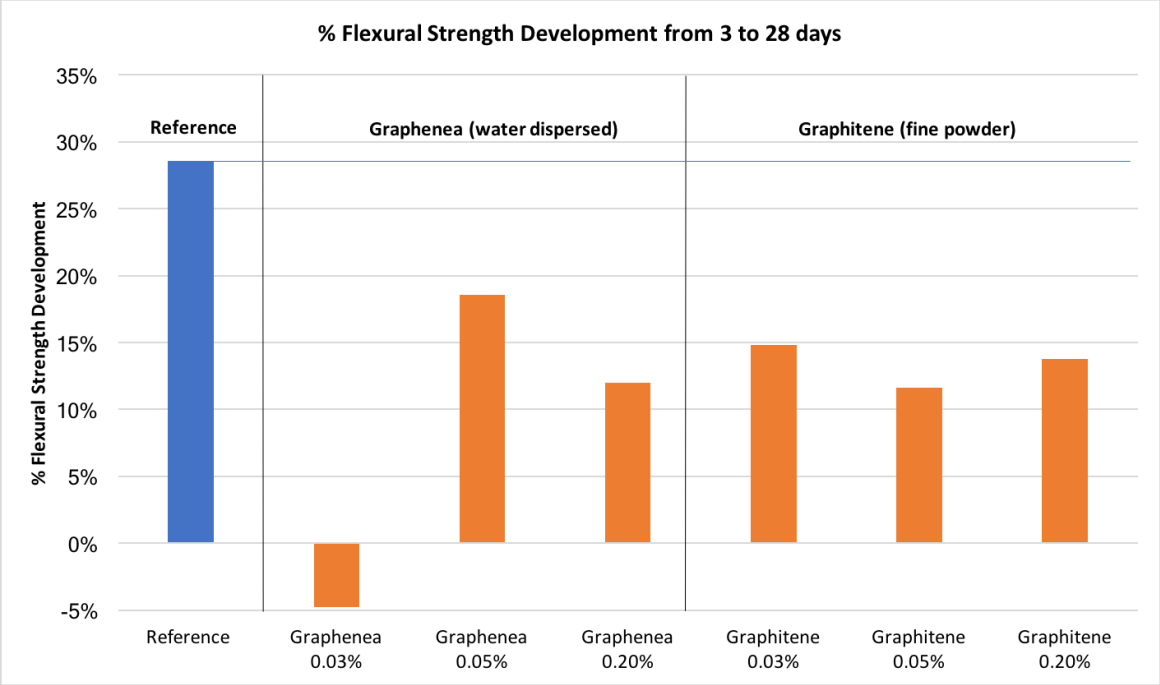

Figure 95. Percent flexural strength development from 3 to 28 days of curing (Kjaernsmo, 2017)

4.4.2 Compressive strength

4.4.2.1 Strain Distribution – Verification of the Compressive Strength Test

The strain distribution during the compressive strength test is presented in Figure 96.
The red zones, which indicate a relatively higher substantial strain compared to other parts of the specimen, are first initiated in the middle of the specimen, as illustrated in Figure 96. The strain distribution propagates then towards the bottom and the top part. The observed strain distribution and the propagation is equivalent to a traditional compressive strength test with cubes, and the selected method of determining the compressive strength can be considered as valid.

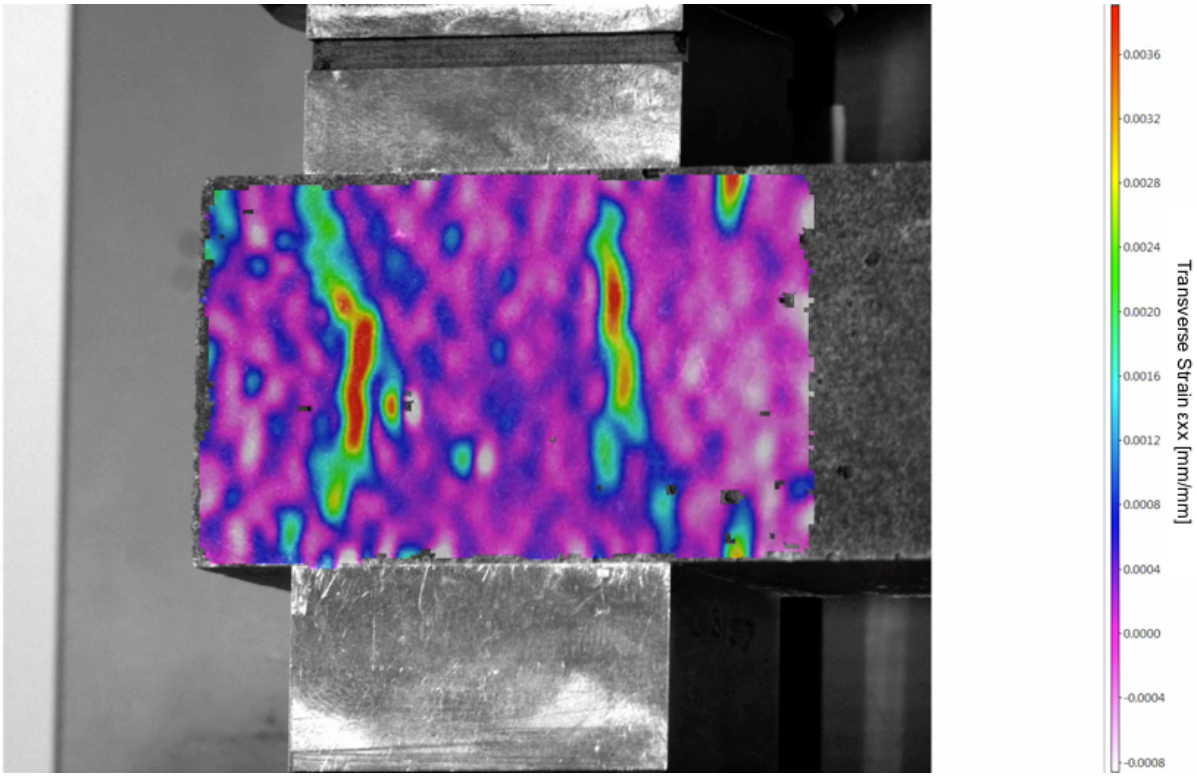

Figure 96. Transverse Strain distribution in the x-direction (Horizontally), (Kjaernsmo, 2017)

4.4.2.2 *Compressive Strength Results*

The compressive strength after three, seven and 28 days of curing is presented in Figure 97. The percent changes and the compressive strength developments are presented in Figure 98 and Figure 99, respectively.

The compressive strength correlates with the flexural strength reported in Section 4.4.1.2. Equivalent to what have been reported in the Section 4.4.1.2, graphene oxide increases the early compressive strength after three and seven days, but have no effect after 28 days of curing. In addition, the compressive strength for Graphenae 0.2% is reduced by 8 % after 28 days, while compressive strength for Graphenea 0.2% & SP 2.0% is improved by 7 % after 28 days. This indicates that the reduced workability, reported in Section 4.1.1, has a considerable effect on the compressive strength and can create a variation of 15 %.

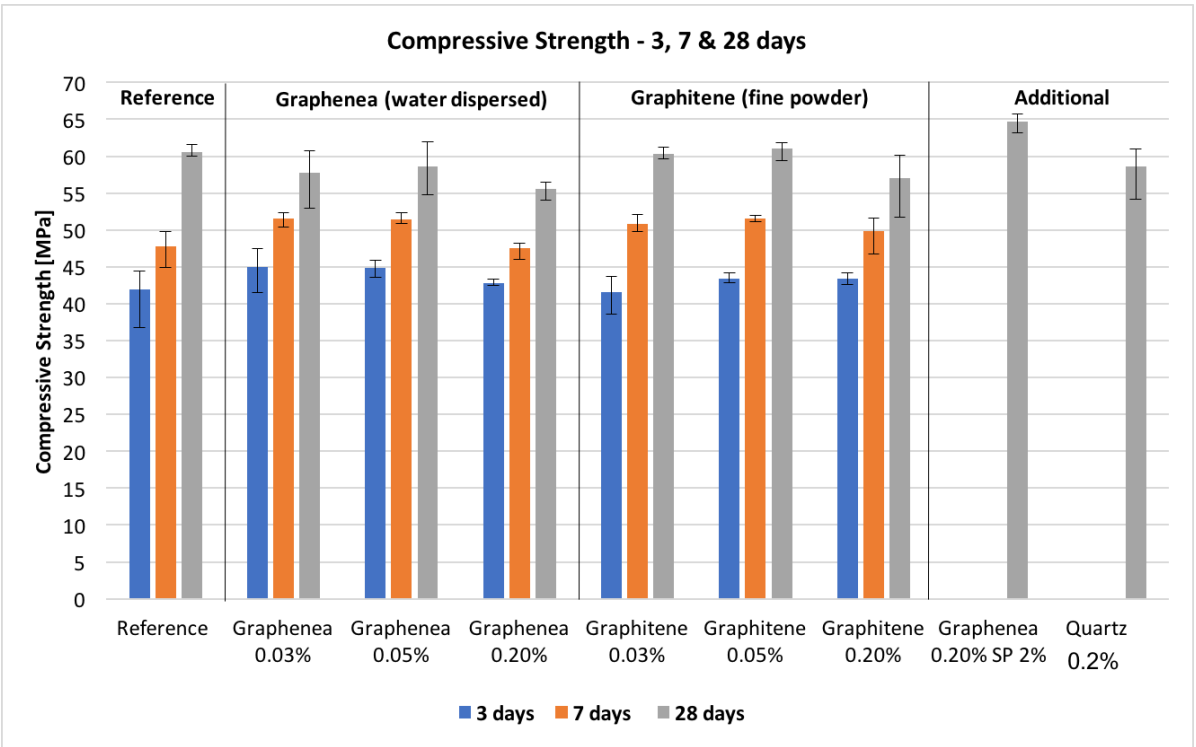

Figure 97. Compressive Strength after 3,7 & 28 days of curing. The error bar represents the maximum and minimum compressive strength within a set of results. (Kjaernsmo, 2017)

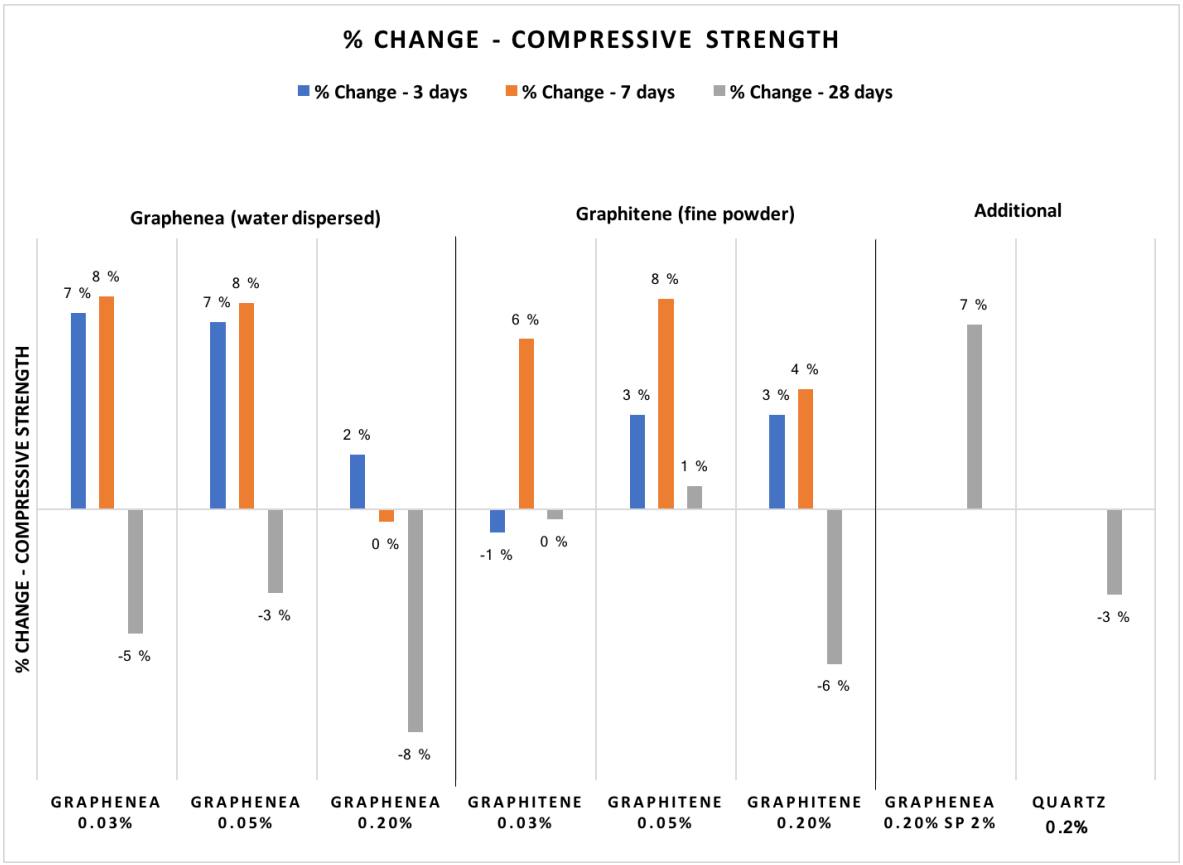

Figure 98. Percent change in the compressive strength with respect to the reference mortar (Kjaernsmo, 2017)

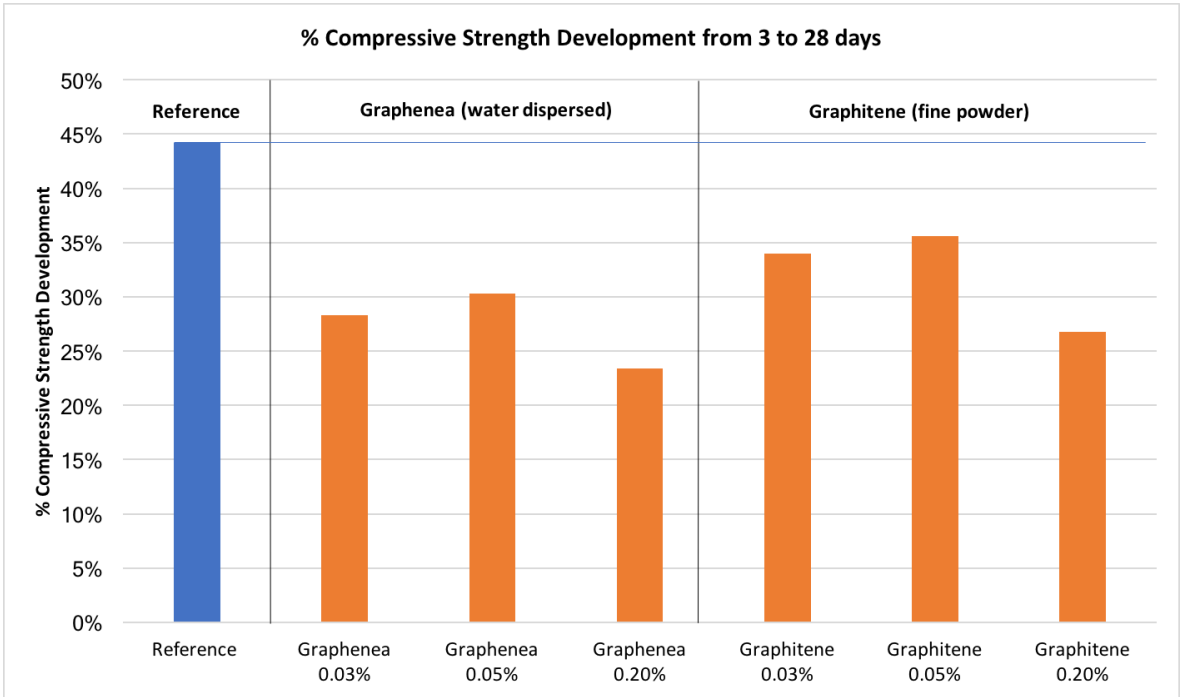

Figure 99. Percent compressive strength development from 3 to 28 days of curing (Kjaernsmo, 2017)

4.4.3 Splitting Tensile Strength

4.4.3.1 Strain Distribution – Verification of the Splitting Tensile Test

According to the theoretical cylinder stress distribution, presented in Section 3.4.9.2, the top and bottom part of the cylinder face are subjected to compression, while the middle is exposed to tension.

Figure 100 presents the horizontal strain (ε_{xx}) evolution on the cylinder face during the splitting tensile test. The images show no substantial strain near the edges of the cylinder, while the red areas in the middle indicate strain. The strain evolution arises first in the middle of cylinder face and propagates outwards to the cylinder edge. This is illustrated by Image #1 to Image #6 in Figure 100. These observations can be associated with the theoretical cylinder stress distribution, presented in Section 9.4.9.2. However, it is important to emphasize that the presented theory of the splitting tensile test is related to stress through the whole cylinder, and the images express the actual strain distribution observed on the cylinder face.

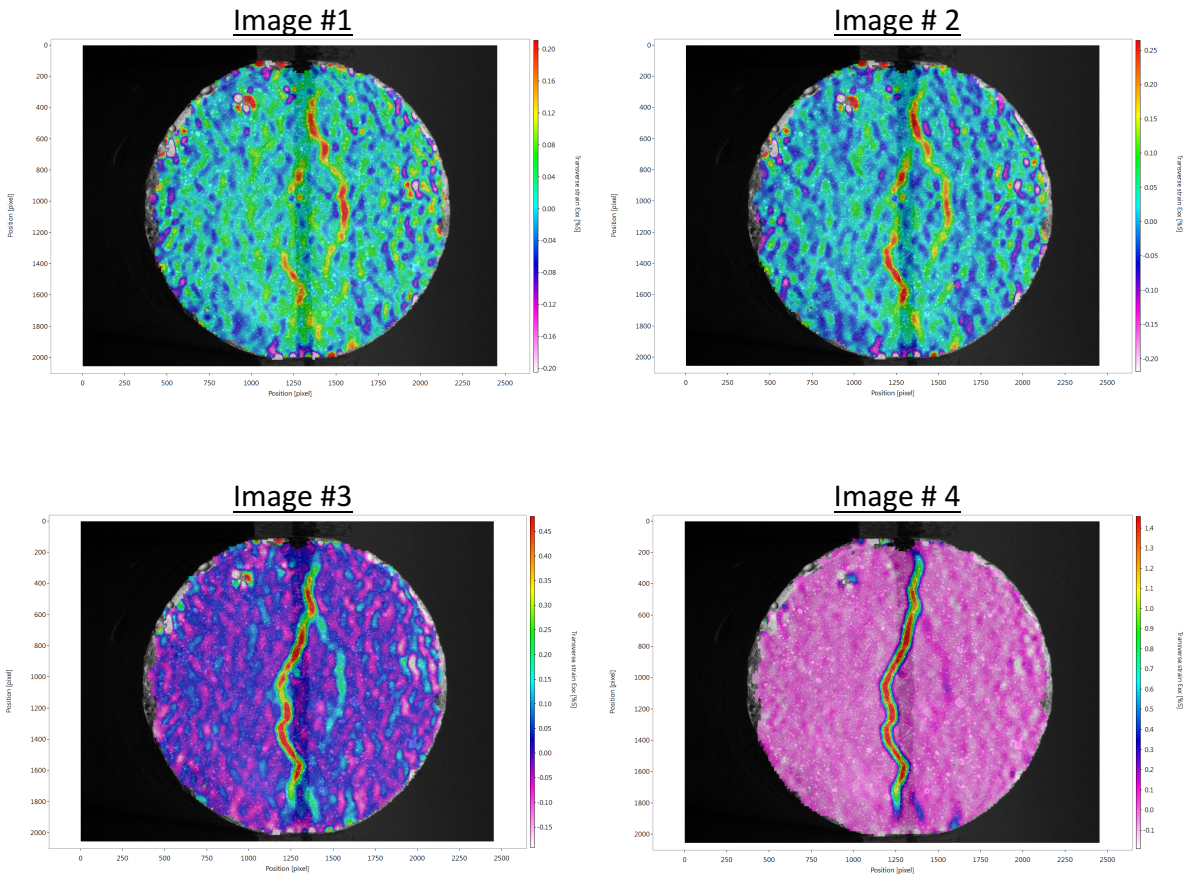

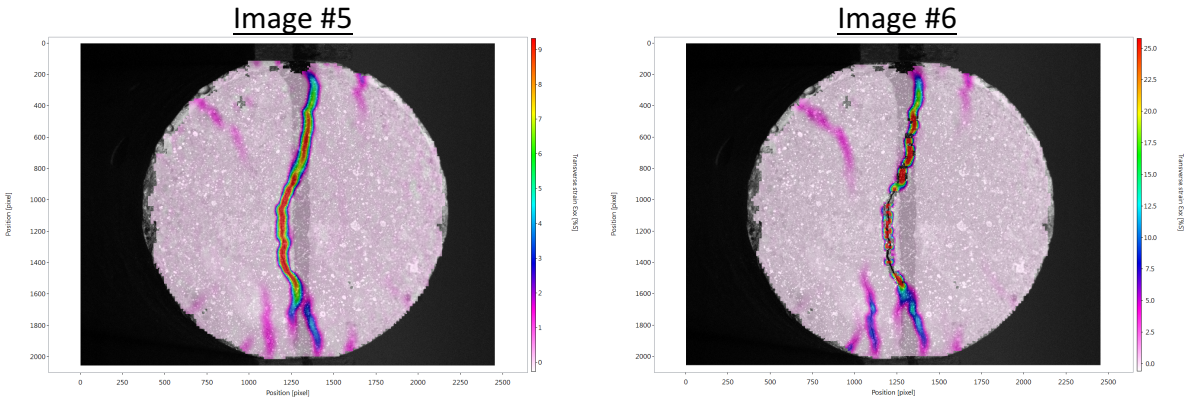

Figure 100. Strain evolution (Transverse Strain [ε_{xx}]) during the splitting tensile test (Kjaernsmo, 2017)

Three virtual strain gauges were arranged as illustrated in Figure 101. The corresponding strain evolutions are presented in Figure 102. The virtual strain gauge positioned in the center of cylinder face (red) show substantial larger strain compared to those located close to the edges (blue & green). Moreover, the bottom strain gauge (green) shows a negative strain in the earlier stages of the strain evolution. These results indicate that the selected setup for the splitting tensile strength test provides equivalent stresses as for a conventional splitting tensile test with a larger cylinder and different loading rate.

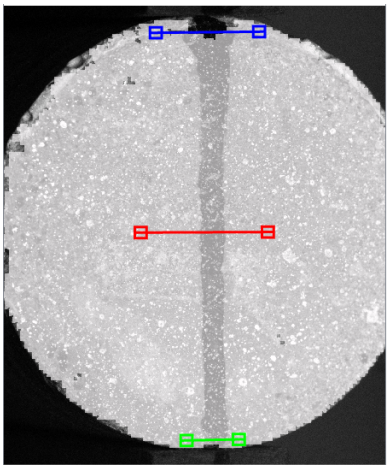

Figure 101. Virtual Strain gauges (extensometers) on the cylinder face (Kjaernsmo, 2017)

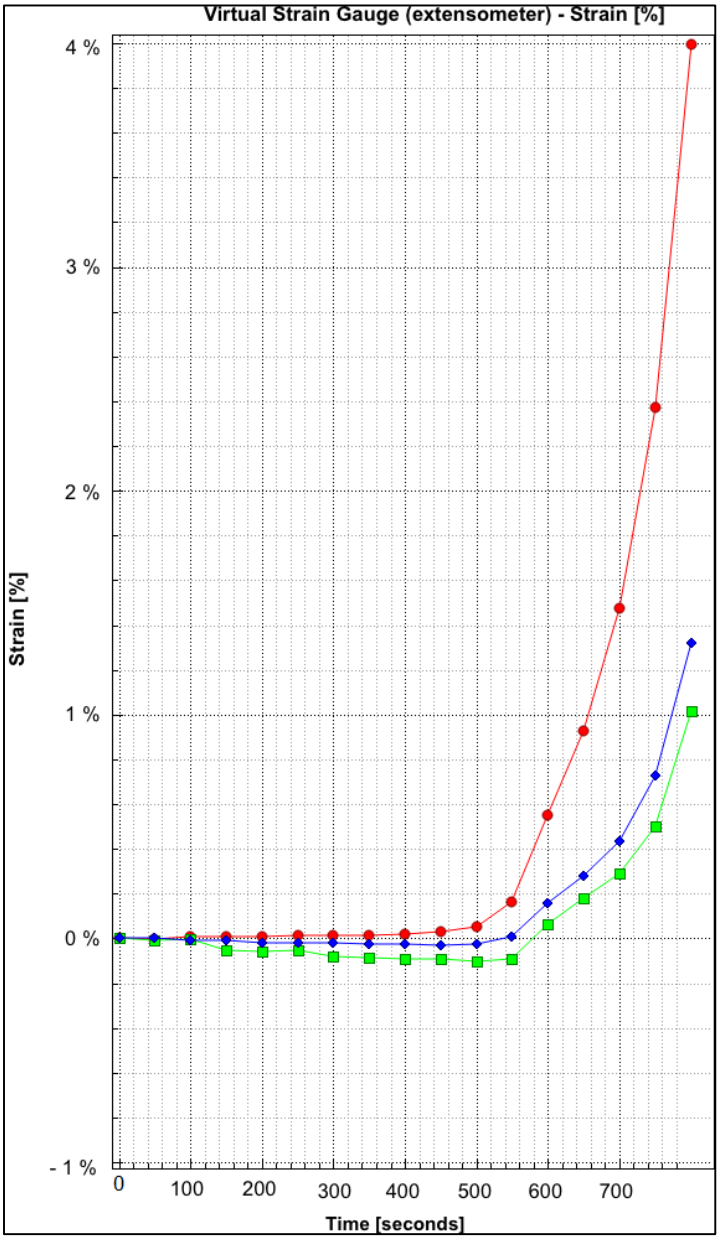

Figure 102. Strain evolution corresponding to the strain gauge (extensometer) color. (Kjaernsmo, 2017)

4.4.3.2 *Splitting Tensile Strength Results*

The splitting tensile strength results and the percent changes compared to reference mortar are presented in Figure 103 and Figure 104, respectively.

The results show an enhanced splitting tensile strength after three and seven days of curing for the cement mortar containing Graphenea. The highest enhancement is 19 % for the cement mortar containing 0.2 % Graphenea and after three days of curing. Moreover, this enhancement seems to decline during the hydration process, and after 28 days the splitting tensile strengths are almost equal or less than the reference mortar. The results are almost equivalent to the reference mortar for the cement mortar containing 0.03% Graphitene. For the other mortar compositions containing Graphitene, the splitting tensile strength is reduced by 6 % and 8 % after 28 days.

The results indicate that graphene oxide produced by Graphena can accelerate the strength development in the early stages of the hydration process. The strength development seems to decline after three days of curing and no improvements are obtained after 28 days. The splitting tensile strength development is shown in Figure 105.

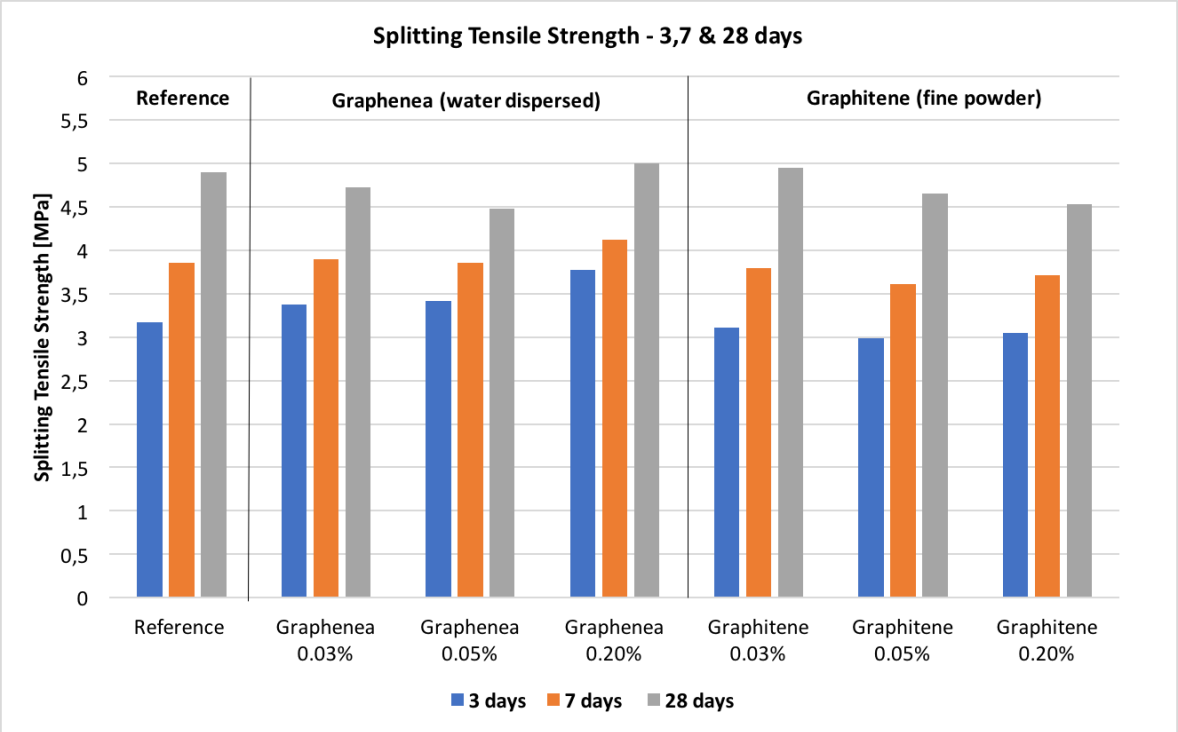

Figure 103. Splitting Tensile Strength after 3,7 & 28 days of curing (Kjaernsmo, 2017)

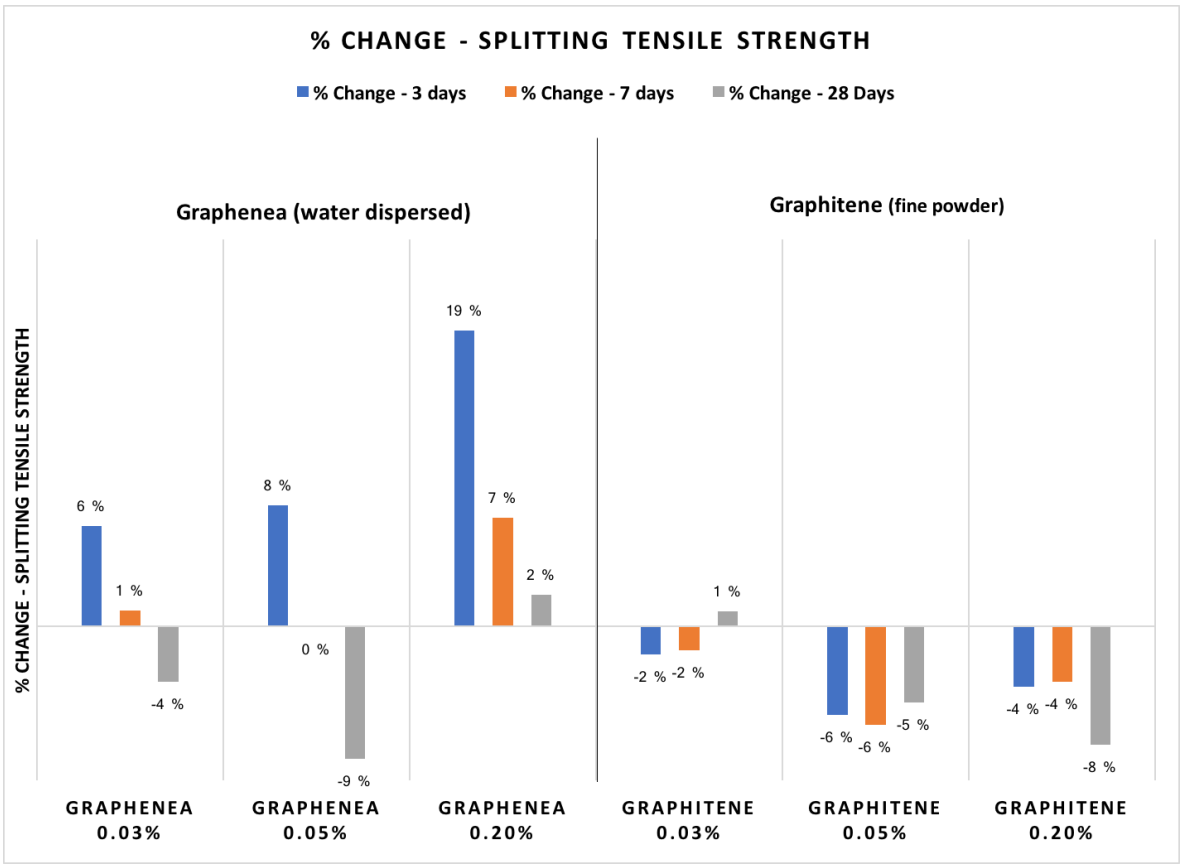

Figure 104. Percent change in splitting tensile strength compared with the reference mortar (Kjaernsmo, 2017)

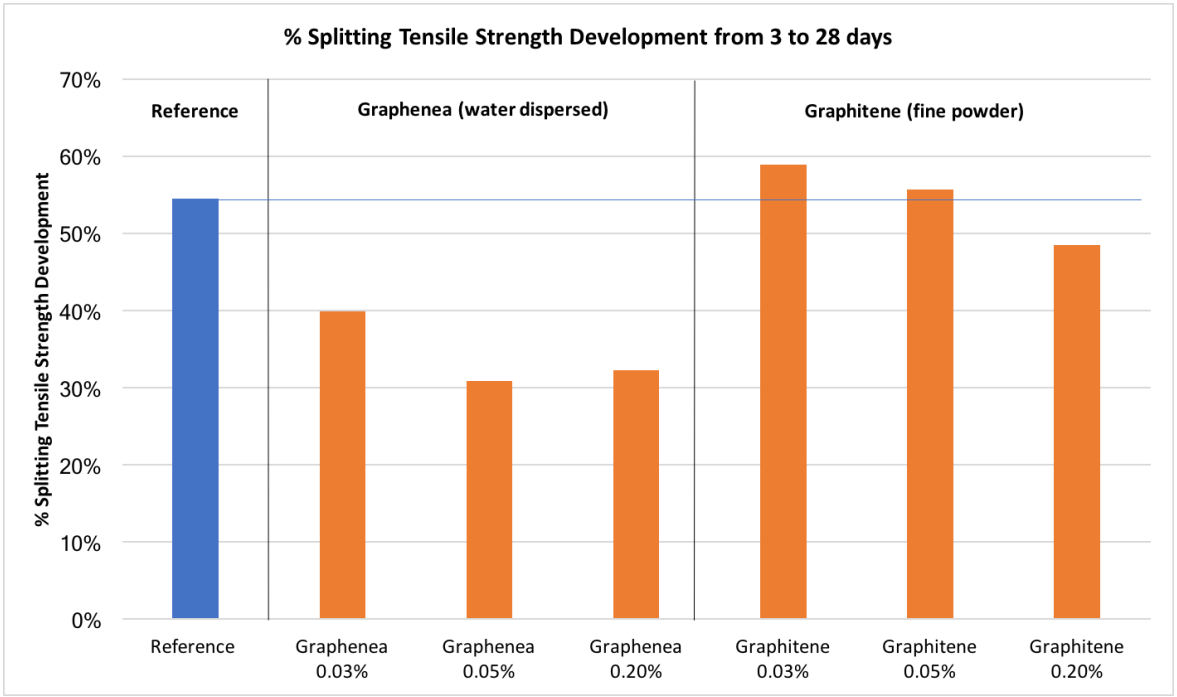

Figure 105. The percent splitting tensile strength development during the hydration process (Kjaernsmo, 2017)

4.4.4 Ultrasonic Velocity Test Results

4.4.4.1 The Modulus of Elasticity

The modulus of elasticity is calculated by the equations presented in Section 3.4.6.2. The modulus of elasticity (M) after seven and 28 days of curing is presented in Figure 106, and the percent changes with respect to the reference mortar are presented in Figure 107. The results show a reduced modulus of elasticity for the mortar cylinders containing Graphenea, especially after 28 days of curing.

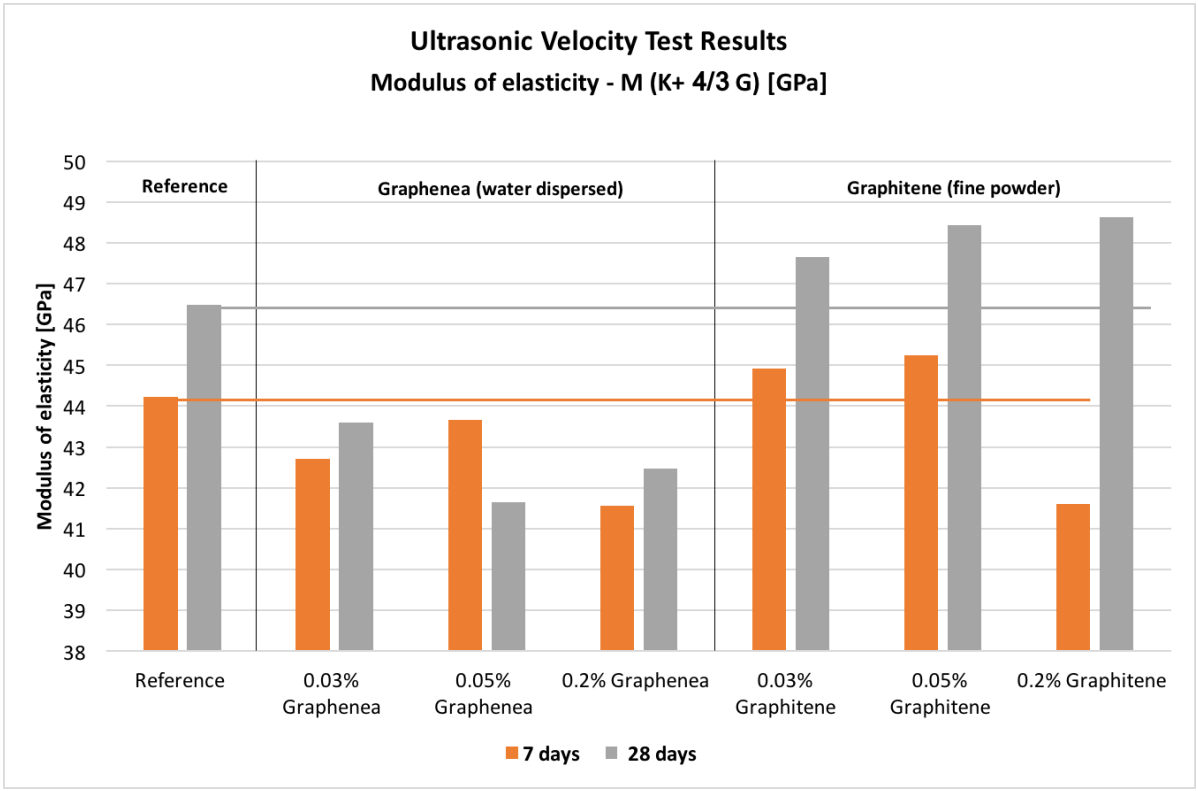

Figure 106. Ultrasonic Test Results - The special modulus of elasticity (Kjaernsmo, 2017)

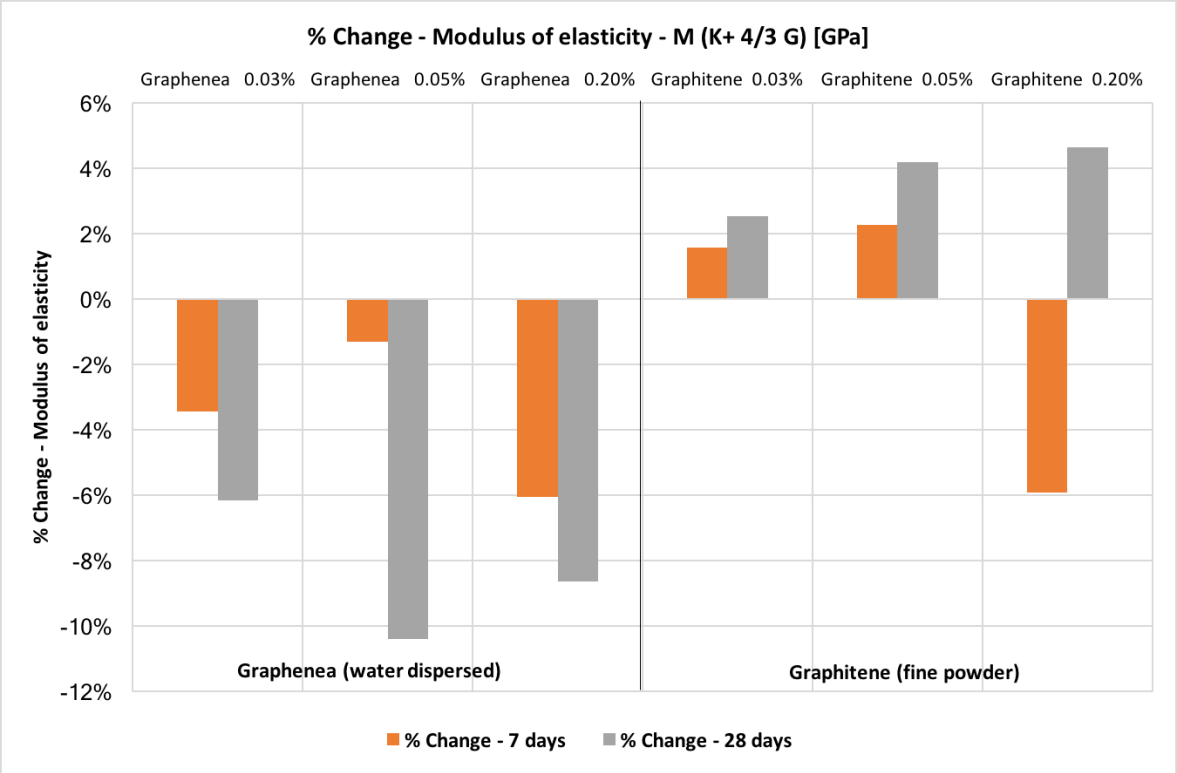

Figure 107. Ultrasonic Test Results - The Percent Change with respect to the reference (Kjaernsmo, 2017)

4.4.4.2 Detecting embedded air voids through sonic velocity

The ultrasonic velocity test results can also indicate how the reduced workability influences the amount of embedded air voids in the mortar. Since the sonic sound is not transmitted through air bubbles and voids, the sonic travel time will increase if large air bubbles or voids lie in the sonic travel path (Pan et al., 2015). With the purpose of investigating this theory, the change of sonic velocity is analyzed and presented Figure 108 and Figure 109. The sonic velocity is considered more accurate since the cylinder lengths have some variance (1-2 mm). In this case, a reduced sonic velocity indicates possible embedded air voids. The sonic test results, presented in Section 4.4.4.1, take the density into account, and can therefore not be used to quantify possible air voids. The sonic velocity is calculated according to equation (4) presented in Section 3.4.6.2.

4.4.4.3 *The Sonic Velocity*

The sonic velocity is reduced for the mortar cylinders containing Graphenea which indicates a higher content of embedded air bubbles and voids. Furthermore, the results from the density of hardened mortar and the mini-flow test indicates both directly and indirectly similar findings. Figure 108 and Figure 109 show a reduced sonic velocity for the cement mortar containing Graphenea.

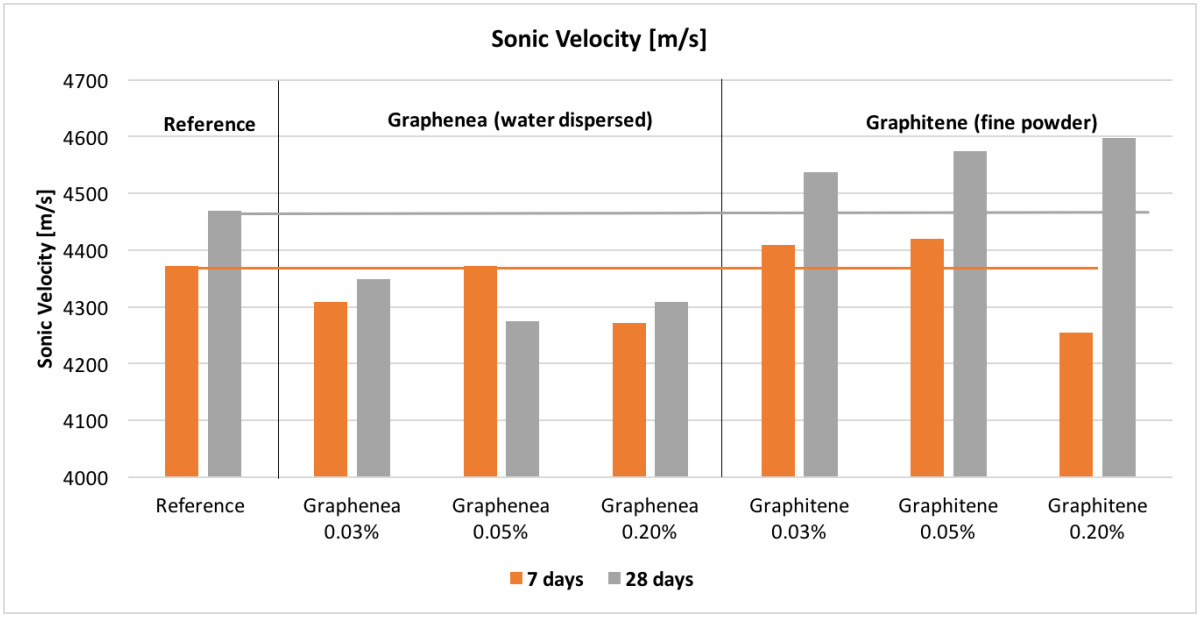

Figure 108. Sonic Velocity [m/s] (Kjaernsmo, 2017)

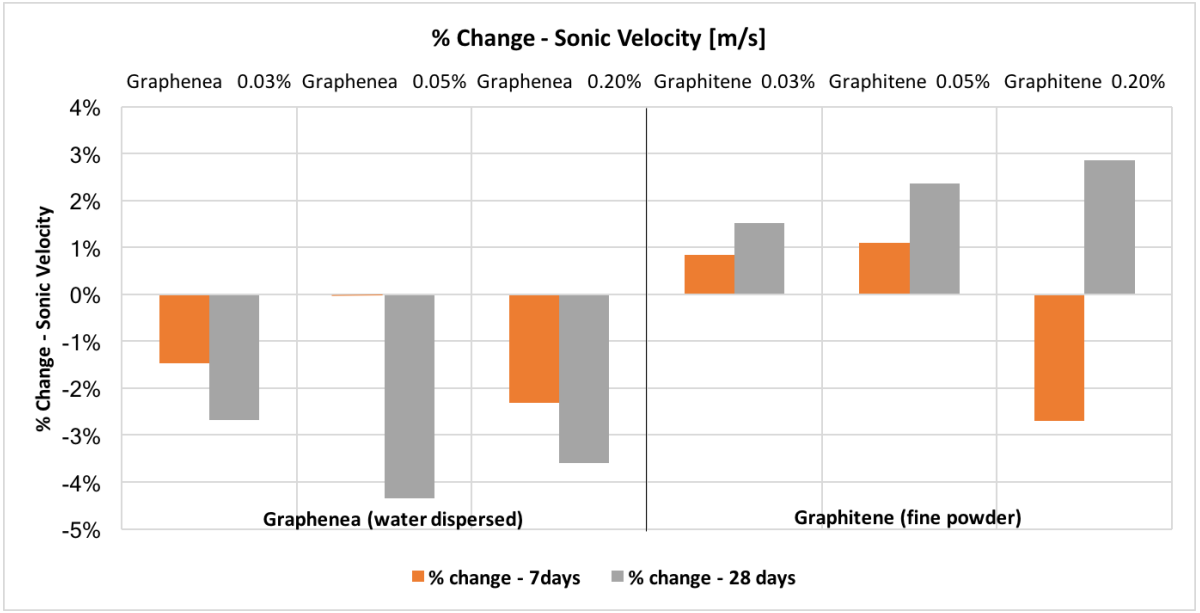

Figure 109. Percent changes in the sonic velocity with respect to the reference mortar (Kjaernsmo, 2017)

4.5 The effect of GO on the Microstructure – SEM & EDS

Graphene oxide sheets were only observed by the scanning electron microscope (SEM) in a sample taken from the cement mortar containing 0.05% Graphenea. The low dosages of GO (0.03 wt%, 0.05 wt%, and 0.2 wt% of cement weight) and the small sample size can explain why graphene oxide sheets were not observed in the other mortar compositions. The graphene oxide sheets were verified by analyzing the bright objects with the energy dispersive X-ray spectroscopy. The analyzed bright objects were selected because they did not look like traditional hydration products and because of their particular shape.

The graphene oxide sheets illustrated in Figure 110, Figure 113, and Figure 114, are observed at different locations on the sample. The size (width or length) varies approximately from 0.865 μm to 16.87 μm (diameter of a human hair is approximately 17 to 181 μm). Figure 110 illustrates a wrinkled graphene oxide sheet located next to a small air bubble. The EDS spectrum and the percent element composition is presented bellow in Figure 112 and Table 14, respectively. The element analysis shows a carbon content of 64.61 % and 16.34 % oxygen. The high content of palladium in the spectrum is a consequence of the sample covering procedure explained in Section 3.4.11. Palladium is therefore eliminated from the element analysis. The element composition indicates with a high probability that the observed object is a graphene oxide sheet or sheets. The spectrums are validated by analyzing several points in the bright objects, and by determining the element composition for objects nearby. Figure 113 and Figure 114 illustrates similar observations as in Figure 110 with equivalent EDS spectra and element analyses (Table 15 & Table 16). Moreover, the GO sheet observed in Figure 113 has a more distinct polyhedron shape compared to Figure 110. The smallest observed graphene oxide sheet is illustrated in Figure 114. Also, similar wrinkled-shaped graphene oxide sheets have been observed in previous research, but the element analysis showed a larger content of calcium (Ca). This is illustrated in Section 2.9 (Figure 17 & Figure 18).

No distinct variation in the interfacial transition zone (ITZ) between the different samples were observed, except for the graphene oxide sheet located in the ITZ for the cement mortar containing 0.05% Graphenea. This is illustrated in Figure 113. The SEM images of ITZ for the different type and dosages of GO are presented in Appendix D.

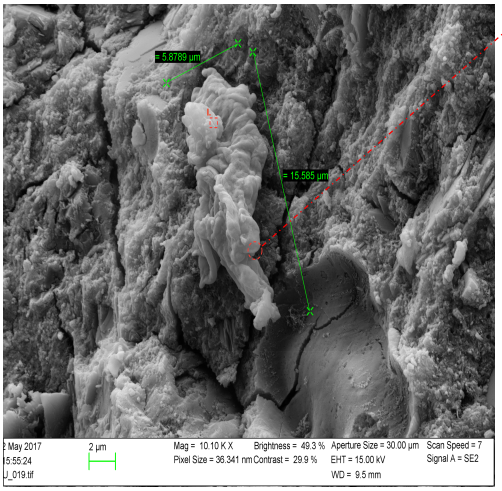

Figure 110. Graphene Oxide sheet & Spectrum 1 (Kjaernsmo, 2017)

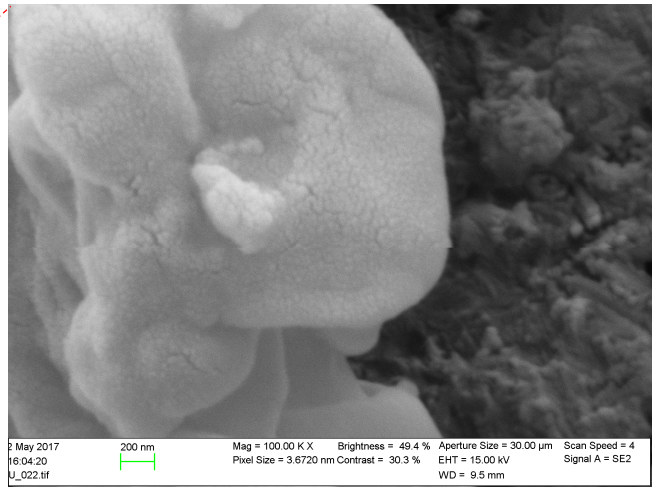

Figure 111. Surface of the graphene oxide sheet (Kjaernsmo, 2017)

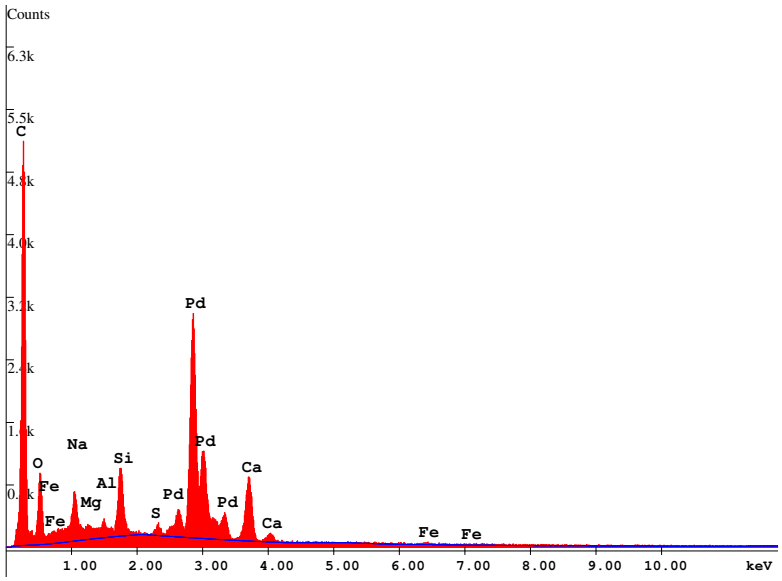

Figure 112. Spectrum I (Kjaernsmo, 2017)

Table 14. Spectrum I - Element Analysis (Kjaernsmo, 2017)

Element	Wt %	At %	K-Ratio	Z	A	F
C K	64.61	76.30	0.3005	1.0189	0.4564	1.0002
O K	16.36	14.50	0.0351	0.9998	0.2144	1.0002
NaK	6.30	3.88	0.0358	0.9333	0.6092	1.0007
MgK	0.74	0.43	0.0050	0.9561	0.6984	1.0012
AlK	0.73	0.38	0.0055	0.9241	0.8097	1.0020
SiK	3.00	1.52	0.0251	0.9442	0.8862	1.0016
S K	1.34	0.59	0.0120	0.9362	0.9589	1.0036
CaK	6.27	2.22	0.0581	0.9178	1.0090	1.0005
FeK	0.65	0.16	0.0054	0.8249	1.0075	1.0000
Total	100.00	100.00				

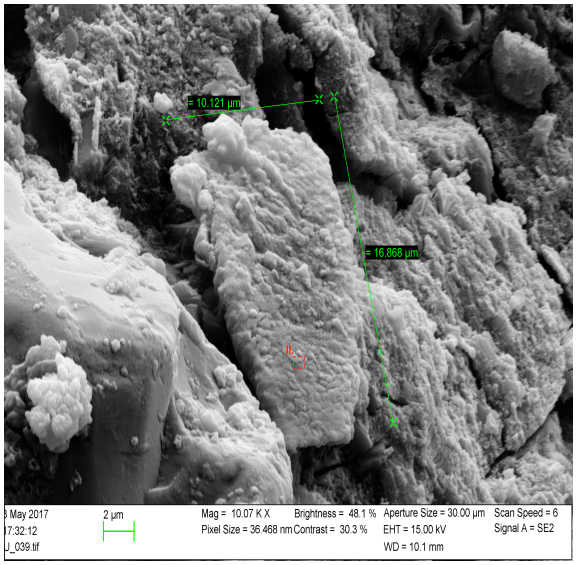

Figure 113. Graphene Oxide Sheet located in the ITZ & Spectrum II (Kjaernsmo, 2017)

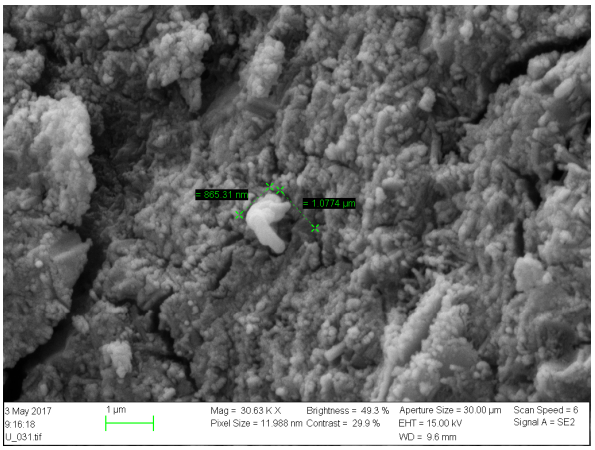

Figure 114. The smallest observed Graphene Oxide sheet. Spectrum III is located in the center of the bright object. (Kjaernsmo, 2017)

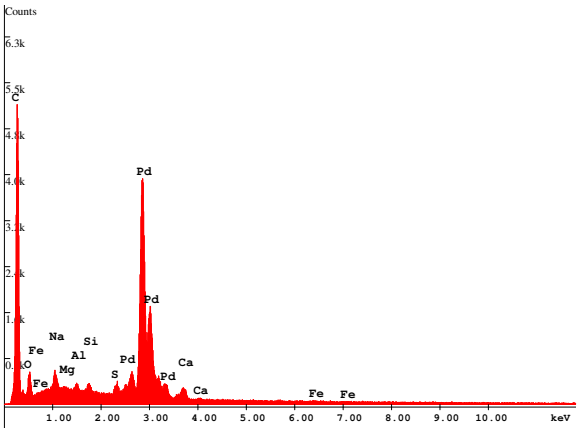

Figure 115. Spectrum II (Kjaernsmo, 2017)

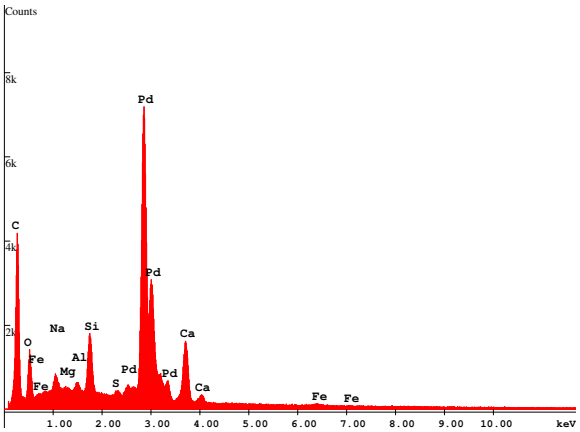

Figure 116. Spectrum III (Kjaernsmo, 2017)

Table 15. Spectrum II - Element Analysis (Kjaernsmo, 2017)

Element	Wt %	At %	K-Ratio	Z	A	F
C K	73.89	83.03	0.3600	1.0140	0.4804	1.0001
O K	11.89	10.03	0.0253	0.9950	0.2139	1.0002
NaK	5.95	3.49	0.0354	0.9289	0.6400	1.0006
MgK	0.98	0.54	0.0068	0.9516	0.7259	1.0009
AlK	0.97	0.48	0.0074	0.9194	0.8294	1.0013
SiK	0.88	0.42	0.0075	0.9389	0.8989	1.0018
S K	2.73	1.15	0.0249	0.9312	0.9763	1.0013
CaK	1.97	0.66	0.0182	0.9130	1.0108	1.0007
FeK	0.74	0.18	0.0062	0.8203	1.0106	1.0000
Total	100.00	100.00				

Table 16. Spectrum III - Element Analysis (Kjaernsmo, 2017)

Element	Wt %	At %	K-Ratio	Z	A	F
C K	55.74	70.05	0.2219	1.0254	0.3881	1.0002
O K	18.57	17.52	0.0397	1.0061	0.2122	1.0002
NaK	5.40	3.54	0.0295	0.9391	0.5821	1.0010
MgK	0.90	0.56	0.0059	0.9620	0.6843	1.0018
AlK	1.19	0.67	0.0088	0.9304	0.7965	1.0030
SiK	4.97	2.67	0.0414	0.9514	0.8725	1.0022
S K	1.60	0.75	0.0143	0.9428	0.9416	1.0052
CaK	10.31	3.88	0.0957	0.9241	1.0033	1.0008
FeK	1.32	0.36	0.0110	0.8311	1.0039	1.0000
Total	100.00	100.00				

4.6 Sources of Errors in the Experimental Program

4.6.1 Preparation of cement mortar – The reduced Workability

The reduced workability because of less free water can create large air voids in the mortar specimens. These air voids should be considered as possible flaws, and since cementitious mortar is a brittle material, these flaws will reduce the mechanical strength. A Similar explanation of a reduced mechanical strength when adding nanomaterials is also reported by Chuah et al. (2014).

Alternatively, the cement mortar compositions could have been prepared with an SP content which provides an equivalent workability as the reference mortar. But potential side-effects of GO will then not be reported precisely.

4.6.2 Preparation of GO - Multiply GO sheets can create weak bonding

The preferred type of graphene oxide consists of only monolayers, because the bonds between the graphene oxide layers (sheets) are created by Van der Waals forces which can generate weakness in the cement mortar in case of bonding failure(Xiangyu Li et al., 2016). This possible weakness can be reduced by using-ultra sonication with the purpose increase the content of monolayers. Ultra-sonic treatment uses high energy sound waves to break the Van der Waals forces and increase the content of monolayers.

4.6.3 Test Setup - Three-point bending test according to NS-196:2016

The three-point bending test provides a very concentrated strain zone, and the final flexural strength can be a result of the weakness in that specific part of the beam. This theoretical assumption is confirmed by analyzing the three-point bending test with a strain camera. Figure 91 (Section 4.4.1.1) illustrates how the maximum strain propagates in a very concentrated part of the beam. Alternatively, the test setup could have been modified to either a four-point bending test or by applying a distributed load with the purpose of allocating the strain propagation in a larger part of the beam.

On the other hand, this test procedure is confirmed to be acceptable by the European Committee of Standardization (CEN), and has the advantages of testing the flexural and compressive strength with the same specimen. In this thesis, the procedure of multiply testing with the same specimen has been found to be acceptable by analyzing the three-point bending test with the strain camera. Figure 91, Section 4.4.1.1, indicates that the prism ends that are used for the compressive test are not exposed to substantial strain during the first mechanical test (three-point bending test).

5 Conclusions

Numerous effects of graphene oxide (GO) on the cement mortar have been observed and quantified by the experimental program. Generally, the water dispersed GO had a larger influence on the properties of cement mortar compared to the fine powder GO. The following conclusions are organized according to the thesis objectives:

1) The effect of GO on fresh cement mortar

Workability

The workability is reduced by the increasing content of water dispersed GO, but is less affected by fine powder GO. The consistency of fresh mortar with the highest content of water dispersed GO (0.2 wt%) is categorized as stiff plastic.

Content of air

GO has almost no effect on the content of air in the fresh mortar, except for the cement mortar with the highest content of water dispersed GO (0.2 wt%) and is an indirect outcome of poor workability.

Density of fresh and hardened mortar

The density of fresh mortar is slightly reduced by both types of GO. There is a more distinct change for the mortar containing the highest content of water dispersed GO (0.2 wt%). This corresponds also with the reduced workability and the increased content of air in the fresh mortar. Furthermore, the density of the hardened mortar is reduced by the increasing content of water dispersed GO, but is constant for the fine powder GO.

Hydration process

The heat of hydration is increased by GO, and especially for the highest content of water dispersed GO. The increased exothermal heat development indicates a chemical reaction between the GO sheets and the cement components.

2) The effect of GO on mechanical properties

Flexural strength

GO enhances the flexural strength after three and seven days, but has no effect after 28 days. The results show no correlation between the content of GO and the flexural strength. Moreover, the highest improved flexural strengths were in the range of 9-17% and observed after three days of curing.

Compressive strength

The effect of GO on the compressive strength corresponds to the flexural strength. Except for a 7 % improvement for the cement mortar with 0.2 wt% water dispersed GO and a content of polycarboxylate which provides an equivalent workability as the reference mortar (additional mortar composition).

Splitting Tensile Strength

Water dispersed GO increases the splitting tensile strength after three days of curing, but the enhancement decreases after seven days, and no effect after 28 days of curing. In addition, the fine powder GO has almost no influence on the splitting tensile strength after three, seven and 28 days.

The dynamic modulus of elasticity & Ultrasonic Velocity

No distinct variations in the dynamic modulus of elasticity are detected after seven days of curing. After 28 days of curing the water dispersed GO reduces the dynamic modulus of elasticity, and the opposite effect is observed for fine powder GO. Moreover, the reduced sonic velocity for cement mortar with water dispersed GO indicates an increased content of air voids due to a diminished workability.

3) The effect of GO on the microstructure

Graphene oxide sheets were observed by scanning electron microscopy and verified by the energy dispersive X-ray detector, but only in sample containing water dispersed GO. The sheet size varies from 0.865 μm to 16.87 μm. The element composition showed a high content of carbon (55.74 - 73.89 wt%) and oxygen (11.89 – 18.57 wt%). Furthermore, no distinct change in the interfacial transition zone or the bulk cement paste have been observed, except for the presence of GO sheets.

6 Future work

The following bullet points are my suggestions for future work within the field of graphene oxide (GO) as an additive in cementitious materials:

- The effect of GO containing only monolayers.
- Investigate possible issues and solutions for the reduced workability, which seems to be not only a case for GO, but also a general concern with other potential nanomaterials according to (Chuah et al., 2014).
- Potential side-effects from mixing GO and polycarboxylate, and especially with respect to the temperature development and the heat of hydration.
- Mechanical properties after 56, 90, and 180 days of curing.
- Permeability.
- Conductivity – Utilize GO as a functional filler in Self-Sensing Concrete. Study the change in electrical resistivity during mechanical testing.

This page intentionally left blank.

References

Bedwani. (2017). X-RAY FLUORESCENCE SPECTROSCOPY (XRF) [Picture]. Retrieved from http://www.bedwani.ch/xrf/xrf_1/xrf.htm

Bruker. (2017). Handheld XRF: How it works [Picture]. Retrieved from https://www.bruker.com/products/x-ray-diffraction-and-elemental-analysis/handheld-xrf/how-xrf-works.html

Chuah, S., Pan, Z., Sanjayan, J. G., Wang, C. M., & Duan, W. H. (2014). Nano reinforced cement and concrete composites and new perspective from graphene oxide. *Construction and Building Materials, 73*, 113-124. doi:http://dx.doi.org/10.1016/j.conbuildmat.2014.09.040

Ghavanini, F. A., & Theander, H. (2015). *Graphene feasibility study - and foresight study for transport infrastructures*. Retrieved from https://www.chalmers.se/sv/nyheter/Documents/Graphene and transport infastructure.pdf

Gong, K., Pan, Z., Korayem, A. H., Qiu, L., Li, D., Collins, F., . . . Duan, W. H. (2015). Reinforcing Effects of Graphene Oxide on Portland Cement Paste. *Journal of Materials in Civil Engineering, 27*(2). doi:doi:10.1061/(ASCE)MT.1943-5533.0001125

Graphenea. (2017). Product Datasheet Graphenea Graphene Oxide Retrieved from https://www.graphenea.com/products/graphene-oxide

GraphiteneLdt. (2017a). Cement Concrete Admixtures – Fine Powder Concentrate Retrieved from https://www.graphitene.com/buy-graphene-online/graphitene-admixture/cement-concrete-admixtures-fine-powder-concentrate/

GraphiteneLdt. (2017b). Eco Graphene Oxide - Product Data Sheet. Retrieved from http://www.gtma.co.uk/wp-content/uploads/2016/10/DS-eco-GO-1525-v1_1.pdf

InTechopen. (2017). Graphene — A Platform for Sensor and Biosensor Applications [Picture]. Retrieved from https://www.intechopen.com/books/biosensors-micro-and-nanoscale-applications/graphene-a-platform-for-sensor-and-biosensor-applications

Kang, D., Seo, K. S., Lee, H., & Chung, W. (2017). Experimental study on mechanical strength of GO-cement composites. *Construction and Building Materials, 131*, 303-308. doi:https://doi.org/10.1016/j.conbuildmat.2016.11.083

LearnXRF. (2017). Wavelength Dispersive X-ray Fluorescence (WD-XRF) [Picture]. Retrieved from http://learnxrf.com/wavelength-dispersive-x-ray-fluorescence-wd-xrf/

Leng, Y. (2013). *Materials Characterization*. Somerset, GERMANY: John Wiley & Sons, Incorporated.

Li, X., Korayem, A. H., Li, C., Liu, Y., He, H., Sanjayan, J. G., & Duan, W. H. (2016). Incorporation of graphene oxide and silica fume into cement paste: A study of dispersion and compressive strength. *Construction and Building Materials, 123*, 327-335. doi:https://doi.org/10.1016/j.conbuildmat.2016.07.022

Li, X., Li, C., Liu, Y., Chen, S. J., Wang, C. M., Sanjayan, J. G., & Duan, W. H. (2016). Improvement of mechanical properties by incorporating graphene oxide into cement mortar. *Mechanics of Advanced Materials and Structures*. doi:10.1080/15376494.2016.1218226

Lv, S., Ma, Y., Qiu, C., Sun, T., Liu, J., & Zhou, Q. (2013). Effect of graphene oxide nanosheets of microstructure and mechanical properties of cement composites. *Construction*

and Building Materials, 49, 121-127. doi:https://doi.org/10.1016/j.conbuildmat.2013.08.022

Magne, M., Sverre, S., O., K. K., Johan, S. E., Jan, L., Rolands, C., . . . Stefan, J. (2016). *Concrete Technology 1. TKT 4215. Compendium*. Trondheim: Institutt for konstruksjonsteknikk, NTNU.

MasterBuildersSolution. (2013). MasterGlenium ACE 434. Retrieved from https://assets.master-builders-solutions.basf.com/Shared Documents/PDF/Norwegian, Nynorsk (Norway)/basf-MasterGlenium-ace-434-db.pdf

Metha, P. K., & Monteiro, P. J. M. (2006). *CONCRETE Microstructure, Properties, and Materials*. United States of America: The McGraw-Hill Companies, Inc. .

Muhit, B. A. A. (2015). *Investigation on the Mechanical, Microstructural, and Electrical Properties of Graphene Oxide-Cement Composite.* (Master of Science (M.S.)), University of Central Florida Florida, USA.

NobelMedia. (2014). The 2010 Nobel Prize in Physics - Press Release [Press release]. Retrieved from http://www.nobelprize.org/nobel_prizes/physics/laureates/2010/press.htm

Norcem. (2017). Norcem = Norsk sement. Retrieved from http://www.norcem.no/no

Pan, Z., He, L., Qiu, L., Korayem, A. H., Li, G., Zhu, J. W., . . . Wang, M. C. (2015). Mechanical properties and microstructure of a graphene oxide-cement composite. *Cement and Concrete Composites*.

Quoracdn. (2017). What are the possible term symbols for the hybridized carbon atom (SP, SP2, SP3)? [Picture]. Retrieved from https://qph.ec.quoracdn.net/main-qimg-d0eb8b57d521980c3e0dcc848547882a

Shang, Y., Zhang, D., Yang, C., Liu, Y., & Liu, Y. (2015). Effect of graphene oxide on the rheological properties of cement pastes. *Construction and Building Materials, 96*, 20-28. doi:https://doi.org/10.1016/j.conbuildmat.2015.07.181

Sheriff, R. E., & Geldart, L. P. (1995). *Exploration Seismology* (Second ed.). The Pitt Building, Trumpington Street, Cambridge CB2 1RP, United Kingdom Cambridge University Press.

Tang, L., Liu, J., Wang, N., & Ye, L. (2014). *Pre-Study of Graphene-Enhanced Cementitious Materials*. Retrieved from Chalmers University of Technology, Gothenburg: http://publications.lib.chalmers.se/records/fulltext/236729/local_236729.pdf

TheManufactor. (2016). Talga Resources makes first delivery of graphene coating product [Picture]. Retrieved from https://www.themanufacturer.com/wp-content/uploads/2014/08/Graphene.jpg

UCL, U. C. L. (2007). University College London UCL- Spectral Emission Line Overlap Checker [Picture]. Retrieved from http://www.ucl.ac.uk/archmat/tools/emission.php

Vjayaraghavan, D. A. (2017). How strong is graphene? Retrieved from http://www.graphene.manchester.ac.uk/discover/video-gallery/what-is-graphene/how-strong-is-graphene/

Wang, Q., Wang, J., Lu, C.-x., Liu, B.-w., Zhang, K., & Li, C.-z. (2015). Influence of graphene oxide additions on the microstructure and mechanical strength of cement. *New Carbon Materials, 30*(4), 349-356. doi:http://dx.doi.org/10.1016/S1872-5805(15)60194-9

Zhao, L., Guo, X., Ge, C., Li, Q., Guo, L., Shu, X., & Liu, J. (2017). Mechanical behavior and toughening mechanism of polycarboxylate superplasticizer modified graphene oxide reinforced cement composites. *Composites Part B: Engineering, 113*, 308-316. doi:http://dx.doi.org/10.1016/j.compositesb.2017.01.056

List of Figures

List of Tables

Appendix

Appendix A – p.102

Mix design

Appendix B – p.104

Speedy Moisture Test Procedure

Appendix C – p.109

Mini-Flow Diameter
Percent Air of Fresh Mortar
Density of Fresh Mortar
Density of Hardened Mortar
Temperature - Max (peak) Temperature and % change
Temperature Development - Data
Cumulative Isothermal Heat Development (Curing-box spreadsheets)
Flexural Strength
Compressive Strength
Splitting Tensile Strength
Ultrasonic Velocity Test (Modulus of Elasticity & Sonic Velocity)

Appendix D – p.141

Interfacial Transition Zone – SEM images

Appendix E – p.144

Quartz Sand W12 (Quarzwerke GmbH) - Product Data

Appendix A

Mix Design

Mix Design:	Reference	Volume:	0,8 L
	Name:	w/c	0,5
Material	**Reference**		
Sand [g]	1350		
Water [g]	225		
Cement [g]	450		
SP wt% of cement weight	0,80 %		
SP [g] (liquid weight)	3,6		

Mix Design:	Graphenea	Volume:	0,8 L
	Name:	w/c	0,5
Material	**Graphenea 0.03%**	**Graphenea 0.05%**	**Graphenea 0.20%**
Sand [g]	1350	1350	1350
Water [g]	191,25	168,75	0
Cement [g]	450	450	450
SP wt% of cement weight	0,80 %	0,80 %	0,80 %
SP [g] (liquid weight)	3,6	3,6	3,6
GO wt % of cement weight	0,03 %	0,05 %	0,20 %
G0 [g]	0,135	0,225	0,900
GO [mg] (1 g = 1000 mg)	135	225	900
Concentration [mg/mL]*	4	4	4
Graphenea [mL]	33,75	56,25	225,00
* Concentration of GO in water dispersed Graphenea = 4 mg/mL			

Mix Design:	Graphitene	Volume:	0,8L
	Name:	w/c	0,5
Material	**Graphitene 0.03%**	**Graphitene 0.05%**	**Graphitene 0.20%**
Sand [g]	1350	1350	1350
Water [g]	225	225	225
Cement [g]	450	450	450
SP wt% of cement weight	0,80 %	0,80 %	0,80 %
SP [g] (liquid weight)	3,6	3,6	3,6
GO wt % of cement weight	0,03 %	0,05 %	0,20 %
G0 [g]	0,135	0,225	0,900
Concentration Factor *	5	5	5
Graphitene [g]	0,675	1,125	4,50
* Concentration of GO in the fine powder: 20 g GO/ 100 g fine powder = Concentration factor of 5			

Mix Design:	Graphenea	Volume:	0,8L
	Name:	w/c	0,5
Material	**Graphenea 0.2% & SP 2.0%**		
Sand [g]	1350		
Water [g]	0		
Cement [g]	450		
SP wt% of cement weight	2,0 %		
SP [g] (liquid weight)	9		
GO wt % of cement weight	0,20 %		
G0 [g]	0,9		
GO [mg] (1 g = 1000 mg)	900		
Concentration [mg/mL]*	4		
Graphenea [mL]	225		
* Concentration of GO in water dispersed Graphenea = 4 mg/mL			

Mix Design:	Quartz	Volume:	0,8L
	Name:	w/c	0,5
Material	**Quartz Sand 0.20 %**		
Sand [g]	1350		
Water [g]	225		
Cement [g]	450		
SP wt% of cement weight	0,80 %		
SP [g] (liquid weight)	3,6		
Quartz Sand (W12) wt % of cement weight	0,20 %		
Quartz Sand (W12) [g]	0,90		

Appendix B

Speedy Moisture Test Procedure

Large Size Speedy – Moisture Test Procedure

The test procedure is simple to follow and takes a just few minutes for most materials. To ensure accurate and consistent results the procedure should be followed precisely.

1. **Clean the Speedy Vessel.** Prior to using the speedy tester ensure that the inside of the Speedy cap and vessel are empty and clean. Use the bristle brush to remove any residues from previous tests as shown.

2. **Select and prepare the sample.** Ensure that the sample to be weighed and placed in the Speedy is representative of the material that is under investigation. Some materials, such as free-flowing powders and sands, need no preparation whereas others may need to be ground prior to testing or pulverised during the test – please refer to the Sample Preparation Table for further information.

3. **Weigh the sample.** Place the empty measuring beaker on the electronic scale and zero the scale – Refer to the electronic balance user instructions for further details. Add small amounts of material from the sample until the correct sample weight is reached. The sample weight is determined by the size and measurement range of the Speedy that is being used as detailed below:

Part No.	Vessel Size	Measurement Range H_2O%W/W	Sample weight (g)
L2000C	Large	0 – 10	40g
L2000D	**Large**	**0 – 20**	**20g**
L2000G	Large	0 – 50	8g

4. **Add the sample to the Speedy vessel.** Pour the sample into the chamber of the Speedy vessel as shown. Place pulverising balls into the chamber if required – refer to Sample Preparation Table.

5. **Add the reagent to the Speedy cap.** Using the metal scoop, add a minimum of two full scoops of reagent to the Speedy cap cavity as shown.

6. Seal **the Speedy.** Hold the Speedy horizontally and position the cap as shown. Swing the stirrup into position and tighten the top screw to seal.

Mix the sample with the reagent. Hold the Speedy vertically with the pressure gauge facing the ground and shake vigorously for 5 seconds. Rotate the Speedy through 180° so that the pressure gauge faces the sky, tap the sides of the Speedy to ensure the sample falls into the cap cavity and prop or hold the Speedy in this position for 1 – 2 minutes.

Alternatively, if the pulverising balls are being used, hold the Speedy horizontally and shake it in an orbital motion to make the balls spin around the inside of the Speedy vessel. Do this for 20 seconds and then rest for 20 seconds. Repeat this process two or three times. The spinning balls pulverise the sample to give a more reliable measurement.

7. **Take the reading.** Hold the Speedy horizontally and at eye level and take the moisture content reading directly from the pressure gauge.

8. **Release the pressure.** Hold the Speedy vertically with the pressure gauge facing the ground. Locate the arrow on the flange of the cap and point this away from yourself and other people in your vicinity. Unscrew the top screw slowly to vent the gas that may have been generated within the Speedy.

9. **Remove the sample and reagent.** Tip the contents of the Speedy directly into a clean and dry open container and dispose of in accordance with **Section 13** of the Calcium Carbide **Material Safety Data Sheet**.

10. **Clean the Speedy.** Clean the Speedy vessel and cap and measuring beaker in preparation for the next moisture measurement.

User Guidance Notes

Proportional Test Technique
If the moisture content of the material exceeds the measurement range of the Speedy being used then the Proportional Test Technique may be used to obtain measurements. This involves halving the normal sample weight and doubling the gauge value. For example:

> Assume a L2000D Speedy with a measurement range of 0 – 20 H_2O%W/W is being used to test soil with a nominal moisture content of 30%. The sample is prepared as required and half the normal weight – 10g – is weighed and placed in the Speedy. The test procedure is followed and a gauge value of 14.7% is recorded. This value is then doubled to give the actual moisture content of 29.4%.

The proportional test may also be used to obtain clearer readings in very dry material by doubling the sample size and halving the gauge value.

Temperature
For optimum performance the Speedy tester and sample should be at 20°C (68°F) when used. If this is not practical, take at least three tests in quick succession to equilibrate temperatures as far as possible. Ignore the first and second test results and record the later results.

Correction Factors
When compared with oven test results, Speedy readings may be low if the material under investigation contains volatile components other than water as these may evaporate with the water at elevated temperatures. Correction factors for given materials can be established by plotting graphs of Speedy test results against oven test results.

Measuring Liquids
Speedy testers may be used to measure the moisture content of certain liquids (most commonly oils) by adapting the test procedure as follows:

1. Weigh the liquid sample as normal
2. Place the liquid in a clean mixing vessel and add two to four scoops of **dry** sand. Mix thoroughly and place the mixture in the Speedy vessel.
3. Continue with the test as detailed in the Moisture Test Procedure.

Wet Weight to Dry Weight Conversion

The pressure gauges used with the Series 2000 Speedy testers are calibrated to give the moisture content expressed as a percentage of the sample's wet weight. If required, the measured value (M_{WW}) can be expressed as a percentage of the sample's dry weight (M_{DW}) by using the following formula:

$$M_{DW} = \frac{100 \times M_{WW}}{100 - M_{WW}}$$

Fault Diagnosis

Suspect Low Reading

If gauge readings are lower than you expect or anticipate check the following:

1. Test procedure has not been followed correctly. Ensure correct sample weight is used. Ensure sample is placed in the Speedy vessel and reagent is placed in the Speedy cap. Ensure Speedy vessel and cap are united and sealed in the horizontal plane to prevent premature contact of reagent and sample.
2. Inadequate cleaning of Speedy vessel and cap between tests. Ensure all residues from previous tests have been removed from the cap and vessel before starting a new test.
3. Insufficient reagent. Repeat the test using an additional scoop of reagent.
4. Ineffective reagent. Ensure that the reagent is fresh. Note that the colour of fresh reagent is dark grey; ineffective reagent (that has been exposed to moisture in the air or other sources) will have turned light grey in colour.
5. Inadequate sample preparation or sample-reagent mixing. Consider grinding the sample prior to weighing and/or (for Large Speedy only) using pulverising balls.
6. Temperature effects. Low readings may be recorded if the Speedy is used in very low temperatures. Take numerous readings in quick succession to raise the operating temperature of the Speedy.
7. Pressure loss. Visually check the cap washer for signs of holes or leak paths. Remove pressure gauge and visually check pressure gauge washer. Visually check Speedy vessel and cap for hairline cracks.
8. Defective pressure gauge. Does the needle sweep smoothly across the scale plate? If not, replace the gauge, or return the Speedy tester to an authorised distributor for service.

Suspect High Reading
If gauge readings are higher than you expect or anticipate check the following:

1. Ensure correct sample weight is used.
2. Ensure Speedy is held in the horizontal plane at eye level when reading the pressure gauge.
3. Temperature effects. High readings may be recorded if the Speedy is used in very high temperatures. If the Speedy is warm/hot to touch as a result of taking many readings in quick succession, allow time for it to cool down before taking more tests.
4. Defective pressure gauge. Does the needle return to zero after releasing pressure from the Speedy? If not, replace the gauge, or return the Speedy tester to an authorised distributor for service.

Recommended Spares and Consumables
It may be wise to consider having the following spares and consumables to hand when using the Speedy tester, especially in remote locations:

Batteries for the electronic scale, 3-off AA/LR6 1.5V
Speedy cap washer
Pressure gauge washer
Pressure gauge (note the measurement range)
Cleaning brushes

Other spares parts for the Speedy vessel are available on request.

Sample Preparation Table

Material Type	Recommended Preparation
Aggregate	Check maximum sample size; crush if larger than maximum recommended particle size
Dust	None required
Liquids	Mix with dry sand – see User Guidance Notes
Powders	None required
Sand	None required
Soils	Grind with mortar and pestle prior to testing, or use pulverising balls. Refer to Large Size Speedy – Moisture Test Procedure

The information contained in this booklet is given in good faith. As the method of use of the instrument (and its accessories) and the interpretation of the readings are beyond the control of the manufacturers, they cannot accept responsibility for any loss, consequential or otherwise, resulting from its use.

Appendix C

Mini-Flow Diameter

	1. test	1. test	1. test	2. test	2. test	2. test	Total Avg.	Total %
Type	**d1 [cm]**	**d2 [cm]**	**1. Avg. Flow Diameter [cm]**	**d1 [cm]**	**d2 [cm]**	**2. Avg. Flow Diameter [cm]**	**Total Avg. Flow Diameter**	**% Change - Flow Diameter**
Reference SP 0.08%	25,5	25,7	25,6	25,0	25,2	25,1	25,4	N/A
Graphenea 0.03 % SP 0.8%	23,8	23,7	23,8	24,0	24,3	24,2	24,0	-6,4 %
Graphenea 0.05 % SP 0.8%	19,4	19,6	19,5	21,5	21,9	21,7	20,6	-19,5 %
Graphenea 0.20 % SP 0.8%	10	10	10,0	10,0	10,0	10,0	10,0	-60,9 %
Graphenea 0.20 % SP 2.0%	25,7	26,5	26,1	24,0	24,5	24,3	25,2	-1,7 %
Graphitene 0.03 % SP 0.8%	24,8	24,5	24,7	24,6	24,2	24,4	24,5	-4,2 %
Graphitene 0.05 % SP 0.8%	24,5	24,0	24,3	25,0	25,2	25,1	24,7	-3,6 %
Graphitene 0.20 % SP 0.8%	23,1	23,0	23,1	26,2	25,5	25,9	24,5	-4,5 %
Quartz Sand 0.20 % SP 0.8%	25,4	24,8	25,1	-	-	-	25,1	-2,0 %

Percent Air of Fresh Mortar

Type	**% Air of fresh mortar**
Reference SP 0.08%	3,2 %
Graphenea 0.03 % SP 0.8%	3,4 %
Graphenea 0.05 % SP 0.8%	3,4 %
Graphenea 0.20 % SP 0.8%	4,9 %
Graphenea 0.20 % SP 2.0%	3,2 %
Graphitene 0.03 % SP 0.8%	2,5 %
Graphitene 0.05 % SP 0.8%	2,7 %
Graphitene 0.20 % SP 0.8%	2,8 %

Appendix C

Density of Fresh Mortar

Type	Density fresh mortar [Kg/L]
Reference SP 0.08%	2,299
Graphenea 0.03 % SP 0.8%	2,264
Graphenea 0.05 % SP 0.8%	2,262
Graphenea 0.20 % SP 0.8%	2,223
Graphenea 0.20 % SP 2.0%	2,266
Graphitene 0.03 % SP 0.8%	2,278
Graphitene 0.05 % SP 0.8%	2,278
Graphitene 0.20 % SP 0.8%	2,261

Appendix C

Density of Hardened Mortar

Type	Sample Name	Density [Kg/m3]	Avg. Density [Kg/m^3]	% Change - Density of hardened mortar
Reference SP 0.08%	A	2364		
	B	2363		
	C	2366	2364	N/A
Graphenea 0,03% SP 0.08%	A	2352		
	B	2342		
	C	2348	2348	-0,7 %
Graphenea 0,05% SP 0.08%	A	2343		
	B	2337		
	C	2341	2340	-1,0 %
Graphenea 0,2% SP 0.08%	A	2282		
	B	2282		
	C	2281	2282	-3,5 %
Grapehena 0,2 % SP 2,0 %	A	2342		
	B	2343		
	C	2344	2343	-0,9 %
Graphitene 0,03% SP 0.08%	A	2366		
	B	2352		
	C	2367	2362	-0,1 %
Graphitene 0,05% SP 0.08%	A	2367		
	B	2351		
	C	2365	2361	-0,1 %
Graphitene 0,2% SP 0.08%	A	2350		
	B	2359		
	C	2378	2362	-0,1 %
Quartz 0,2% SP 0.08%	A	2352		
	B	2355		
	C	2359	2355	-0,4 %

Appendix C

Temperature - Max (peak) Temperature and % change

Type	**Max (peak) Temperature [°C]**	**% Change – Max (peak) Temperature [°C]**
Reference SP 0.08%	40,79	N/A
Graphenea 0.03 % SP 0.8%	42,27	3,6 %
Graphenea 0.05 % SP 0.8%	43,00	5,4 %
Graphenea 0.20 % SP 0.8%	43,41	6,4 %
Graphitene 0.03 % SP 0.8%	41,34	1,3 %
Graphitene 0.05 % SP 0.8%	41,97	2,9 %
Graphitene 0.20 % SP 0.8%	41,10	0,7 %

Temperature Development - Data

Temperature data [°C]									
	Reference	Graphenea			Graphitene				
	-	0.03 %	0.05%	0.2%	0.03 %	0.05%	0.2%	Air 1	Air 2
Time [Hrs]	[°C]	[°C]	[°C]	[°C]	[°C]	[°C]	[°C]	[°C]	[°C]
0,0	23,1	23,2	23,3	23,8	23,5	23,7	23,8	22,4	22,3
0,2	23,2	23,4	23,4	24,0	23,7	23,8	23,9	22,4	22,3
0,3	23,3	23,5	23,5	24,1	23,7	24,0	24,1	22,5	22,3
0,5	23,3	23,6	23,6	24,2	23,8	24,1	24,1	22,4	22,3
0,7	23,4	23,7	23,6	24,2	23,9	24,2	24,2	22,5	22,3
0,8	23,5	23,7	23,6	24,3	24,0	24,4	24,1	22,5	22,4
1,0	23,3	23,7	23,6	24,4	23,9	24,4	24,2	22,5	22,4
1,2	23,3	23,8	23,6	24,4	23,9	24,5	24,2	22,5	22,4
1,3	23,4	23,8	23,7	24,4	23,9	24,4	24,2	22,6	22,3
1,5	23,4	23,8	23,7	24,5	23,9	24,5	24,2	22,6	22,5
1,7	23,5	23,9	23,7	24,5	24,0	24,5	24,2	22,6	22,5
1,8	23,4	23,9	23,8	24,5	24,0	24,4	24,3	22,6	22,4
2,0	23,4	23,9	23,8	24,4	24,1	24,4	24,3	22,6	22,4
2,2	23,4	23,9	23,8	24,5	24,1	24,4	24,3	22,6	22,4
2,3	23,5	23,9	23,8	24,5	24,1	24,5	24,3	22,6	22,4
2,5	23,5	23,9	23,8	24,5	24,1	24,5	24,3	22,6	22,4
2,7	23,5	24,0	23,8	24,5	24,1	24,5	24,3	22,6	22,5
2,8	23,5	23,9	23,9	24,5	24,0	24,4	24,3	22,6	22,5
3,0	23,5	23,9	23,8	24,5	24,1	24,4	24,3	22,6	22,5
3,2	23,5	23,9	23,9	24,6	24,0	24,4	24,3	22,6	22,4
3,3	23,5	23,9	23,9	24,6	24,1	24,5	24,3	22,6	22,4
3,5	23,5	23,9	23,9	24,6	24,1	24,4	24,3	22,6	22,5
3,7	23,5	24,0	24,0	24,6	24,1	24,5	24,3	22,7	22,5
3,8	23,5	23,9	24,0	24,6	24,1	24,4	24,2	22,6	22,4
4,0	23,5	23,9	24,1	24,6	24,1	24,4	24,2	22,6	22,5
4,2	23,5	24,0	24,1	24,7	24,1	24,5	24,2	22,6	22,4
4,3	23,5	24,0	24,1	24,6	24,1	24,5	24,2	22,7	22,5
4,5	23,5	24,0	24,2	24,7	24,1	24,5	24,2	22,7	22,5
4,7	23,6	24,1	24,2	24,7	24,2	24,4	24,2	22,7	22,5
4,8	23,6	24,2	24,2	24,8	24,2	24,4	24,2	22,7	22,5
5,0	23,6	24,2	24,3	24,9	24,2	24,4	24,3	22,7	22,5
5,2	23,6	24,2	24,3	24,9	24,2	24,4	24,3	22,6	22,5
5,3	23,7	24,3	24,4	25,0	24,3	24,5	24,3	22,7	22,5
5,5	23,7	24,3	24,5	25,1	24,3	24,5	24,3	22,7	22,6
5,7	23,8	24,3	24,6	25,3	24,3	24,5	24,4	22,8	22,6
5,8	23,9	24,4	24,7	25,4	24,3	24,6	24,4	22,8	22,7
6,0	24,0	24,5	24,8	25,5	24,3	24,6	24,4	22,8	22,7
6,2	24,0	24,6	24,9	25,7	24,4	24,7	24,5	22,9	22,6
6,3	24,1	24,7	25,1	25,9	24,4	24,7	24,6	22,8	22,6
6,5	24,1	24,9	25,3	26,1	24,5	24,8	24,7	22,8	22,6
6,7	24,2	25,0	25,4	26,3	24,6	25,0	24,8	22,7	22,6
6,8	24,3	25,1	25,6	26,5	24,7	25,1	24,9	22,8	22,6
7,0	24,4	25,3	25,8	26,7	24,8	25,2	25,0	22,8	22,6
7,2	24,6	25,5	26,1	27,0	24,9	25,4	25,2	22,8	22,6
7,3	24,7	25,7	26,3	27,3	25,0	25,5	25,3	22,8	22,6
7,5	24,9	25,9	26,6	27,7	25,2	25,8	25,5	22,8	22,7
7,7	25,0	26,2	26,9	28,0	25,3	26,0	25,7	22,8	22,6

Temperature data [°C]

	Reference	Graphenea			Graphitene				
	-	0.03 %	0.05%	0.2%	0.03 %	0.05%	0.2%	Air 1	Air 2
Time [Hrs]	[°C]	[°C]	[°C]	[°C]	[°C]	[°C]	[°C]	[°C]	[°C]
7,8	25,2	26,4	27,2	28,5	25,5	26,2	25,9	22,8	22,6
8,0	25,4	26,7	27,5	29,0	25,7	26,5	26,1	22,9	22,7
8,2	25,6	27,0	27,9	29,5	26,0	26,8	26,3	22,8	22,8
8,3	25,9	27,4	28,3	30,2	26,2	27,1	26,6	22,8	22,7
8,5	26,1	27,7	28,8	30,9	26,5	27,4	26,8	22,8	22,7
8,7	26,3	28,1	29,4	31,7	26,8	27,8	27,1	22,8	22,6
8,8	26,6	28,6	30,1	32,6	27,1	28,2	27,4	22,7	22,5
9,0	27,0	29,1	30,8	33,6	27,5	28,7	27,8	22,6	22,3
9,2	27,4	29,7	31,6	34,6	27,9	29,1	28,1	22,5	22,2
9,3	27,9	30,4	32,5	35,7	28,3	29,7	28,6	22,5	22,2
9,5	28,2	31,1	33,4	36,7	28,8	30,2	29,1	22,4	22,1
9,7	28,6	31,9	34,4	37,6	29,4	30,9	29,6	22,3	22,0
9,8	29,2	32,8	35,5	38,4	30,0	31,6	30,2	22,3	22,0
10,0	29,7	33,7	36,4	39,1	30,7	32,4	30,8	22,2	21,9
10,2	30,4	34,7	37,2	39,7	31,3	33,2	31,5	22,2	21,9
10,3	31,1	35,6	38,0	40,3	32,1	34,1	32,2	22,1	21,9
10,5	31,8	36,5	38,7	40,8	32,9	35,0	33,0	22,1	21,9
10,7	32,6	37,3	39,3	41,3	33,7	35,9	33,8	22,1	21,8
10,8	33,4	38,0	39,8	41,7	34,5	36,7	34,6	22,1	21,8
11,0	34,2	38,6	40,4	42,1	35,3	37,4	35,4	22,0	21,8
11,2	35,0	39,1	40,8	42,4	36,1	38,1	36,1	22,0	21,8
11,3	35,7	39,7	41,3	42,7	36,8	38,6	36,7	22,0	21,8
11,5	36,3	40,1	41,6	42,9	37,4	39,2	37,3	22,0	21,7
11,7	36,9	40,5	41,9	43,1	37,9	39,6	37,7	22,0	21,8
11,8	37,5	40,9	42,2	43,2	38,4	40,1	38,2	22,0	21,7
12,0	37,9	41,2	42,5	43,3	38,9	40,4	38,6	22,0	21,8
12,2	38,4	41,5	42,7	43,3	39,3	40,7	39,0	22,0	21,9
12,3	38,8	41,7	42,8	43,4	39,6	41,0	39,3	22,1	21,9
12,5	39,1	41,9	42,9	43,3	39,9	41,3	39,6	22,1	22,0
12,7	39,4	42,1	43,0	43,3	40,2	41,5	40,0	22,2	22,1
12,8	39,7	42,2	43,0	43,3	40,4	41,6	40,2	22,2	22,1
13,0	40,0	42,2	43,0	43,2	40,7	41,8	40,4	22,2	22,1
13,2	40,2	42,3	43,0	43,1	40,8	41,8	40,5	22,2	22,1
13,3	40,4	42,2	42,9	42,9	41,0	41,9	40,7	22,2	22,1
13,5	40,5	42,2	42,9	42,8	41,1	42,0	40,8	22,3	22,2
13,7	40,6	42,2	42,8	42,6	41,2	42,0	40,9	22,3	22,2
13,8	40,7	42,1	42,7	42,4	41,3	41,9	41,0	22,2	22,1
14,0	40,8	42,0	42,6	42,2	41,3	42,0	41,0	22,1	21,9
14,2	40,8	41,9	42,4	42,0	41,3	41,9	41,1	22,1	21,8
14,3	40,8	41,7	42,3	41,8	41,3	41,8	41,1	22,0	21,8
14,5	40,8	41,6	42,1	41,6	41,3	41,7	41,1	22,0	21,8
14,7	40,7	41,4	41,9	41,4	41,2	41,6	41,1	22,0	21,8
14,8	40,6	41,2	41,7	41,1	41,2	41,4	41,1	21,9	21,7
15,0	40,5	41,0	41,5	40,9	41,1	41,3	41,0	21,9	21,7
15,2	40,5	40,8	41,3	40,6	41,0	41,2	40,9	21,9	21,7
15,3	40,3	40,6	41,1	40,4	40,9	41,0	40,8	21,9	21,7
15,5	40,2	40,4	40,9	40,1	40,8	40,9	40,7	21,9	21,7

Temperature data [°C]

	Reference	Graphenea			Graphitene				
	-	0.03 %	0.05%	0.2%	0.03 %	0.05%	0.2%	Air 1	Air 2
Time [Hrs]	[°C]	[°C]	[°C]	[°C]	[°C]	[°C]	[°C]	[°C]	[°C]
15,7	40,1	40,2	40,6	39,9	40,6	40,7	40,6	21,8	21,7
15,8	40,0	40,0	40,4	39,6	40,5	40,5	40,5	21,9	21,6
16,0	39,8	39,7	40,1	39,4	40,3	40,3	40,4	21,8	21,7
16,2	39,6	39,5	39,9	39,1	40,2	40,1	40,2	21,8	21,7
16,3	39,5	39,2	39,7	38,9	40,0	39,9	40,1	21,8	21,6
16,5	39,3	39,0	39,4	38,6	39,9	39,7	39,9	21,8	21,6
16,7	39,1	38,8	39,2	38,3	39,7	39,5	39,8	21,8	21,6
16,8	38,9	38,5	38,9	38,1	39,5	39,2	39,6	21,8	21,6
17,0	38,7	38,3	38,7	37,8	39,3	39,0	39,5	21,8	21,6
17,2	38,5	38,0	38,5	37,7	39,1	38,8	39,3	21,8	21,5
17,3	38,3	37,8	38,3	37,4	38,9	38,5	39,1	21,8	21,5
17,5	38,1	37,6	38,0	37,1	38,7	38,4	39,0	21,8	21,6
17,7	37,9	37,3	37,8	36,9	38,5	38,1	38,8	21,8	21,6
17,8	37,7	37,1	37,5	36,7	38,3	37,9	38,6	21,7	21,5
18,0	37,5	36,9	37,3	36,5	38,1	37,7	38,5	21,7	21,5
18,2	37,3	36,6	37,1	36,2	37,9	37,5	38,3	21,7	21,6
18,3	37,0	36,4	36,9	36,0	37,7	37,3	38,1	21,7	21,5
18,5	36,9	36,2	36,6	35,8	37,5	37,1	37,9	21,7	21,5
18,7	36,7	35,9	36,4	35,5	37,3	36,9	37,7	21,7	21,5
18,8	36,5	35,7	36,2	35,3	37,1	36,7	37,5	21,7	21,6
19,0	36,2	35,5	36,0	35,1	36,9	36,5	37,3	21,7	21,5
19,2	36,0	35,3	35,8	34,8	36,7	36,3	37,2	21,7	21,5
19,3	35,8	35,0	35,5	34,6	36,5	36,1	37,0	21,7	21,5
19,5	35,6	34,8	35,3	34,4	36,3	35,9	36,8	21,7	21,5
19,7	35,4	34,6	35,1	34,2	36,2	35,7	36,6	21,7	21,5
19,8	35,2	34,4	34,9	34,0	36,0	35,5	36,4	21,7	21,6
20,0	35,0	34,2	34,6	33,8	35,8	35,3	36,3	21,8	21,8
20,2	34,8	34,0	34,5	33,6	35,6	35,2	36,1	21,9	21,8
20,3	34,6	33,8	34,2	33,5	35,4	35,0	35,9	22,0	21,9
20,5	34,4	33,6	34,1	33,3	35,2	34,8	35,7	21,9	21,8
20,7	34,2	33,4	33,9	33,1	35,0	34,6	35,5	21,9	21,8
20,8	34,0	33,2	33,7	32,9	34,9	34,4	35,4	21,9	21,7
21,0	33,8	33,0	33,5	32,8	34,7	34,2	35,2	21,9	21,7
21,2	33,6	32,8	33,3	32,6	34,5	34,1	35,0	21,8	21,7
21,3	33,4	32,6	33,2	32,5	34,3	33,8	34,8	21,8	21,7
21,5	33,3	32,4	33,0	32,3	34,1	33,7	34,6	21,8	21,6
21,7	33,0	32,2	32,8	32,1	34,0	33,5	34,5	21,8	21,6
21,8	32,8	32,1	32,7	31,9	33,8	33,4	34,3	21,8	21,6
22,0	32,7	31,9	32,5	31,8	33,6	33,2	34,1	21,8	21,6
22,2	32,5	31,7	32,3	31,6	33,5	33,0	34,0	21,9	21,7
22,3	32,3	31,6	32,2	31,5	33,3	32,9	33,8	22,0	21,9
22,5	32,1	31,4	32,0	31,4	33,2	32,7	33,6	22,0	22,0
22,7	32,0	31,3	31,8	31,2	33,0	32,5	33,5	22,1	22,0
22,8	31,8	31,1	31,7	31,1	32,8	32,4	33,3	22,2	22,1
23,0	31,7	31,0	31,5	30,9	32,7	32,3	33,2	22,2	22,1
23,2	31,5	30,9	31,4	30,8	32,5	32,1	33,0	22,2	22,2
23,3	31,4	30,7	31,2	30,6	32,4	32,0	32,8	22,3	22,2

Temperature data [°C]

	Reference	Graphenea			Graphitene				
	-	0.03 %	0.05%	0.2%	0.03 %	0.05%	0.2%	Air 1	Air 2
Time [Hrs]	[°C]	[°C]	[°C]	[°C]	[°C]	[°C]	[°C]	[°C]	[°C]
23,5	31,2	30,6	31,1	30,5	32,2	31,8	32,7	22,3	22,2
23,7	31,1	30,4	31,0	30,4	32,1	31,7	32,5	22,3	22,3
23,8	30,9	30,3	30,8	30,3	31,9	31,5	32,4	22,4	22,3
24,0	30,8	30,2	30,7	30,1	31,8	31,4	32,2	22,4	22,3
24,2	30,7	30,0	30,6	30,0	31,6	31,2	32,1	22,4	22,3
24,3	30,5	29,9	30,4	29,9	31,5	31,1	31,9	22,4	22,3
24,5	30,4	29,8	30,3	29,7	31,4	31,0	31,8	22,4	22,4
24,7	30,2	29,6	30,1	29,6	31,2	30,9	31,6	22,4	22,4
24,8	30,1	29,5	30,0	29,5	31,1	30,7	31,5	22,4	22,4
25,0	30,0	29,4	29,9	29,4	30,9	30,6	31,4	22,5	22,4
25,2	29,8	29,3	29,8	29,3	30,8	30,5	31,2	22,5	22,4
25,3	29,7	29,2	29,7	29,2	30,7	30,4	31,1	22,5	22,4
25,5	29,6	29,1	29,6	29,1	30,5	30,2	31,0	22,5	22,4
25,7	29,5	29,0	29,5	29,0	30,4	30,1	30,8	22,5	22,5
25,8	29,4	28,9	29,3	28,9	30,3	30,0	30,7	22,5	22,4
26,0	29,2	28,8	29,2	28,8	30,2	29,9	30,5	22,5	22,4
26,2	29,1	28,7	29,1	28,7	30,1	29,7	30,4	22,6	22,5
26,3	29,0	28,5	29,0	28,6	29,9	29,6	30,2	22,5	22,5
26,5	28,9	28,4	28,9	28,5	29,8	29,5	30,1	22,5	22,4
26,7	28,8	28,4	28,8	28,4	29,7	29,4	30,0	22,6	22,4
26,8	28,7	28,3	28,7	28,3	29,6	29,2	29,9	22,6	22,4
27,0	28,6	28,2	28,6	28,2	29,5	29,1	29,8	22,6	22,5
27,2	28,4	28,1	28,5	28,1	29,4	29,0	29,6	22,6	22,4
27,3	28,4	28,0	28,4	28,0	29,3	28,8	29,5	22,6	22,4
27,5	28,3	27,9	28,3	27,9	29,2	28,8	29,4	22,6	22,5
27,7	28,1	27,8	28,2	27,8	29,0	28,7	29,3	22,6	22,5
27,8	28,1	27,7	28,1	27,8	28,9	28,6	29,2	22,6	22,5
28,0	28,0	27,6	28,0	27,7	28,8	28,5	29,0	22,7	22,6
28,2	27,9	27,5	27,9	27,6	28,7	28,4	28,9	22,6	22,5
28,3	27,8	27,4	27,8	27,5	28,6	28,3	28,8	22,7	22,7
28,5	27,7	27,4	27,7	27,4	28,5	28,2	28,7	22,6	22,5
28,7	27,6	27,3	27,6	27,3	28,4	28,1	28,6	22,6	22,5
28,8	27,5	27,2	27,6	27,2	28,3	27,9	28,5	22,6	22,5
29,0	27,5	27,1	27,5	27,1	28,2	27,9	28,4	22,7	22,5
29,2	27,3	27,1	27,4	27,0	28,1	27,8	28,3	22,6	22,5
29,3	27,2	27,0	27,3	27,0	28,0	27,7	28,2	22,6	22,6
29,5	27,2	26,9	27,2	26,9	27,9	27,5	28,0	22,6	22,5
29,7	27,1	26,8	27,1	26,8	27,8	27,5	27,9	22,7	22,5
29,8	27,0	26,8	27,1	26,7	27,7	27,4	27,9	22,7	22,6
30,0	26,9	26,7	27,0	26,7	27,6	27,3	27,8	22,7	22,6
30,2	26,8	26,6	26,9	26,6	27,5	27,2	27,7	22,7	22,6
30,3	26,8	26,5	26,8	26,5	27,4	27,1	27,6	22,7	22,6
30,5	26,7	26,5	26,7	26,5	27,3	27,0	27,6	22,6	22,6
30,7	26,6	26,4	26,6	26,3	27,2	26,9	27,5	22,6	22,5
30,8	26,6	26,3	26,6	26,3	27,1	26,8	27,4	22,6	22,6
31,0	26,5	26,2	26,5	26,2	27,1	26,8	27,3	22,6	22,5
31,2	26,4	26,1	26,4	26,1	27,0	26,7	27,2	22,6	22,5

Temperature data [°C]

	Reference	Graphenea			Graphitene				
	-	0.03 %	0.05%	0.2%	0.03 %	0.05%	0.2%	Air 1	Air 2
Time [Hrs]	[°C]	[°C]	[°C]	[°C]	[°C]	[°C]	[°C]	[°C]	[°C]
31,3	26,3	26,0	26,4	26,0	26,8	26,7	27,1	22,5	22,4
31,5	26,3	26,0	26,3	26,0	26,8	26,6	27,0	22,5	22,3
31,7	26,2	25,9	26,2	25,9	26,7	26,6	26,9	22,5	22,2
31,8	26,1	25,9	26,1	25,8	26,6	26,5	26,8	22,4	22,3
32,0	26,0	25,8	26,1	25,8	26,6	26,5	26,7	22,4	22,2
32,2	25,9	25,7	26,0	25,7	26,5	26,4	26,6	22,4	22,2
32,3	25,9	25,7	25,9	25,6	26,4	26,3	26,6	22,4	22,3
32,5	25,8	25,6	25,8	25,6	26,4	26,2	26,5	22,4	22,3
32,7	25,8	25,5	25,7	25,5	26,3	26,1	26,4	22,4	22,3
32,8	25,7	25,5	25,7	25,4	26,2	26,0	26,4	22,4	22,3
33,0	25,6	25,4	25,6	25,4	26,2	25,9	26,3	22,4	22,2
33,2	25,6	25,3	25,5	25,3	26,1	25,8	26,2	22,3	22,2
33,3	25,5	25,3	25,5	25,3	26,0	25,8	26,2	22,3	22,2
33,5	25,4	25,2	25,4	25,3	25,9	25,7	26,1	22,3	22,1
33,7	25,4	25,1	25,4	25,2	25,9	25,6	26,0	22,2	22,1
33,8	25,3	25,1	25,3	25,2	25,8	25,6	25,9	22,2	22,0
34,0	25,2	25,0	25,3	25,1	25,7	25,5	25,9	22,2	22,0
34,2	25,2	24,9	25,2	25,1	25,7	25,5	25,8	22,2	22,0
34,3	25,1	24,9	25,2	25,0	25,6	25,4	25,8	22,2	22,0
34,5	25,0	24,8	25,2	24,9	25,5	25,4	25,7	22,2	22,0
34,7	25,0	24,8	25,1	24,9	25,5	25,3	25,6	22,1	22,0
34,8	24,9	24,7	25,1	24,8	25,4	25,2	25,6	22,1	21,9
35,0	24,9	24,7	25,0	24,8	25,4	25,2	25,5	22,1	21,9
35,2	24,8	24,7	25,0	24,7	25,3	25,2	25,5	22,1	21,9
35,3	24,8	24,7	24,9	24,7	25,2	25,1	25,4	22,1	21,9
35,5	24,7	24,6	24,8	24,6	25,2	25,1	25,3	22,1	21,9
35,7	24,6	24,6	24,8	24,6	25,2	25,0	25,3	22,1	22,0
35,8	24,6	24,6	24,7	24,5	25,1	24,9	25,2	22,1	22,1
36,0	24,6	24,5	24,6	24,4	25,0	24,9	25,2	22,2	22,1
36,2	24,5	24,5	24,6	24,4	25,0	24,8	25,1	22,2	22,2
36,3	24,5	24,4	24,6	24,4	24,9	24,8	25,1	22,2	22,1
36,5	24,5	24,3	24,5	24,3	24,9	24,8	25,0	22,2	22,1
36,7	24,4	24,3	24,5	24,3	24,8	24,7	25,0	22,2	22,1
36,8	24,4	24,2	24,4	24,3	24,8	24,7	24,9	22,2	22,1
37,0	24,4	24,2	24,4	24,2	24,7	24,6	24,9	22,2	22,0
37,2	24,3	24,1	24,3	24,2	24,7	24,6	24,8	22,1	22,0
37,3	24,2	24,1	24,3	24,1	24,6	24,5	24,8	22,1	22,0
37,5	24,2	24,0	24,3	24,1	24,6	24,5	24,8	22,1	21,9
37,7	24,1	24,0	24,2	24,1	24,5	24,5	24,7	22,0	21,9
37,8	24,1	23,9	24,2	24,0	24,5	24,5	24,7	22,0	21,9
38,0	24,0	23,9	24,1	24,0	24,5	24,4	24,6	22,0	21,9
38,2	24,0	23,9	24,1	24,0	24,4	24,3	24,6	22,0	21,9
38,3	23,9	23,9	24,1	24,0	24,4	24,3	24,5	22,0	21,8
38,5	23,9	23,8	24,0	23,9	24,3	24,3	24,5	22,0	21,8
38,7	23,9	23,8	24,0	23,9	24,3	24,3	24,5	22,0	21,8
38,8	23,8	23,8	24,0	23,8	24,3	24,2	24,4	22,0	21,8
39,0	23,8	23,7	23,9	23,8	24,2	24,2	24,4	22,0	21,8

Temperature data [°C]

	Reference	Graphenea			Graphitene				
	-	0.03 %	0.05%	0.2%	0.03 %	0.05%	0.2%	Air 1	Air 2
Time [Hrs]	[°C]	[°C]	[°C]	[°C]	[°C]	[°C]	[°C]	[°C]	[°C]
39,2	23,7	23,7	23,9	23,8	24,2	24,1	24,4	22,0	21,8
39,3	23,7	23,6	23,8	23,7	24,2	24,1	24,3	22,0	21,9
39,5	23,6	23,6	23,8	23,7	24,1	24,1	24,3	22,0	21,9
39,7	23,6	23,6	23,8	23,7	24,1	24,1	24,2	21,9	21,8
39,8	23,7	23,5	23,8	23,7	24,1	24,0	24,2	22,0	21,8
40,0	23,6	23,5	23,7	23,6	24,0	23,9	24,2	22,0	21,8
40,2	23,5	23,5	23,7	23,6	24,0	23,9	24,1	22,0	21,8
40,3	23,5	23,5	23,7	23,6	23,9	23,9	24,1	21,9	21,8
40,5	23,5	23,4	23,6	23,6	23,9	23,9	24,1	22,0	21,8
40,7	23,5	23,4	23,6	23,5	23,9	23,8	24,0	21,9	21,8
40,8	23,4	23,4	23,6	23,5	23,8	23,8	24,0	21,9	21,8
41,0	23,4	23,4	23,5	23,5	23,8	23,8	24,0	21,9	21,8
41,2	23,4	23,3	23,5	23,4	23,8	23,8	24,0	21,9	21,8
41,3	23,3	23,3	23,5	23,4	23,7	23,7	23,9	21,9	21,8
41,5	23,3	23,3	23,5	23,4	23,7	23,7	23,9	21,9	21,8
41,7	23,3	23,3	23,4	23,4	23,7	23,6	23,8	21,9	21,8
41,8	23,3	23,2	23,4	23,3	23,6	23,6	23,8	21,9	21,8
42,0	23,2	23,2	23,4	23,3	23,6	23,6	23,8	21,9	21,8
42,2	23,2	23,2	23,4	23,3	23,6	23,6	23,8	21,9	21,8
42,3	23,1	23,2	23,3	23,3	23,6	23,6	23,7	21,9	21,7
42,5	23,2	23,1	23,3	23,2	23,5	23,6	23,7	21,9	21,8
42,7	23,1	23,1	23,3	23,2	23,5	23,5	23,7	21,9	21,8
42,8	23,1	23,1	23,2	23,2	23,5	23,5	23,6	21,9	21,8
43,0	23,1	23,1	23,2	23,1	23,5	23,4	23,6	21,9	21,8
43,2	23,0	23,0	23,2	23,1	23,4	23,5	23,6	21,9	21,8
43,3	23,1	23,0	23,2	23,1	23,4	23,4	23,6	21,9	21,8
43,5	23,0	23,0	23,2	23,1	23,4	23,4	23,5	21,9	21,8
43,7	23,0	23,0	23,1	23,1	23,4	23,3	23,5	21,9	21,8
43,8	22,9	22,9	23,1	23,1	23,3	23,3	23,5	21,9	21,8
44,0	22,9	22,9	23,0	23,1	23,3	23,3	23,5	21,9	21,7
44,2	23,0	22,9	23,1	23,0	23,3	23,3	23,4	21,9	21,8
44,3	22,9	22,9	23,1	23,0	23,3	23,2	23,4	21,9	21,8
44,5	22,9	22,9	23,0	23,0	23,3	23,3	23,4	21,9	21,7
44,7	22,8	22,9	23,0	23,0	23,2	23,2	23,4	21,9	21,7
44,8	22,8	22,8	23,0	23,0	23,2	23,2	23,3	21,9	21,7
45,0	22,8	22,8	23,0	22,9	23,2	23,2	23,3	21,9	21,7
45,2	22,8	22,8	22,9	22,9	23,1	23,2	23,3	21,9	21,7
45,3	22,8	22,8	22,9	22,9	23,1	23,2	23,3	21,9	21,7
45,5	22,7	22,8	22,9	22,9	23,1	23,1	23,2	21,9	21,7
45,7	22,7	22,8	22,9	22,9	23,1	23,1	23,2	21,9	21,7
45,8	22,7	22,7	22,9	22,8	23,1	23,1	23,2	21,8	21,7
46,0	22,7	22,7	22,8	22,8	23,1	23,0	23,2	21,9	21,7
46,2	22,7	22,7	22,8	22,8	23,0	23,0	23,2	21,8	21,7
46,3	22,7	22,7	22,8	22,8	23,0	23,0	23,2	21,9	21,7
46,5	22,6	22,7	22,8	22,8	23,0	23,0	23,2	21,9	21,7
46,7	22,6	22,7	22,8	22,8	22,9	23,0	23,1	21,8	21,7
46,8	22,6	22,6	22,8	22,8	22,9	23,0	23,1	21,9	21,7

Temperature data [°C]

	Reference	Graphenea			Graphitene				
	-	0.03 %	0.05%	0.2%	0.03 %	0.05%	0.2%	Air 1	Air 2
Time [Hrs]	[°C]	[°C]	[°C]	[°C]	[°C]	[°C]	[°C]	[°C]	[°C]
47,0	22,6	22,6	22,8	22,7	22,9	22,9	23,1	21,8	21,7
47,2	22,6	22,6	22,7	22,7	22,9	22,9	23,0	21,8	21,7
47,3	22,6	22,6	22,7	22,7	22,9	22,9	23,0	21,8	21,7
47,5	22,6	22,6	22,7	22,7	22,9	22,9	23,0	21,8	21,7
47,7	22,5	22,5	22,7	22,6	22,9	22,9	23,0	21,8	21,7
47,8	22,5	22,5	22,6	22,6	22,8	22,9	23,0	21,8	21,7
48,0	22,5	22,5	22,6	22,6	22,8	22,9	23,0	21,8	21,7
48,2	22,5	22,5	22,6	22,6	22,8	22,8	23,0	21,8	21,7
48,3	22,5	22,5	22,6	22,6	22,7	22,8	22,9	21,8	21,7
48,5	22,4	22,5	22,6	22,6	22,8	22,8	22,9	21,8	21,7
48,7	22,4	22,5	22,6	22,5	22,8	22,8	22,9	21,8	21,7
48,8	22,4	22,5	22,5	22,6	22,7	22,7	22,9	21,8	21,7
49,0	22,4	22,4	22,5	22,5	22,7	22,7	22,9	21,8	21,7
49,2	22,4	22,4	22,5	22,5	22,7	22,8	22,9	21,8	21,6
49,3	22,4	22,4	22,5	22,5	22,7	22,7	22,8	21,8	21,7
49,5	22,4	22,4	22,5	22,5	22,6	22,7	22,8	21,8	21,7
49,7	22,3	22,4	22,5	22,5	22,6	22,7	22,8	21,8	21,7
49,8	22,3	22,4	22,5	22,5	22,6	22,7	22,8	21,8	21,7
50,0	22,3	22,4	22,5	22,5	22,6	22,6	22,8	21,8	21,7
50,2	22,3	22,3	22,4	22,4	22,6	22,6	22,8	21,8	21,7
50,3	22,3	22,3	22,4	22,4	22,6	22,6	22,8	21,8	21,7
50,5	22,2	22,3	22,4	22,4	22,5	22,6	22,7	21,8	21,7
50,7	22,3	22,3	22,4	22,4	22,5	22,6	22,7	21,8	21,6
50,8	22,2	22,3	22,4	22,4	22,5	22,6	22,7	21,8	21,6
51,0	22,2	22,3	22,4	22,4	22,5	22,6	22,7	21,8	21,6
51,2	22,2	22,3	22,3	22,4	22,5	22,6	22,7	21,8	21,7
51,3	22,2	22,3	22,3	22,3	22,5	22,6	22,7	21,8	21,7
51,5	22,2	22,3	22,3	22,3	22,5	22,6	22,7	21,8	21,6
51,7	22,2	22,3	22,3	22,3	22,5	22,6	22,7	21,8	21,7
51,8	22,2	22,3	22,3	22,3	22,5	22,5	22,7	21,8	21,6
52,0	22,2	22,2	22,3	22,3	22,4	22,5	22,7	21,8	21,6
52,2	22,1	22,2	22,3	22,3	22,4	22,5	22,7	21,8	21,6
52,3	22,1	22,2	22,3	22,3	22,4	22,6	22,7	21,8	21,6
52,5	22,1	22,2	22,3	22,3	22,4	22,6	22,7	21,8	21,6
52,7	22,1	22,1	22,3	22,3	22,4	22,5	22,7	21,7	21,6
52,8	22,1	22,2	22,3	22,3	22,4	22,5	22,7	21,8	21,6
53,0	22,0	22,1	22,2	22,2	22,4	22,5	22,7	21,8	21,6
53,2	22,1	22,2	22,2	22,2	22,4	22,5	22,7	21,8	21,6
53,3	22,1	22,1	22,2	22,2	22,4	22,5	22,6	21,7	21,6
53,5	22,1	22,1	22,2	22,3	22,4	22,5	22,6	21,7	21,6
53,7	22,0	22,1	22,2	22,2	22,4	22,5	22,6	21,7	21,6
53,8	22,0	22,1	22,2	22,2	22,4	22,5	22,6	21,7	21,6
54,0	22,0	22,1	22,2	22,2	22,4	22,5	22,6	21,7	21,6
54,2	22,0	22,1	22,2	22,2	22,4	22,5	22,6	21,7	21,6
54,3	22,0	22,1	22,2	22,2	22,4	22,5	22,6	21,7	21,6
54,5	22,0	22,1	22,1	22,2	22,4	22,4	22,6	21,7	21,6
54,7	22,0	22,0	22,1	22,2	22,3	22,5	22,6	21,7	21,6

Temperature data [°C]

	Reference	Graphenea			Graphitene				
	-	0.03 %	0.05%	0.2%	0.03 %	0.05%	0.2%	Air 1	Air 2
Time [Hrs]	[°C]	[°C]	[°C]	[°C]	[°C]	[°C]	[°C]	[°C]	[°C]
54,8	22,0	22,1	22,1	22,2	22,3	22,5	22,5	21,7	21,6
55,0	21,9	22,1	22,1	22,2	22,3	22,5	22,6	21,7	21,6
55,2	22,0	22,1	22,2	22,2	22,3	22,4	22,5	21,7	21,6
55,3	21,9	22,0	22,1	22,2	22,3	22,4	22,5	21,7	21,6
55,5	21,9	22,0	22,1	22,2	22,3	22,4	22,5	21,7	21,6
55,7	21,9	22,0	22,1	22,2	22,3	22,4	22,5	21,7	21,6
55,8	21,9	22,0	22,1	22,2	22,3	22,4	22,5	21,7	21,6
56,0	21,9	22,0	22,1	22,2	22,3	22,4	22,5	21,7	21,5
56,2	22,0	22,0	22,1	22,1	22,3	22,4	22,5	21,7	21,6
56,3	21,9	22,1	22,1	22,2	22,3	22,4	22,4	21,7	21,5
56,5	21,9	22,1	22,1	22,2	22,3	22,3	22,4	21,7	21,5
56,7	21,9	22,0	22,1	22,2	22,2	22,3	22,4	21,7	21,6
56,8	21,9	22,0	22,1	22,2	22,2	22,3	22,4	21,8	21,7
57,0	21,9	22,0	22,1	22,2	22,2	22,3	22,4	21,8	21,8
57,2	21,9	22,0	22,1	22,1	22,2	22,3	22,4	21,8	21,8
57,3	21,9	22,0	22,1	22,2	22,2	22,3	22,4	21,8	21,8
57,5	21,9	22,0	22,1	22,1	22,2	22,3	22,4	21,9	21,7
57,7	21,9	22,0	22,1	22,1	22,2	22,3	22,4	21,9	21,7
57,8	21,9	22,0	22,1	22,1	22,2	22,2	22,4	21,8	21,7
58,0	21,9	22,0	22,0	22,1	22,1	22,3	22,4	21,8	21,7
58,2	21,8	22,0	22,1	22,1	22,2	22,2	22,4	21,8	21,7
58,3	21,9	22,0	22,0	22,1	22,1	22,2	22,3	21,8	21,6
58,5	21,9	22,0	22,1	22,0	22,1	22,2	22,4	21,8	21,7
58,7	21,8	22,0	22,0	22,1	22,1	22,2	22,3	21,8	21,7
58,8	21,8	22,0	22,0	22,0	22,1	22,2	22,4	21,8	21,7
59,0	21,8	21,9	22,0	22,0	22,1	22,2	22,3	21,8	21,7
59,2	21,9	22,0	22,0	22,0	22,1	22,2	22,3	21,8	21,7
59,3	21,9	22,0	22,0	22,1	22,1	22,2	22,3	21,7	21,6
59,5	21,9	21,9	22,0	22,0	22,1	22,2	22,3	21,8	21,7
59,7	21,9	21,9	21,9	22,0	22,1	22,2	22,3	21,8	21,7
59,8	21,8	21,9	22,0	22,0	22,1	22,2	22,3	21,8	21,6
60,0	21,8	21,9	21,9	22,0	22,1	22,2	22,3	21,8	21,6
60,2	21,8	21,9	22,0	22,0	22,0	22,2	22,3	21,8	21,6
60,3	21,8	21,9	21,9	22,0	22,1	22,2	22,3	21,7	21,6
60,5	21,8	21,9	21,9	22,0	22,1	22,2	22,3	21,8	21,6
60,7	21,8	21,9	21,9	21,9	22,1	22,2	22,3	21,8	21,6
60,8	21,8	21,9	21,9	22,0	22,0	22,2	22,3	21,8	21,6
61,0	21,8	21,9	21,9	22,0	22,0	22,1	22,3	21,7	21,6
61,2	21,8	21,8	21,9	21,9	22,0	22,1	22,3	21,7	21,6
61,3	21,8	21,9	21,9	21,9	22,0	22,1	22,2	21,7	21,6
61,5	21,8	21,8	21,9	21,9	22,0	22,1	22,2	21,7	21,6
61,7	21,7	21,8	21,9	21,9	22,0	22,1	22,3	21,7	21,6
61,8	21,7	21,8	21,9	21,9	22,0	22,2	22,3	21,7	21,6
62,0	21,8	21,8	21,9	21,9	22,0	22,1	22,2	21,7	21,6
62,2	21,7	21,8	21,9	21,9	22,0	22,1	22,2	21,7	21,6
62,3	21,7	21,7	21,9	21,9	22,0	22,1	22,2	21,7	21,6
62,5	21,7	21,8	21,9	21,9	22,0	22,1	22,2	21,7	21,6

Temperature data [°C]

	Reference	Graphenea			Graphitene				
	-	0.03 %	0.05%	0.2%	0.03 %	0.05%	0.2%	Air 1	Air 2
Time [Hrs]	[°C]	[°C]	[°C]	[°C]	[°C]	[°C]	[°C]	[°C]	[°C]
62,7	21,7	21,8	21,8	21,9	22,0	22,1	22,2	21,7	21,6
62,8	21,7	21,8	21,9	21,9	22,0	22,1	22,2	21,7	21,6
63,0	21,7	21,8	21,9	21,9	22,0	22,1	22,2	21,7	21,6
63,2	21,7	21,8	21,8	21,9	22,0	22,1	22,2	21,7	21,6
63,3	21,6	21,8	21,8	21,9	22,0	22,1	22,1	21,7	21,6
63,5	21,7	21,8	21,8	21,9	22,0	22,1	22,2	21,6	21,6
63,7	21,7	21,8	21,8	21,9	22,0	22,1	22,2	21,7	21,5
63,8	21,7	21,8	21,8	21,9	22,0	22,0	22,2	21,7	21,6
64,0	21,7	21,8	21,8	21,9	21,9	22,0	22,2	21,7	21,6
64,2	21,7	21,8	21,8	21,9	22,0	22,0	22,1	21,7	21,6
64,3	21,7	21,8	21,8	21,9	21,9	22,0	22,2	21,7	21,6
64,5	21,6	21,8	21,8	21,9	21,9	22,0	22,2	21,7	21,6
64,7	21,7	21,7	21,8	21,9	21,9	22,0	22,1	21,7	21,6
64,8	21,6	21,8	21,8	21,9	21,9	22,0	22,1	21,7	21,5
65,0	21,6	21,7	21,8	21,9	21,9	22,0	22,1	21,7	21,5
65,2	21,6	21,7	21,8	21,8	21,9	22,0	22,1	21,7	21,5
65,3	21,6	21,8	21,8	21,9	21,9	22,0	22,1	21,7	21,6
65,5	21,6	21,7	21,8	21,8	21,8	22,0	22,1	21,7	21,5
65,7	21,6	21,8	21,8	21,9	21,9	22,0	22,1	21,7	21,6
65,8	21,6	21,7	21,8	21,8	21,9	22,0	22,1	21,7	21,6
66,0	21,6	21,7	21,8	21,8	21,9	22,0	22,1	21,6	21,5
66,2	21,6	21,8	21,8	21,8	21,9	22,0	22,1	21,7	21,6
66,3	21,6	21,7	21,8	21,8	21,9	21,9	22,1	21,7	21,6
66,5	21,6	21,7	21,8	21,8	21,9	22,0	22,1	21,7	21,6
66,7	21,6	21,7	21,7	21,8	21,9	22,0	22,1	21,7	21,6
66,8	21,6	21,7	21,8	21,8	21,9	22,0	22,1	21,7	21,6
67,0	21,6	21,7	21,8	21,8	21,9	22,0	22,1	21,7	21,6
67,2	21,6	21,7	21,7	21,8	21,8	22,0	22,1	21,7	21,6
67,3	21,6	21,7	21,7	21,8	21,8	22,0	22,1	21,7	21,6
67,5	21,6	21,7	21,7	21,8	21,8	22,0	22,1	21,7	21,6
67,7	21,6	21,6	21,7	21,8	21,8	22,0	22,1	21,7	21,6
67,8	21,6	21,7	21,7	21,8	21,8	22,0	22,1	21,7	21,6
68,0	21,6	21,7	21,7	21,7	21,8	22,0	22,1	21,7	21,6
68,2	21,6	21,7	21,7	21,8	21,8	22,0	22,1	21,7	21,6
68,3	21,6	21,7	21,7	21,7	21,8	22,0	22,1	21,7	21,6

Appendix C

Cumulative Isothermal Heat Development (Curing-box spreadsheets)

Reference

Adiabatic temperature and isothermic heat

(v 2.8 ss 06-02-2012)

Concrete parameters	
Temp. trans. coeff.	0,0935
Density	2299
Heat capacity (fresh)	1,05
Heat capacity (hardened)	1,05
Cement content	450
Set time	10
A - set time	33500
B - set time	1470
A - hydration	33500
B - hydration	1470
Adia. start temperature	20

Temp. trans. coeff.	
dQ/dm	0
m>	22
m<	76

Heat function	
m-limit	80
Q_∞	150
τ	12,58
α	4,22
R^2	0,4504
$\Sigma\Delta_Q$	6140

specific heat capaticy [J/gK]	
water	4,2
cement	0,8
sand	0,8
gravel	0,8

Resept		Sement	Silika	FA
bindemiddel	450	450	0	0
fint tilslag	1350			
fint tilslag				
grovt tilslag	0			
grovt tilslag	0			
vann	225			
densitet	2299			
Heat cap.	**1,04**			

	FA-LVB	CEM III
A	**35000**	**50000**
B	**500**	**1500**

Graphenea 0.03%

Adiabatic temperature and isothermic heat

(v 2.8 ss 06-02-2012)

Concrete parameters

Temp. trans. coeff.	0,0945
Density	2264
Heat capacity (fresh)	1,05
Heat capacity (hardened)	1,05
Cement content	450
Set time	9,7
A - set time	33500
B - set time	1470
A - hydration	33500
B - hydration	1470
Adia. start temperature	20

Temp. trans. coeff.

dQ/dm	0
m>	21
m<	76

Heat function

m-limit	80
Q_∞	155
τ	11,82
α	4,17
R^2	0,4346
$\Sigma\Delta_Q$	6649

	specific heat capaticy [J/gK]
water	4,2
cement	0,8
sand	0,8
gravel	0,8

Resept		Sement	Silika	FA
bindemiddel	450	450	0	0
fint tilslag	1350			
fint tilslag				
grovt tilslag	0			
grovt tilslag	0			
vann	225			
densitet	2264			
Heat cap.	**1,05**			

	FA-LVB	CEM III
A	**35000**	**50000**
B	**500**	**1500**

Graphenea 0.05%

Adiabatic temperature and isothermic heat

(v 2.8 ss 06-02-2012)

Concrete parameters

Temp. trans. coeff.	0,0904
Density	2262
Heat capacity (fresh)	1,05
Heat capacity (hardened)	1,05
Cement content	450
Set time	9,3
A - set time	33500
B - set time	1470
A - hydration	33500
B - hydration	1470
Adia. start temperature	20

Temp. trans. coeff.

dQ/dm	0
m>	21
m<	76

Heat function

m-limit	80
Q_∞	159
τ	11,45
α	4,00
R^2	0,4433
$\Sigma\Delta_Q$	6526

	specific heat capaticy [J/gK]
water	4,2
cement	0,8
sand	0,8
gravel	0,8

Resept		Sement	Silika	FA
bindemiddel	450	450	0	0
fint tilslag	1350			
fint tilslag				
grovt tilslag	0			
grovt tilslag	0			
vann	225			
densitet	2262			
Heat cap.	**1,05**			

	FA-LVB	CEM III
A	**35000**	**50000**
B	**500**	**1500**

Graphenea 0.20%

Adiabatic temperature and isothermic heat

(v 2.8 ss 06-02-2012)

Concrete parameters	
Temp. trans. coeff.	0,0901
Density	2223
Heat capacity (fresh)	1,07
Heat capacity (hardened)	1,07
Cement content	450
Set time	9
A - set time	33500
B - set time	1470
A - hydration	33500
B - hydration	1470
Adia. start temperature	20

Temp. trans. coeff.	
dQ/dm	0
m>	20
m<	76

Heat function	
m-limit	80
Q_∞	157
τ	11,04
α	4,08
R^2	0,4358
$\Sigma\Delta_Q$	7283

	specific heat capaticy [J/gK]
water	4,2
cement	0,8
sand	0,8
gravel	0,8

Resept		Sement	Silika	FA
bindemiddel	450	450	0	0
fint tilslag	1350			
fint tilslag				
grovt tilslag	0			
grovt tilslag	0			
vann	225			
densitet	2223			
Heat cap.	**1,07**			

	FA-LVB	CEM III
A	**35000**	**50000**
B	**500**	**1500**

Graphitene 0.03%

Adiabatic temperature and isothermic heat

(v 2.8 ss 06-02-2012)

Concrete parameters	
Temp. trans. coeff.	0,0848
Density	2278
Heat capacity (fresh)	1,05
Heat capacity (hardened)	1,05
Cement content	450
Set time	10,6
A - set time	33500
B - set time	1470
A - hydration	33500
B - hydration	1470
Adia. start temperature	20

Temp. trans. coeff.	
dQ/dm	0
m>	22
m<	76

Heat function	
m-limit	80
Q_∞	148
τ	12,61
α	4,24
R^2	0,4570
$\Sigma\Delta_Q$	6692

	specific heat capaticy [J/gK]
water	4,2
cement	0,8
sand	0,8
gravel	0,8

Resept		Sement	Silika	FA
bindemiddel	450	450	0	0
fint tilslag	1350			
fint tilslag				
grovt tilslag	0			
grovt tilslag	0			
vann	225			
densitet	2278			
Heat cap.	**1,05**			

	FA-LVB	CEM III
A	**35000**	**50000**
B	**500**	**1500**

Graphitene 0.05%

Adiabatic temperature and isothermic heat

(v 2.8 ss 06-02-2012)

Concrete parameters	
Temp. trans. coeff.	0,0863
Density	2278
Heat capacity (fresh)	1,05
Heat capacity (hardened)	1,05
Cement content	450
Set time	10,4
A - set time	33500
B - set time	1470
A - hydration	33500
B - hydration	1470
Adia. start temperature	20

Temp. trans. coeff.	
dQ/dm	0
m>	22
m<	76

Heat function	
m-limit	80
Q_∞	151
τ	12,30
α	4,20
R^2	0,4462
$\Sigma\Delta_Q$	6806

specific heat capaticy [J/gK]	
water	4,2
cement	0,8
sand	0,8
gravel	0,8

Resept		Sement	Silika	FA
bindemiddel	450	450	0	0
fint tilslag	1350			
fint tilslag				
grovt tilslag	0			
grovt tilslag	0			
vann	225			
densitet	2278			
Heat cap.	**1,05**			

	FA-LVB	CEM III
A	**35000**	**50000**
B	**500**	**1500**

Graphitene 0.20%

Adiabatic temperature and isothermic heat

(v 2.8 ss 06-02-2012)

Concrete parameters	
Temp. trans. coeff.	0,0822
Density	2261
Heat capacity (fresh)	1,05
Heat capacity (hardened)	1,05
Cement content	450
Set time	10,4
A - set time	33500
B - set time	1470
A - hydration	33500
B - hydration	1470
Adia. start temperature	20

Temp. trans. coeff.	
dQ/dm	0
m>	23
m<	76

Heat function	
m-limit	80
Q_∞	145
τ	12,71
α	4,09
R^2	0,4902
$\Sigma\Delta_Q$	6802

specific heat capaticy [J/gK]	
water	4,2
cement	0,8
sand	0,8
gravel	0,8

Resept		Sement	Silika	FA
bindemiddel	450	450	0	0
fint tilslag	1350			
fint tilslag				
grovt tilslag	0			
grovt tilslag	0			
vann	225			
densitet	2261			
Heat cap.	**1,05**			

	FA-LVB	CEM III
A	**35000**	**50000**
B	**500**	**1500**

Appendix C

Flexural Strength

Flexural Strength, 3 days			
Type	**Sample Name**	**[MPa]**	**Avg. Flexural Strength [MPa]**
Reference SP 0.08%	A	6,0	
	B	6,0	
	C	6,2	6,1
Graphenea 0,03% SP 0.08%	A	6,5	
	B	6,2	
	C	7,1	6,6
Graphenea 0,05% SP 0.08%	A	7,4	
	B	7,8	
	C	6.3	7,2
Graphenea 0,2% SP 0.08%	A	7,2	
	B	6,7	
	C	6,8	6,9
Graphitene 0,03% SP 0.08%	A	6,7	
	B	6,6	
	C	6,6	6,6
Graphitene 0,05% SP 0.08%	A	7,4	
	B	6,5	
	C	7,2	7,1
Graphitene 0,2% SP 0.08%	A	6,1	
	B	6,8	
	C	6,9	6,6

Flexural Strength, 7 days			
Type	**Sample Name**	**[MPa]**	**Avg. Flexural Strength [MPa]**
Reference SP 0.08%	A	6,6	
	B	6,8	
	C	7,2	6,9
Graphenea 0,03% SP 0.08%	A	7,2	
	B	6,6	
	C	6,7	7,4
Graphenea 0,05% SP 0.08%	A	7,5	
	B	7,3	
	C	7,3	7,2
Graphenea 0,2% SP 0.08%	A	7,7	
	B	6,9	
	C	7,1	7,5
Graphitene 0,03% SP 0.08%	A	7,2	
	B	8,0	
	C	7,4	7,2
Graphitene 0,05% SP 0.08%	A	7,7	
	B	6,8	
	C	7,3	7,3
Graphitene 0,2% SP 0.08%	A	8,2	
	B	6,6	
	C	5,7	6,8

Flexural Strength, 28 days			
Type	**Sample Name**	**[MPa]**	**Avg. Flexural Strength [MPa]**
Reference SP 0.08%	A	7,9	
	B	7,6	
	C	8,0	7,8
Graphenea 0,03% SP 0.08%	A	7,2	
	B	6,6	
	C	6,7	6,8
Graphenea 0,05% SP 0.08%	A	8,6	
	B	8,3	
	C	6,6	7,9
Graphenea 0,2% SP 0.08%	A	8,0	
	B	7,8	
	C	7,5	7,7
Grapehena 0,2 % SP 2,0 %	A	7,8	
	B	7,9	
	C	8,2	8,0
Graphitene 0,03% SP 0.08%	A	7,5	
	B	8,0	
	C	7,3	7,6
Graphitene 0,05% SP 0.08%	A	7,2	
	B	7,6	
	C	8,8	7,9
Graphitene 0,2% SP 0.08%	A	- [1)]	
	B	7,0	
	C	8,1	7,5
Quartz 0,2% SP 0.08%	A	7,6	
	B	6,2	
	C	7,1	7,0
- [1)]The result was not recorded by the testing machine (Zwick Z020).			

Appendix C

Compressive Strength

Compressive Strength, 3 days				
Type	**Sample Name**	**#1 [MPa]**	**#2 [MPa]**	**Avg. Compressive Strength [MPa]**
Reference SP 0.08%	A	44,5	44,4	
	B	37,3	36,8	
	C	44,1	42,6	42,0
Graphenea 0,03% SP 0.08%	A	44,0	43,5	
	B	44,8	45,7	
	C	45,3	45,9	44,9
Graphenea 0,05% SP 0.08%	A	46,1	47,5	
	B	41,6	42,5	
	C	46,1	46,4	45,0
Graphenea 0,2% SP 0.08%	A	42,6	42,8	
	B	43,3	42,5	
	C	42,6	43,1	42,8
Graphitene 0,03% SP 0.08%	A	42,8	42,9	
	B	38,8	38,5	
	C	43,7	43,0	41,6
Graphitene 0,05% SP 0.08%	A	43,1	43,7	
	B	42,9	42,8	
	C	43,8	44,2	43,4
Graphitene 0,2% SP 0.08%	A	42,6	43,2	
	B	43,9	43,4	
	C	43,4	44,2	43,4

Compressive Strength, 7 days				
Type	**Sample Name**	**#1 [MPa]**	**#2 [MPa]**	**Avg. Compressive Strength [MPa]**
Reference SP 0.08%	A	48,5	49,0	
	B	45,0	45,6	
	C	49,8	48,9	47,8
Graphenea 0,03% SP 0.08%	A	50,6	50,4	
	B	52,2	51,8	
	C	51,8	52,3	51,5
Graphenea 0,05% SP 0.08%	A	52,3	52,2	
	B	51,1	50,9	
	C	51,1	50,9	51,4
Graphenea 0,2% SP 0.08%	A	48,1	47,5	
	B	47,6	48,2	
	C	47,9	46,0	47,5
Graphitene 0,03% SP 0.08%	A	49,7	51,0	
	B	50,6	50,7	
	C	50,6	52,1	50,8
Graphitene 0,05% SP 0.08%	A	51,4	51,3	
	B	51,2	51,3	
	C	52,0	51,8	51,5
Graphitene 0,2% SP 0.08%	A	50,8	50,9	
	B	46,7	48,2	
	C	51,1	51,7	49,9

Compressive Strength, 28 days				
Type	**Sample Name**	**#1 [MPa]**	**#2 [MPa]**	**Avg. Compressive Strength [MPa]**
Reference SP 0.08%	A	60,0	60,4	
	B	60,5	60,0	
	C	60,7	61,6	60,5
Graphenea 0,03% SP 0.08%	A	59,6	60,7	
	B	52,9	54,3	
	C	60,1	58,7	57,7
Graphenea 0,05% SP 0.08%	A	59,7	59,8	
	B	55,5	54,8	
	C	60,2	62,0	58,7
Graphenea 0,2% SP 0.08%	A	54,1	55,3	
	B	56,5	55,5	
	C	56,3	55,7	55,6
Grapehena 0,2 % SP 2,0 %	A	65,5	64,2	
	B	64,6	65,7	
	C	63,1	64,8	64,7
Graphitene 0,03% SP 0.08%	A	60,7	60,1	
	B	59,7	59,7	
	C	60,4	61,2	60,3
Graphitene 0,05% SP 0.08%	A	60,8	61,8	
	B	61,7	59,3	
	C	61,3	61,2	61,0
Graphitene 0,2% SP 0.08%	A	59,0	58,5	
	B	53,8	51,8	
	C	59,3	60,1	57,1
Quartz 0,2% SP 0.08%	A	60,9	60,9	
	B	54,4	54,1	
	C	60,5	60,9	58,6

Appendix C

Splitting Tensile Strength

Splitting Tensile Strength, 3 days			
Type	**Sample Name**	**[MPa]**	**Avg. Splitting Tensile Strength [MPa]**
Reference SP 0.08%	A	2,9	
	B	3,3	
	C	3,3	3,17
Graphenea 0,03% SP 0.08%	A	3,2	
	B	3,6	
	C	3,3	3,38
Graphenea 0,05% SP 0.08%	A	3,4	
	B	3,3	
	C	3,5	3,42
Graphenea 0,2% SP 0.08%	A	3,8	
	B	4,0	
	C	3,6	3,78
Graphitene 0,03% SP 0.08%	A	2,7	
	B	3,4	
	C	3,2	3,11
Graphitene 0,05% SP 0.08%	A	2,9	
	B	3,0	
	C	3,1	2,99
Graphitene 0,2% SP 0.08%	A	2,9	
	B	3,2	
	C	3,1	3,05

Splitting Tensile Strength, 7 days			
Type	**Sample Name**	**[MPa]**	**Avg. Splitting Tensile Strength [MPa]**
Reference SP 0.08%	A	3,9	
	B	4,0	
	C	3,7	3,86
Graphenea 0,03% SP 0.08%	A	3,5	
	B	3,9	
	C	4,3	3,89
Graphenea 0,05% SP 0.08%	A	3,6	
	B	4,1	
	C	3,9	3,85
Graphenea 0,2% SP 0.08%	A	4,4	
	B	4,1	
	C	3,8	4,13
Graphitene 0,03% SP 0.08%	A	3,9	
	B	3,9	
	C	3,6	3,79
Graphitene 0,05% SP 0.08%	A	3,6	
	B	3,5	
	C	3,7	3,61
Graphitene 0,2% SP 0.08%	A	3,4	
	B	3,8	
	C	3,9	3,72

Splitting Tensile Strength, 28 days			
Type	**Sample Name**	**[MPa]**	**Avg. Splitting Tensile Strength [MPa]**
Reference SP 0.08%	A	4,8	
	B	4,9	
	C	5,0	4,90
Graphenea 0,03% SP 0.08%	A	5,1	
	B	4,7	
	C	4,4	4,72
Graphenea 0,05% SP 0.08%	A	4,5	
	B	4,6	
	C	4,4	4,48
Graphenea 0,2% SP 0.08%	A	4,8	
	B	4,9	
	C	5,3	5,00
Graphitene 0,03% SP 0.08%	A	5,1	
	B	4,6	
	C	5,1	4,95
Graphitene 0,05% SP 0.08%	A	4,8	
	B	4,8	
	C	4,4	4,66
Graphitene 0,2% SP 0.08%	A	4,4	
	B	4,5	
	C	4,6	4,53

Appendix C

Ultrasonic Velocity Test (Modulus of Elasticity & Sonic Velocity)

Ultrasonic Velocity Test Results , 7 days					
Type	**Sample Name**	**Velocity[m/s]**	**Modulus of Elasticity M (K+4/3G) [GPa]**	**Avg. [GPa]**	**% Change [Gpa]**
Reference SP 0.08%	A	4416	45,19		
	B	4418	45,25		
	C	4281	42,24	44,23	-
Graphenea 0,03% SP 0.08%	A	4153	39,76		
	B	4361	43,66		
	C	4409	44,70	42,71	-3,44 %
Graphenea 0,05% SP 0.08%	A	4238	41,05		
	B	4425	44,61		
	C	4453	45,30	43,65	-1,30 %
Graphenea 0,2% SP 0.08%	A	4245	41,01		
	B	4362	43,44		
	C	4205	40,21	41,55	-6,05 %
Graphitene 0,03% SP 0.08%	A	4416	45,21		
	B	4413	45,01		
	C	4399	44,54	44,92	1,56 %
Graphitene 0,05% SP 0.08%	A	4482	46,53		
	B	4492	46,69		
	C	4285	42,48	45,24	2,27 %
Graphitene 0,2% SP 0.08%	A	4276	42,06		
	B	4185	40,30		
	C	4300	42,45	41,60	-5,93 %

Ultrasonic Velocity Test Results , 28 days					
Type	**Sample Name**	**Velocity[m/s]**	**Modulus of Elasticity M (K+4/3G) [GPa]**	**Avg. [GPa]**	**% Change[Gpa]**
Reference SP 0.08%	A	4603	49,33		
	B	4330	43,60		
	C	4476	46,49	46,47	-
Graphenea 0,03% SP 0.08%	A	4179	40,36		
	B	4515	46,91		
	C	4352	43,54	43,60	-6,18 %
Graphenea 0,05% SP 0.08%	A	4245	41,28		
	B	4389	43,72		
	C	4192	39,91	41,64	-10,41 %
Graphenea 0,2% SP 0.08%	A	4371	43,71		
	B	4276	42,05		
	C	4277	41,62	42,46	-8,64 %
Graphitene 0,03% SP 0.08%	A	4651	50,22		
	B	4515	47,09		
	C	4445	45,64	47,65	2,53 %
Graphitene 0,05% SP 0.08%	A	4640	49,81		
	B	4445	45,72		
	C	4640	49,73	48,42	4,19 %
Graphitene 0,2% SP 0.08%	A	4594	48,70		
	B	4689	50,52		
	C	4508	46,66	48,62	4,63 %

Sonic Velocity

Sonic Velocity	**Avg. Sonic Velocity [m/s]**		**% Change – [m/s]**	
Type	**7 days**	**28 days**	**7 days**	**28 days**
Reference SP 0.08%	4372	4469	-	-
Graphenea 0.03% SP 0.08%	4308	4349	-1,46 %	-2,69 %
Graphenea 0.05% SP 0.08%	4372	4275	0,00 %	-4,34 %
Graphenea 0.20% SP 0.08%	4271	4308	-2,31 %	-3,60 %
Graphitene 0.03% SP 0.08%	4409	4537	0,85 %	1,52 %
Graphitene 0.05% SP 0.08%	4420	4575	1,10 %	2,37 %
Graphitene 0.20% SP 0.08%	4254	4597	-2,70 %	2,86 %

Appendix D

Interfacial Transition Zone

Reference

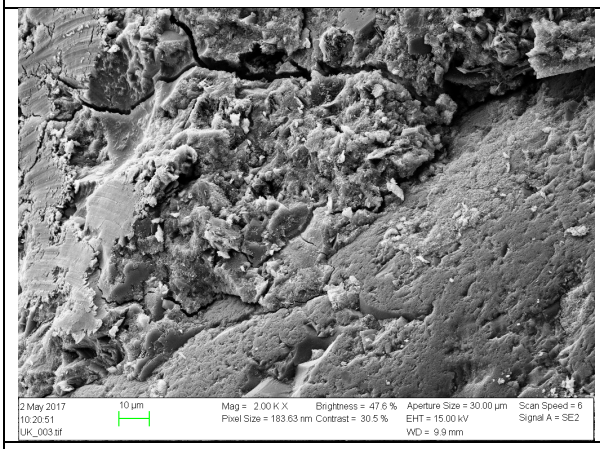

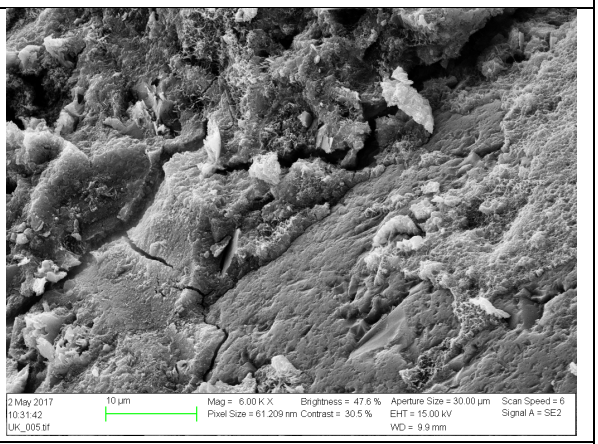

Graphenea 0.03%

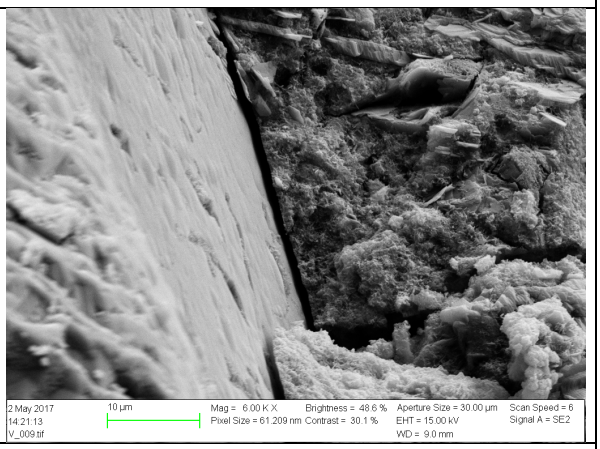

Graphenea 0.05%

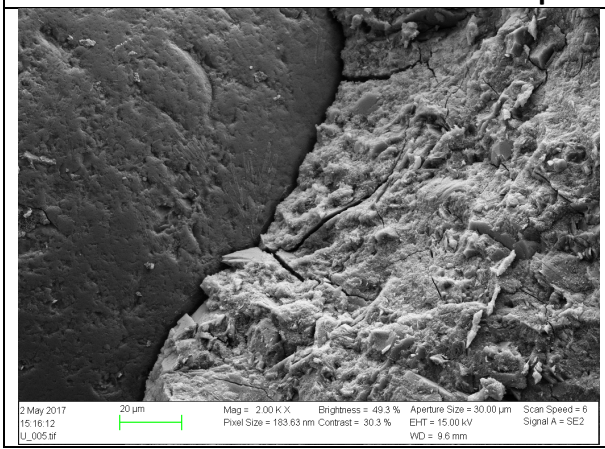

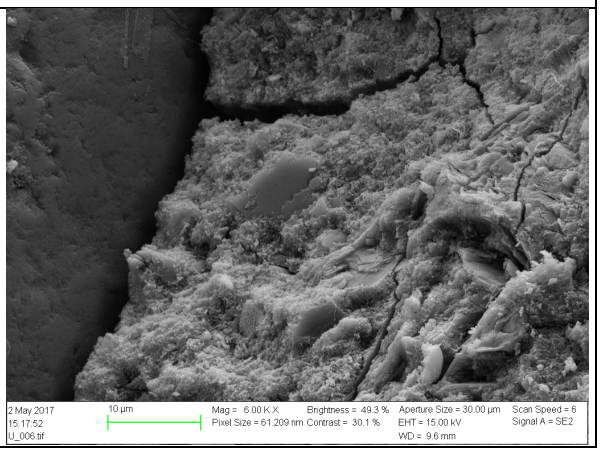

Graphenea 0.20%

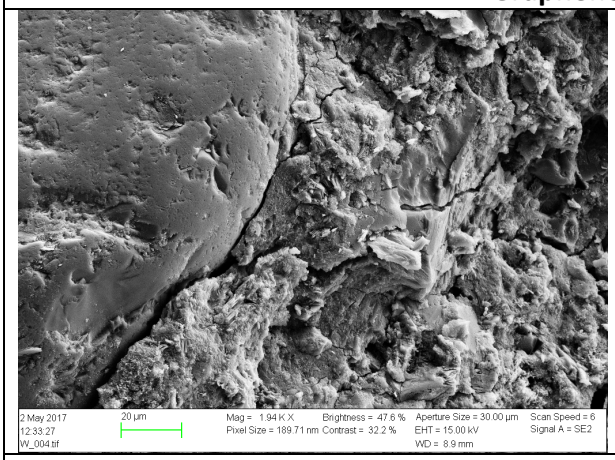

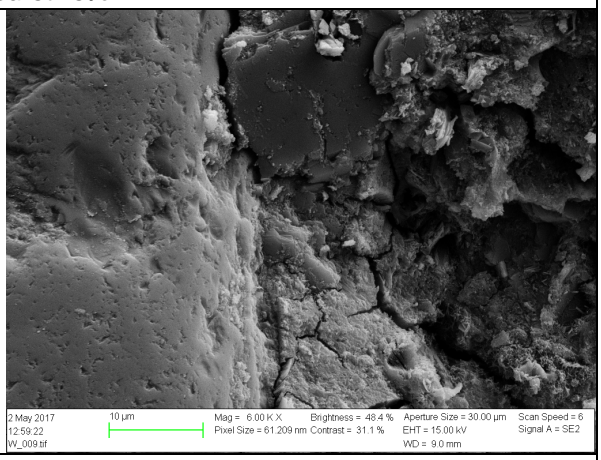

Graphitene 0.03%

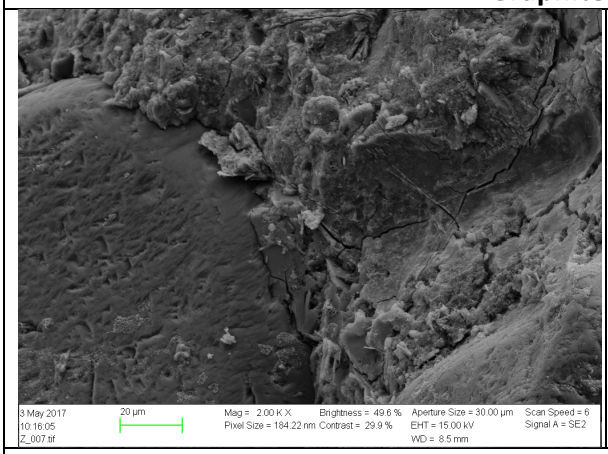

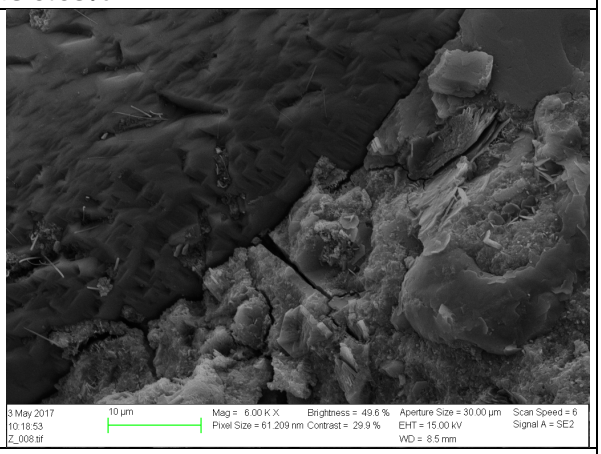

Graphitene 0.05%

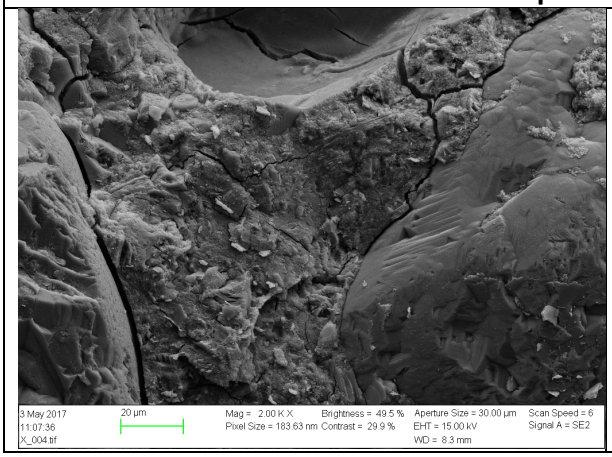

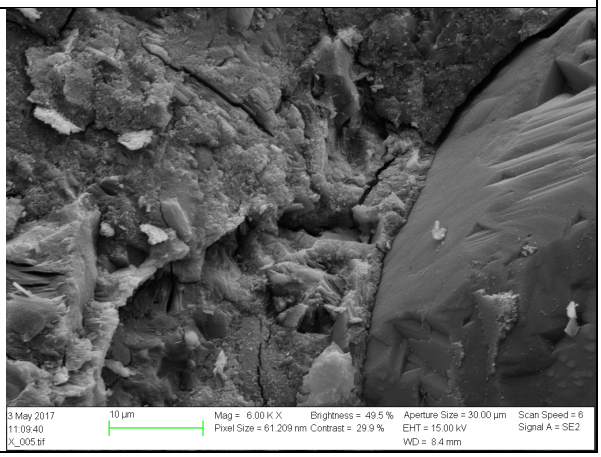

Graphitene 0.20%

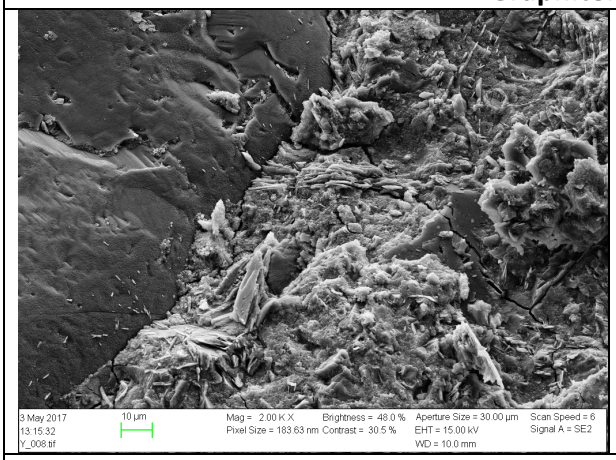

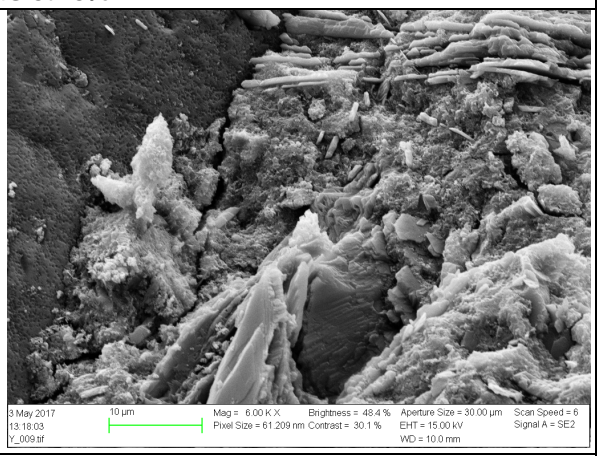

Graphenea 0.20% & SP 2.0%

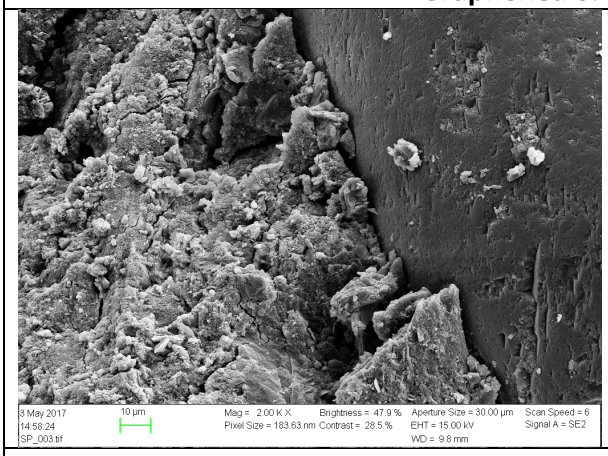

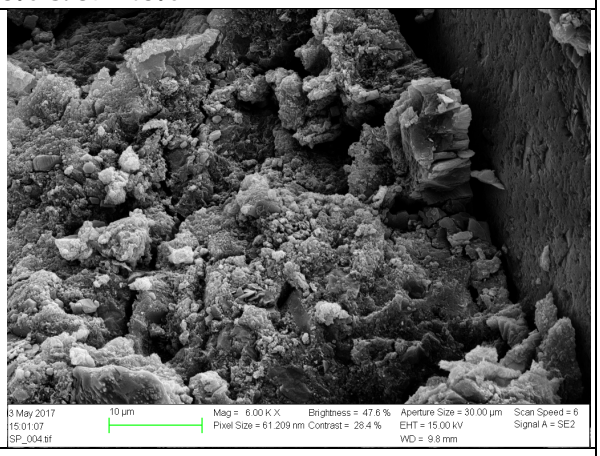

Quartz 0.20%

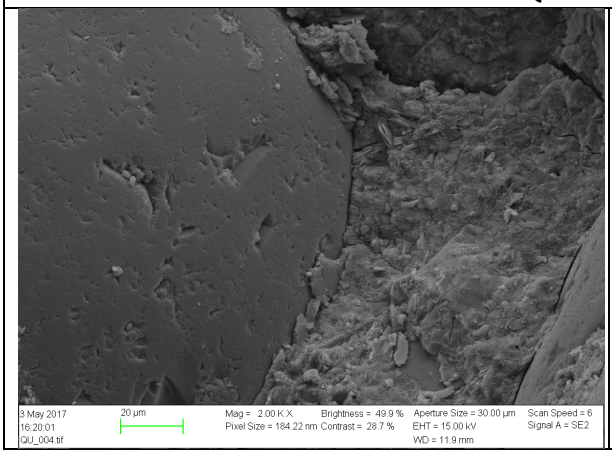

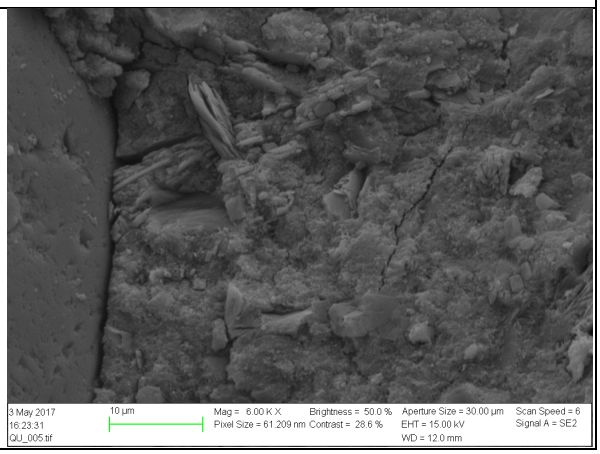

Appendix E

Quartz Sand W12 (Quarzwerke GmbH) - Product Data

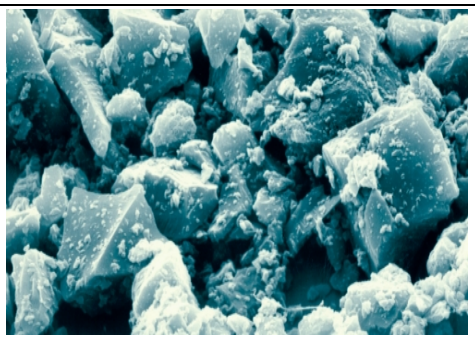

Quarzwerke

Quarzwerke GmbH
Hauptverwaltung | *Head office*

Kaskadenweg 40
50226 Frechen
fon + 49 (0) 22 34 101-0
fax + 49 (0) 22 34 101-400

sales@quarzwerke.com

Stoffdaten | *Product data*

MILLISIL®-Mehle Werk Weferlingen | *MILLISIL® Flours Weferlingen plant*

MILLISIL®-Mehle werden durch eisenfreie Mahlung mit nachfolgender Windsichtung aus aufbereitetem Quarzsand hergestellt

MILLISIL® flours are produced from processed silica sand by iron-free grinding with subsequent air separation.

Typische Korngrößenverteilung und Körnungswerte | *Typical grain size and grain characteristics*

				MILLISIL® Weferlingen | *MILLISIL® Weferlingen*						
				W 3	W 4	W 5	W 6	W 8	W 10	W 12
Obere Korngröße	| *Upper grain size*	$d_{95\%}$	in µm	220	190	160	120	90	70	50
Mittlere Korngröße	| *Average grain size*	$d_{50\%}$	in µm	90	65	50	40	30	20	16
Lichte Maschenweite Alpine Luftstrahlsieb	| *Mesh size* | *Alpine air jet sieve*		in µm	Rückstand in Gew.-% | *Residue in weight-%*						
	400			0,1	0,1					
	315			0,3	0,2	0,1	0,1			
	200			7	4	1	0,5	0,1		
	160			18	10	5	1	0,5	0,1	
	125			32	22	14	4	1	0,5	0,1
	100			42	30	23	7	3	1	0,5
	63			62	51	42	28	15	6	2
	40			75	66	57	49	34	21	12
Korndurchmesser Cilas Granulometer	| *Grain diameter* | *Cilas Granulometer*		in µm	Rückstand in Vol.-% | *Residue in volume-%*						
	32			71	70	59	52	48	38	22
	16			82	80	72	71	68	63	50
	8			90	88	85	81	80	78	69
	6			92	91	87	85	83	82	75
	4			94	93	90	88	87	86	81
	2			97	96	95	94	93	92	90

Quarzwerke

Typische körnungsabhängige Eigenschaften | *Typical grain size related properties*

				MILLISIL® Weferlingen | *MILLISIL® Weferlingen*						
				W 3	W 4	W 5	W 6	W 8	W 10	W 12
Schüttdichte (DIN EN ISO 60)	*Bulk density*		g/cm³	1,35	1,3	1,25	1,2	1,1	1,0	0,9
Stampfvolumen (DIN ISO 787-11)	*Tapped bulk volume*		ml/100 g	52	56	58	60	65	72	75
Spez. Oberfläche	*Spec. surface*									
(DIN 66126-2)		Blaine	cm²/g	1000	1300	1600	1800	2200	2800	3800
(DIN ISO 9277)		BET	m²/g	0,3	0,4	0,45	0,5	0,6	0,8	0,9
Ölzahl (DIN ISO 787-5)	*Oil absorption*		g/100 g	14	15	15	16	18	19	21
Normfarbwert	*Tristimulus values*	X		78	74	82	83	85	86	87
(DIN 5033)		Y		77	78	80	81	83	84	85
		Z		69	79	71	74	76	78	80

Typische physikalische Eigenschaften | *Typical physical properties*

Dichte (DIN EN ISO 787-10)	*Density*	g/cm³	2,65
pH-Wert (DIN ISO 10390)	*pH-value*		7
Mohs Härte (Literaturwert | *Literature value)*	*Hardness*		7
Linearer Ausdehnungskoeffizient (DIN 51045)	*Linear coefficient of thermal expansion*	α 20-300°C	$14 * 10^{-6} * K^{-1}$

Typische chemische Analyse | *Typical chemical analysis*

			Gew.-% | *weight-%*
SiO_2			99
Al_2O_3			0,3
Fe_2O_3			0,05
CaO + MgO			0,1
$Na_2O + K_2O$			0,2
Glühverlust (DIN EN ISO 3262-1)	*Loss on ignition*	1.000°C	0,25
Feuchtigkeit werksfrische Ware (DIN EN ISO 787-2)	*Moisture* | *Material fresh from production*		0,1

Allgemeine Informationen | *General information*

HS-Nummer	*HS number*	2530 9000
Fremdüberwacht nach DIN 4226		
Alle MILLISIL-Sorten entsprechen DIN EN ISO 3262-13 Qualitätsgruppe A		

MILLISIL® wird aus aufbereiteten natürlichen Rohstoffen hergestellt. Alle Daten sind Richtwerte mit vorkommens- und produktionsbedingter Toleranz. Sie dienen nur zur Beschreibung und stellen keine zugesicherten Eigenschaften dar. Gröbere Anteile sind in Spuren möglich.
Dem Benutzer obliegt es, die Tauglichkeit für seinen Verwendungszweck zu prüfen. Wir geben auf Wunsch gerne Auskunft über Toleranzbreiten und anwendungstechnische Erfahrungen. Verkäufe erfolgen gemäß unseren Verkaufs- und Lieferbedingungen.

MILLISIL® is produced from prepared natural raw minerals. All data are approximate values with tolerances depending on occurrences and production. They only serve as description and do not represent any warranty concerning the existence of specific characteristics. Traces of coarser particles may be possible.
It applies to the user to test the suitability for his purposes. If wanted, we are prepared to give further information on tolerances and on our experience in technical applications. Sales are subject to our sales and delivery conditions.

<1238> 2/2 (01/15)